

**University of Strathclyde**  
**Department of Naval Architecture and Marine**  
**Engineering**

**Dynamic modelling of SOFC marine power systems  
and shipboard applications**

**By**

**Baogang San**

A thesis presented in fulfilment of the requirements for  
the degree of Doctor of Philosophy

**2013**

This thesis is the result of the author's original research. It has been composed by the author and has not been previously submitted for examination which has led to the award of a degree.

The copyright of this thesis belongs to the author under the terms of the United Kingdom Copyright Acts as qualified by the University of Strathclyde Regulation 3.51. Due acknowledgement must always be made of the use of any material contained in, or derived from, this thesis.

Signed:

Dated:

## ACKNOWLEDGEMENTS

The thesis would not have been possible without the help of so many people. It was such a privilege, honour and serendipity for me to encounters with people who have changed the course of my academic research and to some extent my life.

I express utmost gratitude to my supervisor Professor Peilin Zhou, for his friendship, encouragement, generosity, guidance and support over the past years. His unwavering enthusiasm for marine engineering and novel ship design kept me constantly engaged with academic research and development work. My special appreciation goes to all the academic staff, research staff and research students at the Department of Naval Architecture and Marine Engineer. Their generous help and inspiration made my time at Strathclyde truly enjoyable.

This work was supported by Universities UK's Overseas Research Students Awards Scheme and University of Strathclyde Postgraduate Scholarships Program. The financial supports provided were greatly appreciated.

I am also deeply indebted to my family whose value to me only grows with age. I finally acknowledge my wife Wei and my daughter Xiwen who championed and blessed me with a life of joy.

## ABSTRACT

Sustainable and efficient provision of shipboard energy is an obvious challenge for the merchant marine industry. Various initiatives have been made to find alternatives to replace the currently used combustion engine for ship power and propulsion. In recent years, fuel cell technology, as has been widely advertised as a clean and efficient means of power generation, is drawing much attention from the marine industry.

Among various types of fuel cells, the Solid Oxide Fuel Cell (SOFC) tops others in terms of energy conversion efficiency as it can be fed with both hydrogen rich fuels and traditional fossil fuels after being chemically reformed. These features make it most promising to meet the large power demands of seagoing ships. However, due to the comprehensive and hazardous working environment, shipboard installation of SOFC power systems is not available. Can the SOFC be a viable proposition for commercial shipping and how will it behave under severe seagoing circumstances? These questions need to be addressed before commercialising SOFC marine power systems. In the thesis, simulation methods are used to predict the performance of marine SOFC systems at both static and dynamic working loads. A mathematical model is developed for describing the thermodynamic nature of a tubular SOFC concerning the thermal equilibrium of the system. Electric-chemical reactions are reflected in the stack modelling. Reforming reactions of the fuel are included in the model. Auxiliary subcomponents within the SOFC power system are modelled based on their own mechanisms and working principles. The whole simulation system is composed by combining subcomponent models via reasonable control strategies to function the system's purpose. SOFC power system models are developed to represent different working scenarios which may possibly occur onboard ship. The dynamic responses of simulation systems are examined. Thermal flow transfer influence, manifold volume influence and controller's influence are also taken into account in the dynamic modelling process. As concluded from the simulation outcomes, the sample SOFC system, while running alone, could satisfy the demand

of dynamic load change for both propulsion and auxiliary power. However, the electric output of the SOFC system would be greatly smoothed if paralleled with a battery.

In addition, risk and safety issues regarding SOFC onboard installation are examined from both design and operating perspectives. Relevant ship rules and regulations for verifications of system installation and maintenance are reviewed in detail. Conceptual design of marine SOFC application are also proposed at the last stage.

## List of previously published papers related to the research topic

Paper A: “B. San, P. Zhou, Dynamic modelling of tubular SOFC for marine power system”, Journal of Marine Science and Application, (2010) Volume 9:231-240

Paper B: “B. San, J. Bradshaw, Fuel cells for ships: systems, risks and regulations”, 11th International Marine Design Conference, Glasgow, UK, Vol 2, P 407-415, 10-14th June 2012

Paper C: “B. San, P. Zhou, Dynamic modelling of PEM fuel cell propulsive system for ship application”, International conference on ship design, production and operation, Harbin, China, 17-18 Jan 2007

## Statement of contributions to the published papers

The contributions by the author of this thesis to the published papers listed above are summarized below:

Paper A: Contributed to the ideas presented, planned the paper, carried out all the numerical simulation and wrote most of the manuscript.

Paper B: Contributed to the ideas presented, planned the paper, carried out all the numerical simulation and wrote most of the manuscript, presenting at the conference.

Paper C: Contributed to the ideas presented, planned the paper, carried out all the numerical simulation and wrote most of the manuscript.

## CONENTS:

ACKNOWLEDGEMENTS .....	iii
ABSTRACT .....	iv
List of previously published papers related to the research topic .....	vi
Chapter 1 Introduction .....	1
1.1 Background and overview of the study .....	1
1.2 Principles and thermodynamics of a fuel cell.....	2
1.2.1 Voltage of a fuel cell .....	2
1.2.2 Fuel cell types and characters .....	4
1.3 Solid oxide fuel cell .....	5
1.3.1 SOFC principles .....	5
1.3.2 Planar design and tubular design.....	7
1.4 SOFC power system and system integration.....	9
1.5 Introduction of SOFC system modelling.....	10
1.6 State of the art on fuel cell marine application and SOFC marine system modelling.....	12
1.6.1 Review of fuel cell application in ships.....	12
1.6.2 Review of SOFC development trends .....	17
1.6.3 Review of SOFC marine system modelling .....	18
1.7 Relevance and objective of the study .....	19
1.8 Methodology .....	20
1.9 Summary and conclusion .....	22
Chapter 2 Models for tubular SOFC systems.....	25
2.1 Introduction.....	25
2.2 Stack models of tubular SOFCs .....	26
2.2.1 SOFC stack layout.....	26
2.2.2 SOFC Stack Modelling.....	27
2.2.3 Pre-reforming and internal reforming modelling .....	33
2.2.4 Modelling of flow, heat transfer and energy balance .....	40
2.3 Auxiliary components models for SOFCs.....	46
2.3.1 Heat exchanger.....	46
2.3.2 Burner .....	47
2.3.3 Battery Modelling.....	47
2.3.4 Power conditioning unit.....	49
2.4 Modelling of system dynamic response .....	51
2.4.1 Dynamic modelling of anode and cathode inlet manifold.....	52
2.4.2 Temperature response time of fuel cell stack .....	56
2.5 Summary and conclusion .....	60
3.1 Introduction.....	61
3.2 Modelling of ship propulsion systems and driving chain.....	61
3.2.1 Propulsion and ship resistance modelling.....	61
3.2.2 Electric motor drive chain.....	62
3.3 Grid bus modelling and power distribution.....	66
3.4 SOFC power system modelling strategy .....	68
3.5 Summary and conclusion .....	70

Chapter 4 Modeling of a 5 (kW) SOFC at steady state .....	72
4.1 The 5 (kW) SOFC power system.....	72
4.2 Configuration of subcomponent models .....	75
4.3 Integration of SOFC stack model.....	77
4.4 Steady state simulation results and analysis .....	78
4.5 Conclusion.....	81
Chapter 5 Dynamic simulation of a 5 (kW) SOFC power system .....	82
5.1 Configuration of dynamic system.....	82
5.2 Execution of simulation.....	86
5.2.1 Starting up of SOFC .....	86
5.2.2 5kW SOFC dynamic simulation result.....	92
5.2.3 SOFC simulation with the use of battery.....	94
5.3 Conclusion.....	99
Chapter 6 Marine SOFC system installation, risks and conceptual design .....	100
6.1 Fuels for fuel cells marine installation .....	100
6.2 Risks for SOFC marine installation .....	102
6.2.1 Risks management procedures and methodology .....	102
6.2.2 Risks associated with SOFC unit .....	106
6.2.3 Risks associated with low flash point fuels .....	107
6.2.4 System level risks .....	108
6.3 Classification regulations for marine SOFC application.....	110
6.4 Improvement and modification of the SOFC marine system .....	112
6.5 Conceptual design of 750 (kW) SOFC power system on LNG carrier.....	116
6.5.1 Introduction and assumptions .....	116
6.5.2 System arrangement .....	121
6.5.3 Operating strategy .....	130
6.5.4 Economical analysis .....	132
6.6 Conclusion.....	139
Chapter 7 Thesis summary and conclusion.....	141
7.1 Summary of the thesis .....	141
7.2 Simulation results validation .....	142
7.3 Conclusions.....	145
Reference.....	148
Appendix A1: Classification regulations for marine SOFC application .....	158
A1.1 SOFC stack .....	159
A1.2 Fuel cell room (housing) and operating environment .....	160
A1.3 General arrangement.....	160
A1.4 Ventilation.....	161
A1.5 Fuel storage container.....	162
A1.6 Bunkering and fuel transfer.....	162
A1.7 Control and electric .....	163
A1.8 Piping system .....	165
A1.9 Fire fighting.....	165
A1.10 Materials .....	166
A1.11 Seagoing circumstances .....	166
A1.12 Trial.....	167

A1.13 Dependability and maintenance .....	168
A1.14 Quality control system and manufacturing control procedure .....	168

## LIST OF FIGURES

Figure 1.1: Chemical-electric reaction of tubular SOFC .....	6
Figure 1.2: Siemens tubular SOFC.....	7
Figure 1.3: Structure of Siemens tubular SOFC.....	8
Figure 1.4: 5 (kW) tubular SOFC system layout.....	9
Figure 1.5: SOFC marine power system modelling block diagram.....	21
Figure 1.6: MATLAB SIMULINK modelling block diagram.....	22
Figure 2.1: 5 (kW) SOFC system layout and inside structure.....	26
Figure 2.2: Chemical reaction of at electrolyte .....	28
Figure 2.3: Methane reacted rate during reforming process.....	39
Figure 2.4: Reforming gas composition with circulation rate change.....	39
Figure 2.5: Single tubular SOFC structure.....	41
Figure 2.6: Temperature profiles along the tube length.....	44
Figure 2.7: Equivalent open voltage circuit of lithium-ion battery.....	48
Figure 2.8: MATLAB SIMULINK block diagram of battery modelling.....	49
Figure 2.9: Circuit diagram of DC/DC chopper.....	50
Figure 2.10: Block model of DC/AC converter.....	51
Figure 2.11: Anode fuel flow diagram.....	53
Figure 2.12: Output flow rate change of reformer and manifold after a step input change.....	55
Figure 2.13: Block diagram of stack temperature control.....	56
Figure 2.14: Control block diagram of fuel cell stack thermal model.....	59
Figure 3.1: Control diagram of AC permanent magnet synchronous motor.....	65
Figure 3.2: Block diagram of drive chain for propulsion.....	66
Figure 3.3: Current distribution strategy of power bus.....	68
Figure 4.1: 5 (kW) SOFC lay out.....	73
Figure 4.2: FCT 5 (kW) SOFC system outlook.....	73
Figure 4.3: Diagram of SOFC stack model integration.....	77
Figure 4.4: Polarization curve of the fuel cell.....	79
Figure 4.5: Partial pressure of reforming reactants.....	79
Figure 4.6: Simulation result of stack voltage drop.....	80
Figure 4.7: Stack power and efficiency at different current density.....	80
Figure 5.1: SOFC temperature change with load change.....	84
Figure 5.2: Stack temprature during starting process if equation (5.4) is applied.....	88
Figure 5.3: Amplified figure of 5.2.....	89
Figure 5.4: Stack temprature during starting process if equation (5.5) is applied.....	89
Figure 5.5: Amplified figure of 5.4.....	90
Figure 5.6: Feed back control of SOFC stack starting process.....	90
Figure 5.7: Stack temprature change under optimized control process.....	91
Figure 5.8: Amplified figure of 5.7.....	91
Figure 5.9: Programed electric load change for dynamic simulation.....	92
Figure 5.10: Dynamic simualtion of SOFC with load changes.....	93
Figure 5.11: Response of step load change at 4-6 seconds.....	93
Figure 5.12: Response of step load change at 40-42 seconds.....	94
Figure 5.13: Structure of fuel cell power system.....	95

Figure 5.14: Control scheme of power distribution.....	96
Figure 5.15: SOFC and battery output at full load.....	97
Figure 5.16: Battery discharge status at full load.....	97
Figure 5.17: SOFC output responses at different load changes.....	98
Figure 5.18: Battery output responses at different load changes.....	98
Figure 6.1: Fuels for fuel cells.....	101
Figure 6.2: Lloyd's Register risk management process for unconventional design.	103
Figure 6.3: Risk assessment and governance process of SOFC marine installation	105
Figure 6.4: 12,000 ( $\text{m}^3$ ) LNG ship Bahrain Vision.....	118
Figure 6.5: 250 (kW) SOFC power system.....	121
Figure 6.6: 12,000 ( $\text{m}^3$ ) LNG ship general arrangement plan.....	123
Figure 6.7: SOFC room arrangement plan (unit in meters) .....	124
Figure 6.8: Typical working conditions for the Siemens CHP250 SOFC.....	126
Figure 6.9 (a): Natural boil off gas fuel supply to SOFC.....	127
Figure 6.9 (b): Forced boil off gas fuel supply to SOFC.....	128
Figure 6.10: CAPEX and OPEX estimation for 750 (kW) diesel generation and SOFC.....	135
Figure 6.11: Comparison of 750 (kW) dual fuel engine and SOFC using methane as fuel.....	138

## LIST OF TABLES

Table 1.1: Thermodynamic data of reactions.....	3
Table 1.2: Types of fuel cell and characters.....	4
Table 1.3: Inventory of marine fuel cell application and design.....	22
Table 2.1: Geometry parameters of Siemens standard tubular cell.....	30
Table 2.2: Coefficients in equation (2.31).....	35
Table 2.3: SOFC cell tube materials by layers.....	43
Table 2.4: Main parameter settings for the computation of figure 2.6.....	46
Table 2.5: Response time of subsystems.....	52
Table 3.1: Composition of integrated SOFC power system.....	70
Table 4.1: Characteristics of 5 (kW) SOFC Beta system.....	74
Table 4.2: Parameter settings for 5 (kW) SOFC stack.....	75
Table 4.3: Natural gas composition.....	76
Table 4.4: Simulation result at steady state for 5 (kW) tubular SOFC model.....	78
Table 6.1: List of fuel properties.....	101
Table 6.2: Load distribution at different operation modes.....	118
Table 6.3: Characteristics of 250 (kW) SOFC.....	119
Table 6.4: Operation strategy of designed power system.....	131
Table 6.5: Fuel oil bunker price versus LNG bunker price at July 2013.....	133
Table 6.6: Economic comparison between diesel generating and SOFC system....	134
Table 7.1: Comparison of simulation result wit test data.....	101

## NOMENCLATURE

A	Unit area
$A_{act}$	Coefficient in natural logarithm form of Tafel equation
$B_m$	Viscous friction coefficient
C	Thermal capacity of elements
$C_{battery}$	Storage capacity of battery
c	Specific heat capacity
$c_p$	Heat capacity
$D_{i,m}$	Diffusion coefficient for species
d	Hydrodynamic diameter of tubular flow channel in Reynolds number equation
E	Thermal potential
$E_0$	Electromotive force at standard condition with pure reactant
$e^-$	Electro
F	Faraday constant, 96485 Coulombs
$F_{x,y,z}$	Body forces
$f_{ng}$	Methane percentage rate in natural gas contains
G	Proportion coefficient in transfer function
$\Delta G$	Change in Gibbs free energy
$\Delta G_0$	Change in Gibbs free energy at standard temperature and pressure, and with pure reactant
$\Delta g_f$	Mol Gibbs free energy change
$\Delta \bar{g}_f^0$	Change of Gibbs free energy of formation per mole
$g_{H_2O}$	Mol Gibbs free energy of water
$g_{H_2}$	Mol Gibbs free energy of hydrogen
$g_{O_2}$	Mol Gibbs free energy of oxygen
$\Delta H$	Reaction enthalpy change
$H^+$	Hydrogen ion
$H_{react}$	Enthalpy change of chemical reaction
I	Rotation inertia of motor
$I_a$	Armature current

$I_{\min}, I_{\max}$	Minimum, maximum current
$i$	Current density
$i_0$	Exchange current density
$J$	Advance number
$\vec{J}_i$	Diffusion flux of species
$K_E$	Voltage constant of electric motor
$K_{\text{reform}}$	Coefficient in reforming reaction
$K_{\text{shift}}$	Coefficient in shift reaction
$K_T$	Torque constant
$k$	Thermal conductivity
$k$	Constant in Darcy's equation
$L$	Current flow length
$L_{\text{af}}$	Field-armature mutual inductance of electric motor
$L_q, L_d$	q and d axis inductances
$m$	Mass
$m_{\text{con}}, n_{\text{con}}$	Coefficient in concentration voltage drop equation
$n, n_e$	Number of moles or number of cells
OCV	Open circuit voltage
$P$	Power
$P$	propeller driving force
$P_e$	Electricity power output
$p$	Partial pressure
$p$	Number of pole pairs
$R$	Gas constant, $8.314 \text{ JK}^{-1} \text{ mol}^{-1}$
$R_i$	Net rate of production of species
$R_{\text{ohm}}$	Ohmic resistance
$R_t$	Hull resistant
$r_a$	Recirculation rate
SOC	State of charge
$S_i$	The rate of creation
$S_T$	Heat of chemical reaction and other volumetric heat sources

T	Temperature
$T_e$	Electromagnetic torque of electric motor
$T_f$	Friction torque from transmission system
$T_f$	Coulomb friction torque
$T_L$	Torque applied to electric motor shaft
$T_m$	Shaft mechanical torque
$T_p$	Resistant torque from propeller and hydrodynamic force
t	Propulsion force deduction factor
$U_f$	Fuel utilization factor of reforming process
$U_{\min}, U_{\max}$	Minimum, maximum voltage
u	Flow velocity in Reynolds number equation
u v w	Velocities vectors in directions of x y z coordinates
$\vec{u}$	Velocity vector
V	Open voltage
$V_A$	Average inflow speed
$V_s$	Ship speed
$\Delta V_{\text{ohm}}$	Ohmic voltage drop
$\Delta V_{\text{act}}$	Activation voltage drop
$\Delta V_{\text{trans}}$	Transport or concentration voltage drop
v	Fluid viscosity in Reynolds number equation
v	Velocity of fuel inlet in Darcy' equation
w	Specific flow rate
$\bar{x}$	Reacted mole numbers rate of $\text{CH}_4$
Yi	Local mass fraction of each species
$\bar{y}$	Reacted mole numbers rate of CO
$\bar{z}$	Reacted mole numbers rate of $\text{H}_2$
$\nabla$	partial derivative for a vector quantity

## GREEK LETTERS

$\alpha_a$	Charge transfer coefficient at anode
$\alpha_c$	Charge transfer coefficient at cathode
$\alpha_{H_2}$	Activity of reactant, hydrogen
$\alpha_{H_2O}$	Activity of reactant, steam water
$\alpha_{O_2}$	Activity of reactant, oxygen
$\eta$	Efficiency
$\xi_{th}$	Max thermal efficiency
$\lambda$	Amplitude of the flux induced by the permanent magnets of the rotor in the stator phases
$\rho$	Resistivity of materials
$\tau$	Time constant
$\tau$	Stress tensor
$\omega$	Wake fraction
$\omega_e$	Motor rotation speed.
$\omega_r$	Angular velocity of the rotor

## SUBSCRIPTS

AC	Alternative current
air	Air flow
bus	Electric grid bus
CH4	Methane
CO	Carbon monoxide
CO2	Carbon dioxide
charge	Battery charge
cov	Converter
DC	Directive current
discharge	Battery discharge
exh	Exhaust gas
f	Fuel
gas	Gas or natural gas flow
H <sub>2</sub>	Hydrogen
H <sub>2</sub> O	Water
HE	Heat exchanger
Lim_startup	Limitation during SOFC starting up process
in	In flow
Mani,manifold	Fuel cell inlet and outlet manifolds of gas and air
max	Maximum
min	Minimum
mix	Mixed gases
O <sub>2</sub>	Oxygen
out	Out flow
react	Reaction
stack	Fuel cell stack
water	Water

## SUPERSCRIPTS

0	Properties of free bulk flow
in	Inflow or input
out	Outflow or output
*	Active sites

## Acronym

AC	Alternative Current
AFC	Alkaline Fuel Cell
AIP	Air Independent Propulsion
AUV	Autonomous Underwater Vehicle
BOG	Boil Off Gas
BOP	Balance Of Plant
BSI	British Standards Institution
CCS	Chinese Classification Society
CEMF	Counter Electromotive Force
CFD	Computational Fluid Dynamic
DC	Direct Current
DME	Dimethyl Ether
DMFC	Direct Methanol Fuel Cell
DNV	Det Norske Veritas
EU	European Union
FCT	Fuel Cells Technologies Ltd
FMEA	Failure Mode Effect and Criticality Analysis
GT	Gas turbine
HAZID	Hazard Identification
HAZOP	Hazard and Operability Analysis
HDW	Howaldswerke Deutsche Werft
IACS	International Association of Classification Societies
IEC	International Electrotechnical Commission
IGBT	Insulated Gate Bipolar Transistor
IGC Code	International Code for the Construction and Equipment of Ships Carrying Liquefied Gases in Bulk
IGF Code	International Code of Safety for Ships Using Gases or Other Low Flash Point Fuels
IMO	International Maritime Organization

ISO	International Organization for Standardization
LCA	Life Cycle Assessment
LHV	Lower Heat Value
LNG	Liquid Natural Gas
LR	Lloyd's Register
MCFC	Molten Carbonate Fuel Cell
MCR	Max Continuous Rated Power
NAME	Department of Naval Architecture and Marine Engineering
NATO	North Atlantic Treaty Organization
NEDO	New Energy and Industrial Technology Development Organization
PAFC	Phosphoric Acid Fuel Cell
PEMFC	Proton Exchange Membrane Fuel Cell
PHL	Preliminary Hazard List
PI	Proportional Integral
PPA	Potential Problems Analysis
PWM	Pulse Width Modulation
ROPAX	Roll On and Roll Off Passenger
SOC	Status Of Charge
SOFC	Solid Oxide Fuel Cell
SOLAS	Safety of Life at Sea

# Chapter 1 Introduction

## 1.1 Background and overview of the study

As of today, marine power systems are dominated by residual and distillate oil fuelled thermal machinery. However, with the worldwide desire to shift to a sustainable future, looking for alternative fuels and efficient systems for the marine industry have become impending tasks with the increasingly stringent exhaust emission regulations. Fuel cell technology, although immature, has been identified as an energy efficient option for marine power systems to offer long term benefits. Fuel cells have fewer moving components than internal combustion engines. They can potentially improve the reliability, and reduce the noise and vibration level of machinery. Fuel cells prefer to use low flash point ( $<60^{\circ}\text{C}$ ) fuels which could reduce the emission level dramatically depending on type of fuel used. The application of fuel cells to road vehicles is at a pre-commercial stage whereas the move to use fuel cells for ships has only gained momentum in recent years due to the more comprehensive and hazardous environment on-board ships.

Among types of fuel cells, the Solid Oxide Fuel Cell (SOFC) tops others in terms of efficiency and can be fed with both hydrogen rich gases and traditional fossil fuels. These features make it most promising for large power propulsion for seagoing ships. However, in practice marine SOFC applications are very rare due to the complexity of the system, very high principal investment and unavailability of internationally agreed shipping rules and regulations. In this respect, fuel scale simulation is identified as a viable method to predict the performance of fuel cell systems in marine environments.

Modelling of a SOFC marine power system is a complicated process which needs to consider influences of both fuel cell stack and peripheral components of the whole system. The challenge of SOFC modelling is to imitate the whole system performance at an acceptable accuracy level while reflecting the various influential factors caused by subcomponents. In the thesis, a tubular SOFC power system model is provided which considers thermodynamic and electrochemical reaction of the SOFC. Subcomponents of

lithium ion battery, power conditioning unit, stack structure, heat exchanger and controller are integrated. The dynamic response of the system is illustrated by the inertia of the subcomponent and controller strategy. Results of the whole system simulation at a steady state and transit period are presented with detailed discussion on the effects of thermal inertia and control strategy on system performance.

To install an SOFC system onboard ship, many practical issues need to be addressed. To safely use fuel cells and low flash point fuels, potential risks that might be brought on board ships need to be minimized. This paper identifies and addresses the risk and safety problems for using fuel cells on board commercial ships from both design and operational perspectives. A detailed safety assessment of an SOFC marine system is performed, complying with current available marine rules and regulations. Conceptual designs of SOFC shipboard installation are also provided in the thesis.

The contents of the thesis are composed in eight chapters as follows. In chapter 1, a review of literature is presented in light of the SOFC technology and its marine applications. In chapter 2, modelling methods for a tubular SOFC stack are given. In chapter 3, the SOFC power system and its modelling strategy are introduced. In chapter 4, a 5 (kW) tubular SOFC system is simulated at steady state by using the modelling methods mentioned above, while in chapter 5, dynamic simulation of the 5 (kW) SOFC is performed. In Chapter 6, shipboard installation issues for the SOFC are discussed in detail with conceptual design provided.

## 1.2 Principles and thermodynamics of a fuel cell

### 1.2.1 Voltage of a fuel cell

The theoretical voltage of a fuel cell can be calculated according to the thermodynamic property of reactants. For instance, the basic reaction of hydrogen and oxygen for fuel cells is expressed as equation 1.1



The energy released by this reaction is the change in Gibbs free energy of formation  $\Delta G$ . If we take one mole of hydrogen and half a mole of oxygen as reactants then the Gibbs free energy change is:

$$\Delta g_f = g_{H_2O} - g_{H_2} - \frac{1}{2} g_{O_2} \quad (1.2)$$

Accordingly, the convertible voltage potential of a single fuel cell is shown as equation (1.3) at standard conditions at 25 ( $^{\circ}\text{C}$ ):

$$E_0 = \frac{-\Delta G_0}{nF} = \frac{237100}{2 \times 96485} = 1.228(V) \quad (1.3)$$

The maximum efficiency possible or the ideal efficiency is the ratio of Gibbs free energy change to reaction enthalpy:

$$\xi_{th} = \frac{\Delta G}{\Delta H} \quad (1.4)$$

To sum up, the thermodynamic property of reactions at standard conditions at 25 ( $^{\circ}\text{C}$ ) are listed in table 1.1

**Table 1.1: Thermodynamic data of reactions**

Reactions	$-\Delta H^0$ (kJmol $^{-1}$ )	$-\Delta G^0$ (kJmol $^{-1}$ )	$E_0$ (V)	$\xi_{th}$
$H_2 + \frac{1}{2} O_2 \rightarrow 2H_2O(l)$	286	237	1.23	0.83
$CH_4 + 2O_2 \rightarrow CO_2 + 2H_2O(l)$	890	817	1.06	0.92
$CO + \frac{1}{2} O_2 \rightarrow CO_2$	283	257	1.33	0.91
$CH_3OH(l) + \frac{3}{2} O_2 \rightarrow CO_2 + 2H_2O(l)$	727	703	1.21	0.97
$NH_3 + \frac{3}{4} O_2 \rightarrow \frac{1}{2} N_2 + \frac{3}{2} H_2O(l)$	383	338	1.17	0.88

### 1.2.2 Fuel cell types and characters

To achieve the best performance, different electrolytes and manufacturing methods have been attempted. So, among most of the publications, fuel cells are categorised by their electrolyte. The most well recognised types are: Alkaline Fuel Cell (AFC), Proton Exchange Membrane Fuel Cell (PEMFC), Direct Methanol Fuel Cell (DMFC), Phosphoric Acid Fuel Cell (PAFC), Molten Carbonate Fuel Cell (MCFC) and SOFC. The properties of the five types of fuel cells are listed in table 1.2.

**Table 1.2: Types of fuel cell and characters**

		AFC	PEMFC	PAFC	MCFC	SOFC
Electrolyte	Electrolyte	KOH	PEM	H <sub>3</sub> PO <sub>4</sub>	Li <sub>2</sub> CO <sub>3</sub> Na <sub>2</sub> CO <sub>3</sub>	Z <sub>r</sub> O <sub>2</sub> +Y <sub>2</sub> O <sub>3</sub>
	Electric ion	OH <sup>-</sup>	H <sup>+</sup>	H <sup>+</sup>	CO <sub>3</sub> <sup>2-</sup>	O <sup>2-</sup>
	Temp(°C)	50-150	80-100	190-200	600-700	700-1000
	Corrosion	Medium	Medium	strong	Strong	No
Electrode	Catalyst	Ni, Ag	Pt	Pt	No	No
	Anode	$H_2 + 2OH^- \rightarrow 2H_2O + 2e^-$	$H_2 \rightarrow 2H^+ + 2e^-$	$H_2 \rightarrow 2H^+ + 2e^-$	$H_2 + CO_3^{2-} \rightarrow H_2O + CO_2 + 2e^-$	$H_2 + O^{2-} \rightarrow H_2O + 2e^-$
	Cathode	$\frac{1}{2}O_2 + H_2O + 2e^- \rightarrow OH^-$	$\frac{1}{2}O_2 + 2H^+ + 2e^- \rightarrow H_2O$	$\frac{1}{2}O_2 + 2H^+ + 2e^- \rightarrow H_2O$	$\frac{1}{2}O_2 + CO_2 + 2e^- \rightarrow CO_3^2$	$\frac{1}{2}O_2 + 2e^- \rightarrow O^{2-}$
Reactants		Hydrogen	hydrogen	Hydrogen	Hydrogen, carbon monoxide	Hydrogen, carbon monoxide
Fuel source		Pure hydrogen	Natural gas, methanol	Natural gas, methanol	Petroleum, natural gas, methanol, coal	Petroleum, natural gas, methanol, coal
System efficiency (%)		45-50	30-40	40-45	50-65	55-70

Fuel type and fuelling infrastructure also have a great influence on applying fuel cell power onboard. Hydrogen is ideal for all types of fuel cell. However, the reformation of hydrogen from hydrocarbon is a complex process. It is clear from table 1.2 that high temperature fuel cells like SOFCs and MCFCs could use both hydrogen and carbon monoxide as fuel. However, to use fossil fuel, the resources must be reformed to contain hydrogen and carbon monoxide rich gases.

The net efficiency of PEMFC is approximately 35-45%, much lower than the high temperature fuel cell, but it is competitive enough to replace the car petrol engine. The merit of PEMFC is its low working temperature, easy operation and short starting time.

The exhaust temperature of MCFC is very high, which could be used to co-generate with gas turbine and steam turbine to achieve maximum electric power output. One of the potential markets for MCFC is to replace the traditional power plant with coal and gas as a power source.

SOFC bears the highest operation temperature and could reform natural gas internally without a catalyst. For large SOFC power plants, if combined with exhaust gas energy, the net output efficiency can be 65-70% when fuelling with natural gas and 55-60% with coal as fuel. This feature is very attractive for large scale power generations, like ship-board electric power generation.

## 1.3 Solid oxide fuel cell

### 1.3.1 SOFC principles

Unlike other fuel cells, the electrolyte of SOFC is a solid ion conducting ceramic material. The highlights of this type of fuel cell are high efficiency, high exhaust temperature, catalyst free and no electrolyte leakage. These features make it very attractive for large power plant application with co-generation systems. Based on cell structure, there are mainly two types of SOFCs: tubular and planar. Figure 1.1 shows the reaction of SOFC

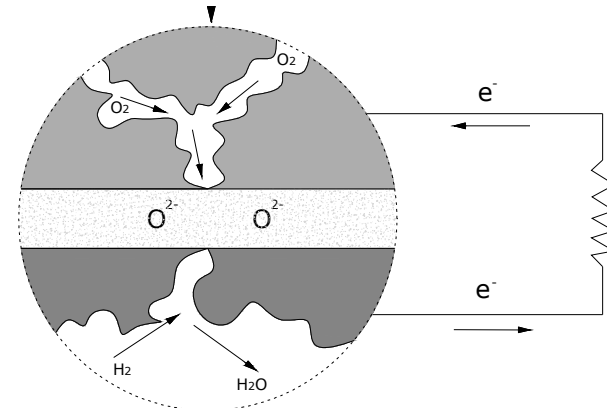


**Figure 1.1 Chemical-electric reaction of tubular SOFC**

The reaction taking place at the cathode is shown in table 1.2. The oxygen working as an oxidant obtains an electron to form an oxygen ion. The oxygen ion replaces the cavity in the electrolyte and is conducted to the anode to react with hydrogen or carbon monoxide.

So, the ion is transferred negatively from the cathode to anode through the electrolyte. Water or carbon dioxide and an electron are formed at the anode. The electrons generated move from anode to cathode via external circuit and provide electric power to load.

The open circuit voltage of a SOFC varies with different working temperature, type of fuel and oxidant, e.g. theoretically below 1.2 (V). However the voltage of a single cell in practice is normally under 0.7 (V). This voltage difference is because of the voltage drop at the electrode and resistance of cell and interconnection.

The merits of the SOFC are:

- It could achieve very high net efficiency in terms of electrical output, e.g. over 50% of Lower Head Value (LHV) and high power density, e.g.  $0.3 \text{ (W/cm}^2\text{)}$ ;
- It could use coal gas as a fuel directly;
- It is not toxic to carbon monoxide and there is no need for an expensive catalyst to accelerate reaction;

- The system can be optimized because the fuel is reformed internally;
- There is no need to consider leakage of the electrolyte;
- The high temperature exhaust can be used to co-generate to improve electric output;

A weak point of the SOFC is that ceramic material is relatively fragile and vulnerable at temperature changes.

### 1.3.2 Planar design and tubular design

There are mainly two types of designs in terms of formation of cell structure, *i.e.* planar and tubular.

A planar design of SOFC uses a series of flat plates to compose a cell stack. Similar to other fuel cell sandwich structures, a bipolar plate is used to connect the anode with the cathode. A planar SOFC has a more compact structure compared with tubular designs, but the drawback is that extra consideration of stack sealing is needed to avoid mixture of oxygen and fuel.

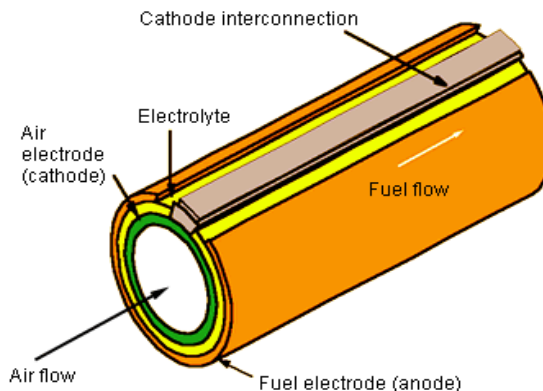


**Figure 1.2 Siemens tubular SOFC (Siemens tubular SOFC, 2013)**

A tubular fuel cell, mainly discussed in the thesis, is normally a cylinder like tube with one closed end. The most prestigious tubular design is developed by Siemens (used to

be Siemens-Westinghouse) as indicated in figure 1.2. The current generation tube design is a three layer cylinder structure. The air electrode supported cathode is made of lanthanum manganite. Other layers of material are deposited on this ceramic support cathode structure. The electrolyte is a 40 ( $\mu\text{m}$ ) yttria stabilized zirconia and the anode is composed of porous nickel or zirconia cermet.

Single tubular cells are connected with a nickel interface into a bundle, normally twenty four cells, as seen from figure 1.3. Further assembly is achieved by putting many bundles together in a specific serial and parallel order to form a fuel cell stack as indicated in figure 1.3.

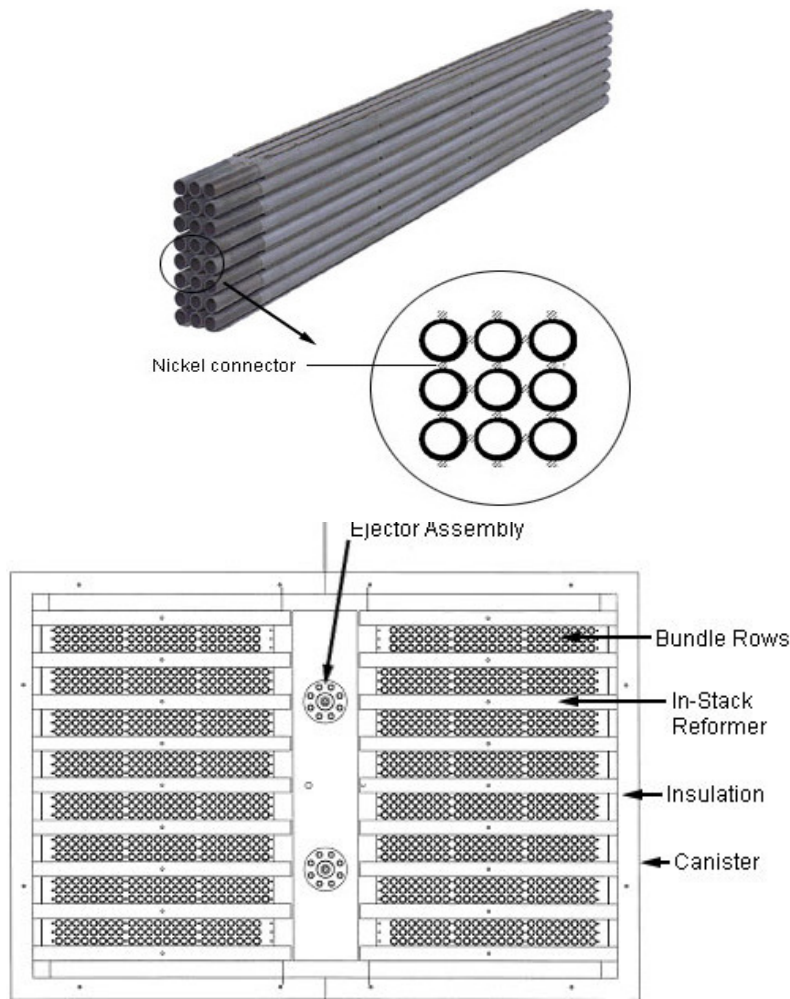


**Figure 1.3 Structure of Siemens tubular SOFC**

## 1.4 SOFC power system and system integration

The SOFC power system is an integration of a fuel cell stack and other peripheral device to maintain individual components to work effectively as a whole. Actually, the fuel cell stack appears to be very small compared with other subcomponents, which is usually called the Balance Of Plant (BOP). These extra devices depend on the type of fuel cell. Take the SOFC for instance; blowers or compressors are needed to circulate air and fuel. A power conditioning unit will be used to regulate electric output. Control and monitoring equipment is used for maintaining system operation. Fuel processing and heat exchangers also take a large share of system volume. Figure 1.4 shows a system diagram of a 5 (kW) tubular SOFC.

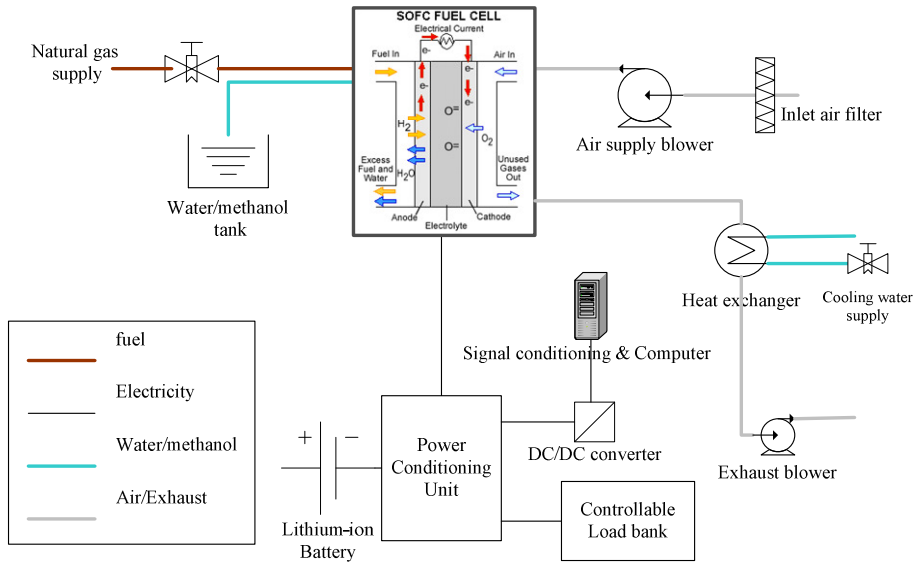


**Figure 1.4: 5 (kW) tubular SOFC system layout**

The system performance of the SOFC depends on stack temperature and pressure. To further utilise the exhaust, a steam turbine could be combined in a bottom cycle. For a pressurised SOFC system of a larger power range, a gas turbine is favourable for exhaust utilisation.

To achieve the best system performance, the following factors need to be considered:

- a) Sealing of stack and sealing between different layers inside the tube
- b) Balance of mass and energy
- c) Electrical connection and isolation
- d) Fuel storage and process
- e) Heat balance and effective use of exhaust
- f) Structure optimisation to reduce system size

## 1.5 Introduction of SOFC system modelling

Simulation of the SOFC system is different from modelling of the SOFC stack itself. Modelling of the fuel cell stack normally reflects the behaviours of electrochemical reactions, ionic conduction, reforming and heat transfer. Some detailed stack modelling explains porosity of microstructure and material conductivity. However, system modelling is concerned more with integrated system performance and the relation and influence among each subcomponent. As this point, some detailed modelling of subcomponents can be simplified under limited accuracy to predict system performance. For instance, experimental equations can be used to model some subcomponents to reduce computational time.

The core of the fuel cell power system is the fuel cell stack. The numerical modelling of the SOFC stack has been tried from different approaches by many researchers. Detailed stack models, like some 1D and 2D models (Chan and Xia, 2001; Costamagna, *etc.*, 1998), describe cell behaviours at various operation status. The property of thermal and electrical conduction is assumed to be identified for repeat elements and sections.

3D modelling flourished in the past decade with the maturity of Computational Fluid Dynamic (CFD) theory. Sets of partial equations are established regarding the conservation equations for species mass, momentum, energy and heat. The solution of these equations is calculated by CFD method according to selected assumptions and boundary conditions. 3D modelling needs massive computational calculation and, sometimes, may not reach an exact numerical solution. So, a 3D model is normally used to emphasise specific interests rather than universal reactions of all details, for instance, single channel models provided by Yakabe *et al* (1999) and Yakabe *et al* (2001), stack models with repeat elements proposed by Recknagle *et al* (2003), Autissier *et al* (2004) and Khaleel *et al* (2001), local reactants' properties suggested by Iora *et al* (2005), Janardhanan and Deutschmann (2005) and Liu *et al* (2007), degradation and reliability models provided by Tu and Stimming (2004) and Yang *et al* (2003).

System modelling of SOFCs has been tried by some authors such as Yerramalla *et al* (2003), Cheddie and Munroe (2005), Liu and Leong (2006), Bessett (1994) and Padulles *et al* (2000). Most models are developed to simulate power systems or combined systems under steady state conditions. Padulles *et al* (2000) addressed a dynamic model for SOFC power systems; however, his research mainly concentrates on electrical and chemical reaction of stacks but neglects the influences of temperature, fuel process and auxiliary components. The factors being neglected take more time to system response and should not be missed for dynamic simulation.

Dynamic and real time simulation of an SOFC system is of great importance to evaluate system control and monitoring. A fair system model could be regarded as a reference for SOFC system optimisation and provide an indication for conceptual design. Therefore, a real time system model with reasonable simulation time is very important.

## 1.6 State of the art on fuel cell marine application and SOFC marine system modelling

### 1.6.1 Review of fuel cell application in ships

There is no commercially available marine fuel cell power system in contrast with the pre-commercial demonstrations in vehicles. Nevertheless, the request for fuel cell power, tailored for marine circumstances, has never stopped. Originating as Germany's first installed hydrogen fuel cell in submarines, there have been many cases of marine fuel cell demonstrations and research projects. The following paragraph is a short review.

The review is not an exhaustive list of fuel cell marine applications; however, it illustrates a trend that fuel cell marine application is shifting from research activities in the early 2000s to physical ship installations in recent years. These demonstration projects delivered a clear message to the marine industry that fuel cells are ready for ship use once proper risk mitigating measures are addressed.

#### **U212 class submarine**

The new generation of submarines were developed by Howaldswerke Deutsche Werft (HDW). 240 (kW) PEMFC is used as Air Independent Propulsion (AIP) on board a 1400 (tons) Germany submarine. HDW and Nordseewerke delivered the 212A class fuel cell powered submarine to the German Office for Defence Technology and Procurement in 2006. Another two 212A class submarines were scheduled for delivery in 2012 and 2013 (German Navy orders tow more fuel cells subs, 2006) for the German Navy. The HDW fuel cell AIP system was installed with a total amount of over 3 (MW) for at least 12 submarines for the German, Greek, South Korean and Italian Navies.

#### **URASHIMA**

Urashima (DeepC project, 2005) is a deep sea probe with a fuel cell and battery hybrid power system. The large class autonomous underwater vehicle, developed by the Japanese Marine Science and Technology Centre since 1998, uses either a fuel cell or a

lithium ion battery as the power source to cruise for over 300 (km). The fuel cell system uses tank stored hydrogen and oxygen to produce energy. It has achieved a record of continuous, 220 (km), cruising using a fuel cell in June 2003.

### **FCTESTNET**

FCTESTNET project (FCTESTNET project introduction, 2005) is a European Union (EU) funded thematic network project. The aim of this project is to collect and exchange information on application-oriented testing of fuel cells and to promote the development and harmonisation of appropriate test procedures applicable to transport applications, stationary power sources, and portable fuel cells. FCTESTNET focuses on fuel cells and stacks, BOP components and fuel cell systems for various applications. The project addresses all aspects of fuel cell testing procedures in a top down perspective from the point of view of application-oriented needs. A harmonised set of requirements and a harmonised view to applications and technology will foster a common communication between system integrators and component developers.

### **ONR/NAVSEA/USCG**

The project provides a conceptual design of a diesel oil fuelled molten carbonate fuel cell powered US coastguard cutter as part of a potential demonstration programme. The content of the design study includes fuel processing, fuel storage, power generation and power conversion. The fuel cell generator systems deliver alternating current electrical power and integrate with an existing ship design and with existing ships systems. In accordance with the IEC fuel cell system definition, the fuel cell generator is considered to include fuel processing, power generation and power conversion subsystems. In the meantime, the environmental impact of sea going on the fuel cell has been tested, e.g. salinity and vibration influences.

### **METHAPU**

Project METHAPU (METHAPU project, 2010) aims to use Wartsila SOFC on board a cargo vessel by using methanol as the fuel. Methanol is renewable fuel but not

permitted on board for its inherently low flashpoint. So, the justification of safety and regulation is one of the main concerns in the project. The major work is to develop technology for the use of renewable methanol on board commercial vessels in order to support the necessary regulations to allow the use of methanol as a marine fuel. The specific components of the technology have been validated, like methanol fuel bunkering, distribution, storage system, and methanol consumption.

The conclusion of the project confirms that utilisation of methanol fuel is good for seaborne vessels. The SOFC is a suitable type of fuel cell for using methanol on board ships.

## FCSHIP

FCSHIP (FCSHIP project, 2005) is the first EU funded research and technology development project for applying FC technologies in ships. The project was initiated under the coordination of the Norwegian Shipowners Association with the participation of a 21-partner consortium representing the European maritime industry.

Findings from the FCSHIP project conclude that ‘no major obstacles have been identified for development of fuel cell systems that will fulfil basic requirements to safety and operation in ships’ (FCSHIP working file, 2004). The main reasons for the application of fuel cell technology in shipping are not only reduction of emissions but also sustainability, reduction of consumption of fossil fuels and moving towards a regenerative power supply.

In the project, two conceptual designs of marine fuel cell systems were performed. One used a high temperature fuel cell on board a seagoing Roll On/ Roll Off Passenger (ROPAX) ship as auxiliary power with diesel and natural gas as the fuels. Another design is to install a PEMFC on board a harbour ferry for both propulsion and electricity supply with pressurised hydrogen as the fuel.

## **Hydroxy 3000**

The Technical University of Western Switzerland has developed several small boats for testing of fuel cell propulsion. The largest example is a 4-6 persons boat powered by a 3 (kW) PEMFC (Hydroxy3000 Hydrogen ship, 2004).

## **MTU sailing boat**

MTU has provided a fuel cell system for a sailing boat on Lake Constance. The boat is equipped with a 4 times 1.2 (kW) PEMFC and a battery which replaces the conventional diesel or gasoline engines. At a normal cruising speed of around 6 (km/h), the boat has a sailing range of 225 (km) (MTU Sailing boat, 2003).

## **Deep C project**

Similar to the URASHIMA project, the German project DeepC (DeepC project, 2005), sponsored by the German Ministry of Education and Research, is to develop a transportable Autonomous Underwater Vehicle (AUV) with a PEMFC to power electrical motors. The 3.6 (kW) PEMFC system has two stacks with 60 cells at each. The AUV is planned to be used for the oil and energy underwater inspection market. This includes survey, inspection, monitoring, production support and exploitation in general.

## **FellowSHIP**

Initiated in 2003 by Det Norske Veritas (DNV) and its partners the FellowSHIP project (HotModule power for FellowSHIP project, 2008) is targeted to build a fuel cell powered offshore supply ship by 2010. The CFC Solution is to supply a MCFC HotModule power unit to cover some 320kW electricity power onboard a gas fuelled ship, Viking Energy, in late 2008. The MCFC unit could produce alternative circuit electricity with a net efficiency of 47%.

### **San Francisco Water Transit Authority fuel cell system study**

The project (Development of a Hybrid Fuel Cell Ferry, Summary Report, 2003) is to apply hydrogen fuelled solid polymer fuel cells on to a harbour ferry for auxiliary power and propulsion. Hydrogen is stored in the form of pressurised gas supplied to the fuel cell through two hydrogen supply lines. Fail closed solenoid valves are provided at both inlet and outlet of hydrogen storage. The fuel cell system, with two fuel cell modules, is installed in a separate compartment on the main deck. A ventilation system is provided for this compartment to move fresh air through the internal space to dilute hydrogen concentrations below combustible range.

### **NATO Naval frigate fuel cell system**

The four years' research and development work (Electric warship technology, 2001) documents the conceptual design of a fuel cell system for a naval frigate. Two diesel oil fuelled MCFC generators supply both propulsion and auxiliary power in combination with a gas turbine onboard the ship. As concluded by Selow and Kraaij (2005), the fuel cell generator system includes diesel oil processing, power conversion and a control unit. Each fuel cell generator could deliver 5500 (kW) electric power, while a gas turbine generator capable of providing 22000 (kW) works in parallel with fuel cells to produce propulsion power and auxiliary power.

### **Passenger boat ‘Hydra’**

Hydra (Hydra ship, 2002) is a small passenger boat built in 2000 with an alkaline fuel cell for power. The single hydrogen fuelled alkaline fuel cell supplies all propulsion power in combination with a battery. The net output of the fuel cell is approximately 5.5 (kW). The novelty of the fuel cell boat is its two metal hydride storages with a storage capacity of 16 ( $m^3$ ) hydrogen each. In these storages the hydrogen is not compressed in a pressurised chamber, but chemically absorbed in a metal powder.

## BP Shipping's SOFC project

BP Shipping is to install a 5 (kW) Fuel Cells Technologies Ltd (FCT) SOFC system on a Liquid Natural Gas (LNG) tanker to test the operating characters of the fuel cell in a marine environment. The fuel cell system will be fuelled by LNG boil-off gas to generate electricity. The system's conceptual design is provided by the Department of Naval Architecture and Marine Engineering (NAME) of the University of Strathclyde. The SOFC system will first be tested at the laboratory of NAME before being moved on board the LNG tanker.

### 1.6.2 Review of SOFC development trends

The main players of SOFC research and development are from the EU, Japan and USA. The target of SOFC development is to improve energy efficiency and reduce carbon dioxide emissions.

European funding is the major source to support SOFC research within Europe member states. In the past five years European companies and institutions have obtained approximately 15% of the world's SOFC related patents. The interest of most of the EU work is focused on the planar design and micro tubular design. The 5<sup>th</sup> and 6<sup>th</sup> Research, Technology and Development (RTD) Framework Program was completed with over 11 projects being supported in terms of fuel cell technology.

Japan's SOFC development is funded mostly by the New Energy and Industrial Technology Development Organization, which was established by the Japanese government in 1980 to develop new oil-alternative energy technologies. The interest of Japanese research is to develop, design and manufacture co-generation and combined cycle SOFC systems that can be used in small and medium-scale distributed power source markets. They also plan to improve the reliability against degradation and lower SOFC system costs by size reduction.

The major U.S. funding source of SOFC research and development comes from the US Department of Energy and Department of Defence. The US research was in favour of tubular SOFCs since the milestone success of tubular design from Siemens Westinghouse in the 1980s. But, the US funding strategy has now changed to small APU units, planar designs and SOFC hybrid systems in recent years.

### 1.6.3 Review of SOFC marine system modelling

Unlike the numerous studies on SOFC modelling, simulation and modelling for marine SOFC systems is extremely rare.

Kar *et al* (2011) investigated a so called “tri-generation” SOFC system, which includes a SOFC stack, exhaust gas turbine and absorption heat pump to drive the heat ventilation and air conditioning system. A 50 meter long ship with a 250 (kW) SOFC tri-generation system was simulated by using static thermodynamic models. It is found that compared to the SOFC-GT system, the overall efficiency of a tri-generation system is far higher when waste heat recovery is used.

Ovrum, and Dimopoulos (2012) were heavily involved with the FellowShip research project (HotModule power for FellowSHIP project, 2008). They built up a dynamic model for a MCFC system, used to test data for the ship “Viking Lady” of FellowShip Project to verify the MCFC model. Like most of the numerical models, the fuel cell model considers the nature of fuel cell thermodynamics, heat transfer and electrochemical reaction. The ship test data shows the calibrated model has a relatively low error prediction rate of within 4%. The author also claims that some operating aspects, such as over-heating, voltage fluctuation and catalyst degradation, can be demonstrated via the simulation model.

Strazza *et al* (2010) used a Life Cycle Assessment (LCA) method to evaluate the use of methanol as a fuel for SOFC auxiliary power systems for commercial vessels. A 20 (kW) SOFC system is examined to compare the different fuel options and technologies. The

environmental effect of the sample SOFC system was also studied. The study concluded that bio-fuel can significantly reduce the environmental impact on operations perspectives. The similar LCA analysis method is also found in Alkaner and Zhou's research (2006) in 2006 on MCFC in a marine application. Alkaner and Zhou compare the LCA simulation results with conventional auxiliary diesel engines. The LCA includes manufacturing of MCFC, fuel supply, operation and decommissioning stages of the system's life cycle.

## 1.7 Relevance and objective of the study

As reviewed in sections 1.5 and 1.6 of the thesis, there are many publications in SOFC modelling, such as fuel cell stack model and lump sum model for SOFC systems. However these models cannot be directly or readily applied to simulate marine power systems. To simulate an integrated marine fuel cell system, lump sum models for all the key components need to be included as a whole under both steady state conditions and dynamic load conditions. From the review of fuel cell marine system modelling in section 1.7, it is also found that dynamic models for SOFC marine systems are extremely rare. Furthermore, some key components for real ship operation are missing, such as battery, heat exchanger, power conditioning and propulsion equipment.

To further support the author's findings, a survey of shipbuilding engineers, ship designers, and classification surveyors was conducted from June to October 2012 (see also chapter 7 for details of the survey). The survey shows that a "relatively accurate" dynamic simulation model covering all key components of the system and with a reasonable simulation time is desired and appreciated. The tolerable overall error range for modelling can be as high as 2% to 5%. The ideal simulation model shall cover all the adjustable configuration of components in the system.

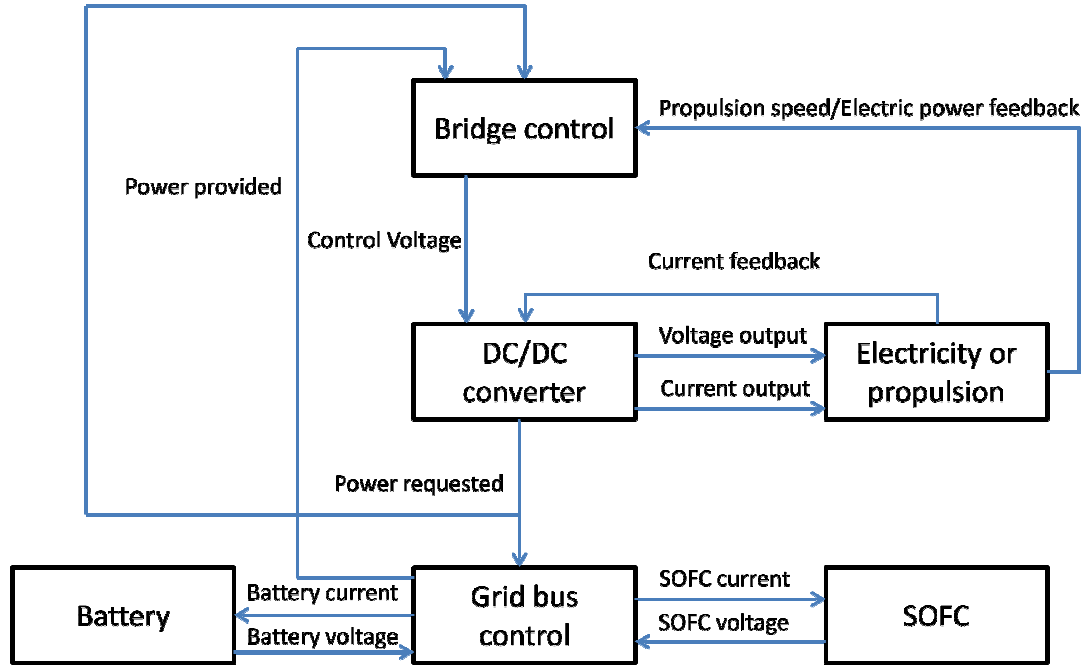
Therefore, it is identified that a thorough lump sum marine SOFC system model, which can mimic the dynamic marine operating environment, is the objective of the thesis. In this paper:

- A real time SOFC stack model is to be provided concerning the dynamic response of parameters.
- SOFC pre-reforming and internal reforming process is to be modelled. Temperature change of fuel cell causes the most time delay of system response. Its influence is also to be integrated in the model.
- All the subcomponents used in SOFC power system is to be provided
- SOFC power system integration and control logic is to be explained in detail

Another difference from other research is that the thesis also emphasises the practical installation issues for SOFC marine power system and propulsion system, which is a blank area and seldom touched by other scholars. The risks and hazardous associated with SOFC marine installation will be assessed in an analytical manner. Risk assessment methodology and risk mitigation practices will be examined in details.

## 1.8 Methodology

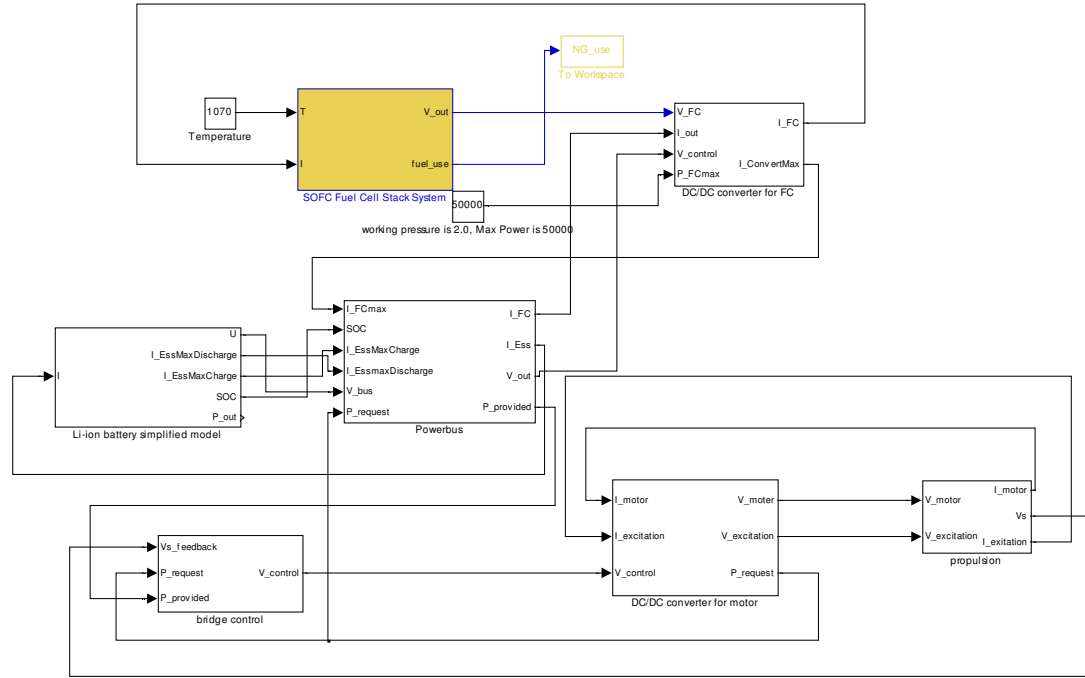
As explained in section 1.7, an integrated SOFC simulation system is the objective of the thesis. The development of the simulation models is similar to building up a block. It starts with detailed modelling of each subcomponent being used in the SOFC system. The subcomponents are then linked together by suitable control logic. The main subcomponents used in the integrated model includes: SOFC stack (including modelling of reforming, mass flow and heat transfer), battery, electric converter, grid bus and electric propulsion/electricity output. The control block diagram for the main components is indicated in figure 1.5 as direct below.



**Figure 1.5: SOFC marine power system modelling block diagram**

The system control starts with a control voltage from the bridge control block. The control voltage and the current feedback from the electric drive train define the power requested from the grid bus. The grid bus control will justify the power needed from SOFC and battery based on the control logic and the status of charge of the battery. The final propulsion speed or the electricity power output will be fed back to the bridge control to adjust the control voltage.

The integrated system model is validated by using software MATLAB SIMULINK. SIMULINK is a data flow graphical programming language tool for modeling, simulating and analyzing multi-domain dynamic systems. SIMULINK is widely used in control theory and digital signal processing for dynamic simulation and model-based design. The SIMULINK model of the overall SOFC system is generally indicated by figure 1.6. The details of models will be introduced in the later chapters.

**Figure 1.6: MATLAB SIMULINK modelling block diagram**

## 1.9 Summary and conclusion

This chapter started with an introduction of the basic principles of fuel cell reactions. SOFC power system design and modelling were also introduced. A review of fuel cell modelling, marine application and SOFC development was presented. It should be pointed out that at the current stage the application of fuel cell technology on board seagoing ships is immature compared with automotive and stationary power generation. The demonstration projects mentioned in section 1.6 are the major sources easily accessible by the public. This information is categorised in table 1.3.

**Table 1.3: Inventory of marine fuel cell application and design**

Fuel cell type	Power range(kW)	Ship type	Application	Fuel	Project
PEMFC	240	Submarine	AIP	Hydrogen	German Navy
PEMFC	4	AUV	Propulsion	Hydrogen	URASHIMA

PEMFC	250	Harbour ferry	Propulsion & Auxiliary	Hydrogen	FCSHIP(conceptual)
PEMFC	3	boat	Propulsion	Hydrogen	Hydroxy
PEMFC	4.8	Sailing boat	Propulsion	Hydrogen	MTU sailing boat
PEMFC	3.6	AUV	Propulsion	Hydrogen	Deep C
PEMFC	240	Harbour ferry	Propulsion & Auxiliary	Hydrogen	San Francisco WTA
AFC	5.5	Passenger boat	Propulsion	Hydrogen	Hydra
MCFC	625	cutter	Propulsion & Auxiliary	Diesel Oil	USCG (conceptual)
MCFC	1000	ROPAX	Auxiliary	Diesel Oil	FCSHIP(conceptual)
MCFC	320	Offshore supply ship	Auxiliary	Natural Gas	FellowSHIP
MCFC	11000	Naval frigate	Propulsion & Auxiliary	Diesel Oil	NATO(conceptual)
SOFC	2500	ROPAX	Auxiliary	Natural Gas	FCSHIP(conceptual)
SOFC	20	Cargo ship	Auxiliary	Methanol	METHAPU
SOFC	5	LNG ship	Auxiliary	Natural Gas	BP shipping (conceptual)

Table 1.3 shows that the most frequently chosen fuel cell types for marine application are PEMFC, MCFC and SOFC. But the fuel storage and recharging limits the PEMFC applications for large seagoing ships. Accordingly, the PEMFC is preferred for propulsion and auxiliary power for boats and small ferries, which is easy to connect to charging points along coast. As for seagoing ships, high temperature fuel cells are favoured for high efficiency and ability to use fossil fuels, like natural gas and other low flash point fuels. Therefore, in this thesis, the author mainly casts light on the SOFC which is possibly one of the most applicable fuel cells onboard seagoing ships in the near future.

From the review of SOFC modelling, it can be seen that modelling of the SOFC has been tried from different perspectives. These models include both analytical models and experimental models. However, very little modelling work has been found in the field of marine power systems especially simulation works on both steady and dynamic status of fuel cells in seagoing circumstances.

Consequently, a model for marine SOFC power systems is provided in this thesis considering thermodynamic and electrochemical reactions of tubular solid oxide fuel cells. Subcomponents of a lithium ion battery, power conditioning unit, stack structure and controller are integrated. The dynamic response of the system is illustrated according to the inertia of subcomponent and controller strategy. Results of the whole system simulation at steady state and transit period are presented, with detailed discussion on the effects of thermo inertia and control strategy on system performance.

Besides modelling and simulation of SOFC marine power systems, the later part of the thesis emphasises onboard installation of an SOFC power system and its safety issues. This is also the main barrier from applying fuel cell systems on seagoing ships. The discussion and assessment of onboard installations strictly complies with current ship rules and ongoing discussion of international standards such as the International Code of Safety for Ships Using Gases or Other Low Flash Point Fuels (IGF Code).

In the next chapter, modelling methods for tubular SOFC marine power systems are provided in detail.

## Chapter 2 Models for tubular SOFC systems

### 2.1 Introduction

Research and development in the solid oxide fuel cell is currently drawing intensive interest for the benefits of its high efficiency and low cost compared with other types of fuel cells. The technology is now in the stage of prototype demonstration. A record of continuous running hours for tubular SOFC power systems was renewed every day to a milestone of over 10,000 hours. Beside the progress in SOFC manufacturing, theoretical research for tubular SOFC modelling has improved in recent years. The mathematical models for tubular SOFCs have been tried from different angles; however, less attempts are available in terms of system models for tubular SOFCs compared with fuel cell stack models, especially dynamic modelling of fuel cell power systems. To simulate an SOFC power system, each component involved in the system needs to be considered, in particular, those subcomponents that contribute more to systems operation characters that have more influence on other parts. This chapter presents a lump-sum method to model tubular SOFC systems. Subcomponents of the fuel cell system, masked into blocks, are simulated according to the mechanism of components within each part. Then it integrates these sub-models to compose an SOFC system model. In the first section the modelling method for an SOFC stack is introduced, followed by a description of auxiliary component models in later sections.

System modelling of SOFC has been tried by many authors, such as Yerramalla *et al* (2003), Cheddie and Munroe (2005), Liu and Leong (2006), Bessett (1994) and Padulles *et al* (2000). Most models are developed to simulate a power system or combined system under steady state conditions. Padulles *et al* (2000) addressed a dynamic model for a SOFC power system; however, his research mainly concentrates on electrical and chemical reaction of stack but neglects influences of temperature, fuel process and auxiliary components that weight more in terms of time delay. In this chapter, a complete system model for tubular SOFC is proposed. An SOFC pre-reforming and internal reforming process is modelled. The influence of stack

temperature change, which causes the most time delay of system response, is also integrated in the model.

## 2.2 Stack models of tubular SOFCs

### 2.2.1 SOFC stack layout

As shown in figure 2.1, the target SOFC system is a 5 (kW) power unit with natural gas as fuel and standard air pressure. Methane rich natural gas is fed into the centre of the stack through a catalysed pre-reformer and then flows into the anode side of the tube through the anode manifold and orifices. Meanwhile, air enters into the stack from the bottom. The inlet air is heated by the high temperature of the stack and goes into the inner side of tube. Part of the anode exhaust is redirected to mix with the fuel inlet by a controlled re-circulator in order to enhance steam content and improve temperature. The exhaust heat is carried away by a heat exchanger. There is a controller to monitor and operate the SOFC power system. The fuel cell output is connected in parallel with battery to power conditioning unit.

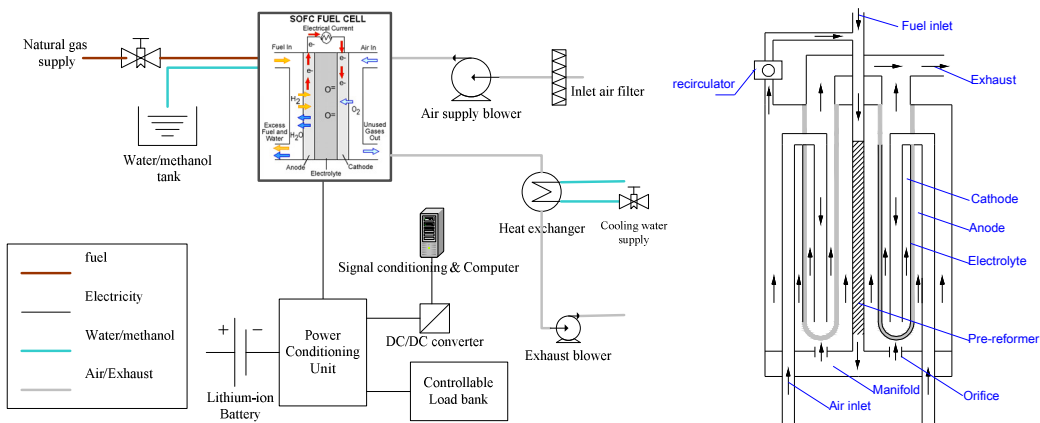


**Figure 2.1: 5 (kW) SOFC system layout and inside structure**

As indicated by the system layout, components within the system include SOFC stack (comprising of internal reformer), battery, electric converter, power conditioning unit

and heat exchanger and burner. The models for these components will be discussed in the following sections.

### 2.2.2 SOFC Stack Modelling

Cheddie and Munroe (2005) categorised fuel cell models into three: analytic, semi-empirical and mechanistic. Though an empirical model is obtained from experimental data by an interpolation method, this kind of model is limited only to the power range of experimental scale, and cannot be used for the prediction of system performance. Thus, in this study SOFC models are performed in a more analytical way. For a tubular solid oxide fuel cell, the chemical reaction is expressed as an equation (2.1-2.3) if considering hydrogen and oxygen as reactants. Figure 2.2 is the transect view of the tubular SOFC and sketch of its chemical reactions. At the cathode side, oxygen is ionized and sets up a flow of oxygen ions. The oxygen ions will then penetrate the electrolyte and reach the anode side to react with hydrogen to produce water. In doing so electrons are released during the reaction. If the anode and cathode are externally connected then the flow of electrons becomes the electric current.

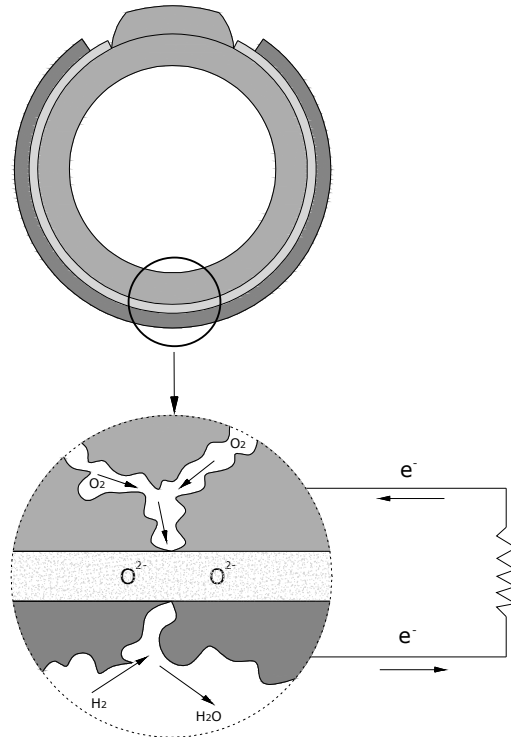


**Figure 2.2: Chemical reaction at electrolyte**



As widely accepted, the operating voltage of the fuel cell is calculated as equation (2.4):

$$V = E - \Delta V_{ohm} - \Delta V_{act} - \Delta V_{con} \quad (2.4)$$

Where: E is the thermodynamic potential,  $\Delta V_{ohm}$  is the ohmic voltage drop,  $\Delta V_{act}$  is the total activation voltage losses,  $\Delta V_{con}$  is mass transport or concentration losses. These voltage drops will be discussed in the following part of this section.

According to the Nernst equation, thermodynamic potential can be expressed as equations (2.5 and 2.6):

$$E = \frac{-\Delta \bar{g}_f^0}{2F} + \frac{RT}{2F} \ln \left( \frac{a_{H_2} \cdot a_{O_2}^{1/2}}{a_{H_2O}} \right) \quad (2.5)$$

$$E = E_0 + \frac{RT}{2F} \ln \left( \frac{a_{H_2} \cdot a_{O_2}^{1/2}}{a_{H_2O}} \right) \quad (2.6)$$

Where:  $E_0$  is the electromotive force at a standard pressure, R is the gas constant (J/mol K), T is the cell temperature, F is Faraday's constant (96485 C/mol),  $a$  is the activity of reactant, which is represented by partial pressure.  $E_0$  is approximately linear with the change of temperature as concluded by Bossel (1992) and Reid *et al* (1987).

$$E_0 = aT^2 + bT + c \quad (2.7)$$

To identify thermodynamic potential, the partial pressure of gas composition and cell temperature need to be confirmed. The chemical composition of reacting gas at either side of the tube is calculated according to the reforming reaction. The detailed process of identifying cell temperature and gas composition will be explained in section 2.2.3.

### Ohmic voltage loss

The Ohmic voltage loss  $\Delta V_{ohm}$  is calculated according to the fuel cell resistance. The current flow inside a cell is described as reference (Li and Chyu, 2003 and Jiang *et al*, 2006). The current accumulates electrons circumferentially around the anode and the cathode tubes. Oxide ions move perpendicularly across the electrolyte. Based on Ohm's law, the resistance of each material is expressed as:

$$\Delta V_{ohm} = R_{ohm} \cdot i \quad (2.8)$$

$$R_{ohm} = \rho \frac{L}{A} (\Omega) \quad (2.9)$$

L stands for current flow length which is also the thickness of each layer, A is the unit area respectively and  $\rho$  is resistivity of material. As also concluded by Jiang *et al* (2006), Campanari and Iora (2004), the resistivity for anode, cathode, electrolyte and interconnection are functions of temperature. The geometry parameters of the cells are listed in table 2.1 according to the reports of Singhal (1998) and Hagiwara *et al* (1999).

$$\rho_{anode} = 2.98 \times 10^{-5} \cdot e^{-1392/T} (\Omega \cdot m) \quad (2.10)$$

$$\rho_{cathode} = 8.114 \times 10^{-5} \cdot e^{600/T} (\Omega \cdot m) \quad (2.11)$$

$$\rho_{electrolyte} = 2.94 \times 10^{-5} \cdot e^{10350/T} (\Omega \cdot m) \quad (2.12)$$

$$\rho_{interconnect} = 0.0012568 \cdot e^{4690/T} (\Omega \cdot m) \quad (2.13)$$

**Table 2.1: Geometry parameters of Siemens standard tubular cell**

Items	Outer diameter (m)	Thickness (m)	Length (m)
Air inducting tube	0.012	$1 \times 10^{-3}$	1.450
Anode	0.022	$1 \times 10^{-4}$	1.5
Cathode	0.021720	$2.2 \times 10^{-3}$	1.5
Electrolyte	0.0218	$4 \times 10^{-5}$	1.5
Inter connection	1/8 of perimeter	$8.5 \times 10^{-5}$	1.5
Fuel boundary	0.02487		1.5

As for the layers of anode, cathode and electrolyte, the circumferential current pathway needs to be considered to calculate ohmic loss. However, when the SOFC working temperature is around 527 to 1027 ( $^{\circ}\text{C}$ ), the order of magnitude of resistivity of anode, cathode, electrolyte and interconnection are  $10^{-6}$ ,  $10^{-4}$ ,  $10^{-1}$ ,  $10^{-1}$  respectively. So the thesis neglects the circumferential current pathway of anode and cathode and looks at them as the current penetrates these layers straight in the model.

## Activation loss

The activation voltage drop is defined as the minimum voltage drop needed to overcome the activation energy from both cathode and anode. The activation polarisation is related to surface over potential and the rate of reaction as a conclusion by Newman and Thomas-Alyea (2004). It can be determined from the Butler–Volmer equation:

$$i = i_0 \left[ \exp\left(\frac{\alpha_a n_e F \Delta V_{act}}{RT}\right) - \exp\left(\frac{\alpha_c n_e F \Delta V_{act}}{RT}\right) \right] \quad (2.14)$$

Where  $i$  is net current density,  $i_0$  is exchange current density or the current densities for the forward and reverse reaction at equilibrium, and  $\alpha_a$   $\alpha_c$  is the charge transfer coefficient which is an additional kinetic parameter and represents how an applied potential favours one direction of reaction over the other or the change in the electrical potential across the reaction interface changes the sizes of the forward versus reverse activation barrier (Kakac *et al*, 2007, Costamagna and Honegger, 1998, Wendt and Kreysa, 1999). The exchange current density is approximately calculated as:

$$i_{0,a} = \gamma_a \left( \frac{p_{H2}}{p_{amb}} \right) \left( \frac{p_{H2O}}{p_{amb}} \right)^m \exp\left(-\frac{E_{act,a}}{RT}\right) \quad (2.15)$$

$$i_{0,c} = \gamma_c \left( \frac{p_{O2}}{p_{amb}} \right)^{0.25} \exp\left(-\frac{E_{act,c}}{RT}\right) \quad (2.16)$$

The values of  $m$ ,  $E_{act}$ ,  $\gamma_a$  and  $\gamma_c$  can be found in reference (Costamagna and Honegger, 1998). In practice, the Butler-Volmer equation can be linearly deduced as equation (2.17) when activation polarisation is low.

$$\Delta V_{act} = \frac{RT}{n_e F i_0} i \quad (2.17)$$

If activation loss is high, the second part of the Butler-Volmer equation could be neglected and is rewritten as a Tafel equation in equation (2.18)

$$\Delta V_{act} = A_{act} \log\left(\frac{i}{i_0}\right) \quad (2.18)$$

The condition of low activation polarisation is determined by

$$\frac{F \Delta V_{act} n_e}{RT} < 1 \quad (2.19)$$

According to the empirical graph plotted by Larminie and Dicks (2003:59), the numerical value of exchange current density varies greatly from different types of fuel cells. In low and medium-temperature fuel cells, the activation polarisation plays the most important role on total losses causing voltage drop from the ideal voltage but the activation polarisation in high temperature fuel cells is less significant. The activation polarisation of electrode-supported SOFC occurs in both electrodes. The activation polarisation of the cathode is obviously higher than that of the anode due to its lower exchange current density (Kakac *et al*, 2007). The activation polarisation increases steeply at low current density but gradually at higher current density (Chan and Xia, 2002). As for small power range SOFC the activation loss is relatively small and changes slightly at the operation temperature range of 627-927 ( $^{\circ}$ C). So assume  $A_{act}$  is 0.002 ( $\text{cm}^2$ ) and  $i_0$  is 10 ( $\text{mA}/\text{cm}^2$ ) for low power output SOFCs.

## Concentration loss

Concentration loss is caused by concentration change at the cell electrodes. Species flows at electrode are caused by concentration gradients between bulk flow and active

site (Sanchez *et al*, 2006). When reactant is spent, the slow diffusion process would cause a voltage drop, which can be expressed by

$$\Delta V_{con} = \Delta V_{trans}^{anode}(i) + \Delta V_{trans}^{cathode}(i) \quad (2.20)$$

$$\Delta V_{con} = \frac{RT}{n_e F} \ln\left(\frac{p_{H_2}^* p_{H_2O}^0}{p_{H_2}^0 p_{H_2O}^*}\right) + \frac{RT}{n_e F} \ln\left(\frac{p_{O_2}^*}{p_{O_2}^0}\right) \quad (2.21)$$

Where superscript “<sup>0</sup>” means properties at free bulk flow and superscript “\*” stands for active sites. The calculation of hydrogen, steam and oxygen molar fraction concentration at cell reaction site is discussed in section 2.2.3. One empirical solution is used by Larminie and Dicks (2003) shows very good results. This method is shown by equation (2.22) if  $m_{con}$  and  $n_{con}$  are properly chosen.

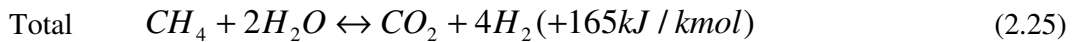
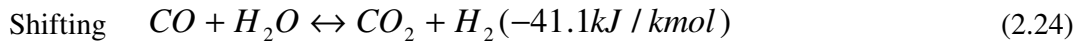
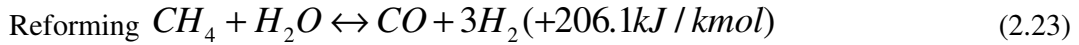
$$\Delta V_{con} = m_{con} \exp(n_{con} i) \quad (2.22)$$

Sometimes concentration loss is negligible because the diffusion process is very fast in terms of high temperature fuel cells. So, the empirical method could be accepted referring to system accuracy.

### 2.2.3 Pre-reforming and internal reforming modelling

Fuel for SOFC anodes is reformed at the internal reformer and pre-reformer. The fuel of SOFCs is methane rich natural gas. Delivered natural gas can be desulfurized and filtered as requested, which is eligible for feeding fuel cells. The natural gas normally contains 75% to 95% methane and other gases like dioxide and low saturated hydrocarbons. Methane reforming is achieved by a catalysed steam reforming method and its chemical reaction is expressed as equation (2.23-2.25). Steam reforming is an endothermic reaction. So, temperature is low at the first sections of the fuel tube. With the reaction of methane, heat is released according to equation (2.26), which causes a

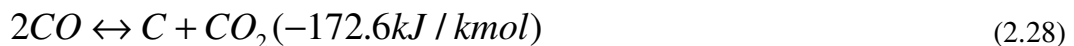
significant temperature increase along the axial direction. Therefore, methane needs to be partially pre-reformed (Meusinger *et al*, 1998). A re-circulator in the system is responsible for ensuring that the appropriate amount of semi-utilised fuel is re-circulated to the pre-reformer with a fresh fuel feed. In addition, the re-circulator is used to achieve sufficient mixing of gases in the stack.



The produced hydrogen could also be oxidised to steam due to electrochemical reaction.



However, deposit of carbon particles will possibly be produced according to the reactions below as equation (2.27 and 2.28). These two reactions would decrease the activity of anodes by depositing carbon on the surface.



Changes of Gibbs free energy influence the reactions. The positive change of Gibbs free energy at certain temperatures will shift towards reactions. On the contrary, reaction would shift towards products if free energy change were negative at that temperature according to Sanchez *et al* (2006). The comparatively high operating temperature of solid oxide fuel cell enhances those reactions whose behaviour is more endothermic (Bossel, 1992). In practice, the concentration of steam is increased in order to enhance the conversion of methane into hydrogen and not into atomic carbon. The equilibrium of the reforming reaction is shifted to the products. The exhaust gas of the anode is

somewhere near 1000 ( $^{\circ}\text{C}$ ) and it contains up to fifty percent of water steam. This gas is re-circulated and mixed with the fuel before it enters the cell.

When reactions reach equilibrium, the composition of reforming products are expressed in equation (2.29 to 2.31) based on temperature and partial pressure over the standard state pressure at  $1.013 \times 10^5$  (MPa).

$$K_{reform} = \frac{p_{H_2}^3 \cdot p_{CO}}{p_{CH_4} \cdot p_{H_2O}} \quad (2.29)$$

$$K_{shift} = \frac{p_{H_2} \cdot p_{CO_2}}{p_{CO} \cdot p_{H_2O}} \quad (2.30)$$

$$\begin{aligned} \log K_{reform} &= aT^4 + bT^3 + cT^2 + dT + e \\ \log K_{shift} &= aT^4 + bT^3 + cT^2 + dT + e \end{aligned} \quad (2.31)$$

The factors in equation (2.31) are listed in table 2.2.

**Table 2.2: Coefficients in equation (2.31) (Bossel, 1992)**

Parameters	Reforming reaction	Shift reaction
a	$-2.6312 \times 10^{-11}$	$5.47 \times 10^{-12}$
b	$1.2406 \times 10^{-7}$	$-2.5748 \times 10^{-8}$
c	$-2.2523 \times 10^{-4}$	$4.6374 \times 10^{-5}$
d	$1.9503 \times 10^{-1}$	$-3.915 \times 10^{-2}$
e	-66.1395	13.2097

As explained previously regarding pre-reforming, the anode duct is fed by the effluent of the pre-reformer. If assumed that the methane reforming in the pre-reformer reaches equilibrium, there are still about 10-30% unreformed methane and carbon monoxide

remains. Similarly, the reforming process happens internally in the anode with the oxidation of hydrogen and monoxide. According to the research of Sanchez *et al* (2006), the reforming procedure is calculated in the methods of both kinetics and equilibrium. The results show that maximum error difference of the two methods is 1% on the main parameters of performance. So, when undertaking SOFC system dynamic simulation, this error range is acceptable, because the objective of dynamic simulation concentrates more on the system inertia and response at time domain.

If internal reform reaches equilibrium, the reactions are looked at as the same as equation (2.29) and (2.30). Let  $\bar{x}$ ,  $\bar{y}$ ,  $\bar{z}$  (mol/s) represent the reacted mole numbers rate of CH<sub>4</sub>, CO and H<sub>2</sub> respectively during the reactions of equation (2.23)-(2.26). The mole changes of species composition in anode channel are shown as follows:

$$CH_4^{out} = CH_4^{in} - \bar{x} \quad (2.32)$$

$$CO^{out} = CO^{in} + \bar{x} - \bar{y} \quad (2.33)$$

$$CO_2^{out} = CO_2^{in} + \bar{y} \quad (2.34)$$

$$H_2^{out} = H_2^{in} + 3\bar{x} + \bar{y} - \bar{z} \quad (2.35)$$

$$H_2O^{out} = H_2O^{in} - \bar{x} - \bar{y} + \bar{z} \quad (2.36)$$

The total mole numbers change from inlet flow to outlet flow is:  $M_f^{out} = M_f^{in} + 2\bar{x}$

So, the equilibrium equations could be transformed as follows:

$$\begin{aligned}
 K_{reform} &= \frac{p_{H_2}^3 \cdot p_{CO}}{p_{CH4} \cdot p_{H_2O}} = \frac{\frac{CO^{in} + \bar{x} - \bar{y}}{M_f^{in} + 2\bar{x}} \cdot (\frac{H_2^{in} + 3\bar{x} + \bar{y} - \bar{z}}{M_f^{in} + 2\bar{x}})^3 \cdot p^2}{\frac{CH_4^{in} - \bar{x}}{M_f^{in} + 2\bar{x}} \cdot \frac{H_2O^{in} - \bar{x} - \bar{y} + \bar{z}}{M_f^{in} + 2\bar{x}}} \\
 &= \frac{(CO^{in} + \bar{x} - \bar{y}) \cdot (H_2^{in} + 3\bar{x} + \bar{y} - \bar{z})^3 \cdot p^2}{(CH_4^{in} - \bar{x}) \cdot (H_2O^{in} - \bar{x} - \bar{y} + \bar{z}) \cdot (M_f^{in} + 2\bar{x})^2}
 \end{aligned} \tag{2.37}$$

$$\begin{aligned}
 K_{shift} &= \frac{p_{H_2} \cdot p_{CO2}}{p_{CO} \cdot p_{H_2O}} = \frac{\frac{H_2^{in} + 3\bar{x} + \bar{y} - \bar{z}}{M_f^{in} + 2\bar{x}} \cdot \frac{CO_2^{in} + \bar{y}}{M_f^{in} + 2\bar{x}}}{\frac{CO^{in} + \bar{x} - \bar{y}}{M_f^{in} + 2\bar{x}} \cdot \frac{H_2O^{in} - \bar{x} - \bar{y} + \bar{z}}{M_f^{in} + 2\bar{x}}} \\
 &= \frac{(H_2^{in} + 3\bar{x} + \bar{y} - \bar{z}) \cdot (CO_2^{in} + \bar{y})}{(CO^{in} + \bar{x} - \bar{y}) \cdot (H_2O^{in} - \bar{x} - \bar{y} + \bar{z})}
 \end{aligned} \tag{2.38}$$

P stands for the reforming pressure which is the ratio of overall pressure over standard pressure. The current could be counted from equation (2.39) if the hydrogen and oxygen are fully reacted.

$$I = 2F \cdot \bar{z} = 4F \cdot O_2^{react} \tag{2.39}$$

It is noted that other consumable gases, like hydrogen and monoxide, are of small portions in the fuel inlet. So the small portions of hydrogen and monoxide can be looked as an equivalent amount of methane. Then the natural gas input is assumed to contain mainly pure methane of  $f_{ng}$  in percentage. So equation (2.40) can be deduced to (2.43). But this  $f_{ng}$  may vary with different gas suppliers. Fuel utilisation factors of the reforming process  $U_f$  is changed with temperature and other parameters. The fuel utilisation factor could be obtained from the experimental test. Hence,  $z$  is confirmed if known hydrogen reaction rate  $U_f$  and anode recirculation rate  $r_a$  according to the deduction of equation (2.40-2.43)

$$\bar{z} = (4 \cdot \alpha_{CH_4}^{in} + \alpha_{H_2}^{in} + \alpha_{CO}^{in}) \cdot U_f \quad (2.40)$$

$$\alpha_{CH_4}^{in} = f_{ng} \cdot \alpha_{ng}^{in} + \alpha_{CH_4}^{out} \cdot r_a = f_{ng} \cdot \alpha_{ng}^{in} + \alpha_{CH_4}^{in} \cdot (1 - U_f) \cdot r_a \quad (2.41)$$

$$\alpha_{CH_4}^{in} = \frac{f_{ng} \cdot \alpha_{ng}^{in}}{1 - r_a + U_f \cdot r_a} \quad (2.42)$$

$$\bar{z} = 4 \cdot \alpha_{CH_4}^{in} \cdot U_f = \frac{4 \cdot U_f \cdot f_{ng} \cdot \alpha_{ng}^{in}}{1 - r_a + U_f \cdot r_a} \quad (2.43)$$

Considering high temperature and rich steam circumstance, assume methane reforming and shifting reaches thermodynamic equilibrium. So, nonlinear equations (2.29-2.31) are applied, which are solved by using the Gauss-Newton method. In the SOFC system model of this thesis, the real time calculation of non-linear equation group may take a long simulation time. Hence, the composition of gas at different temperatures and flux is calculated beforehand. The outcome is imported into a database for the use of the following up dynamic simulation. Figure 2.3 indicates a reforming rate of methane with change of temperature and fuel flow. Figure 2.4 shows the chemical composition of reforming gas when the circulation rate varies. The two figures are calculated based on the 5 (kW) FCT's SOFC system parameters.

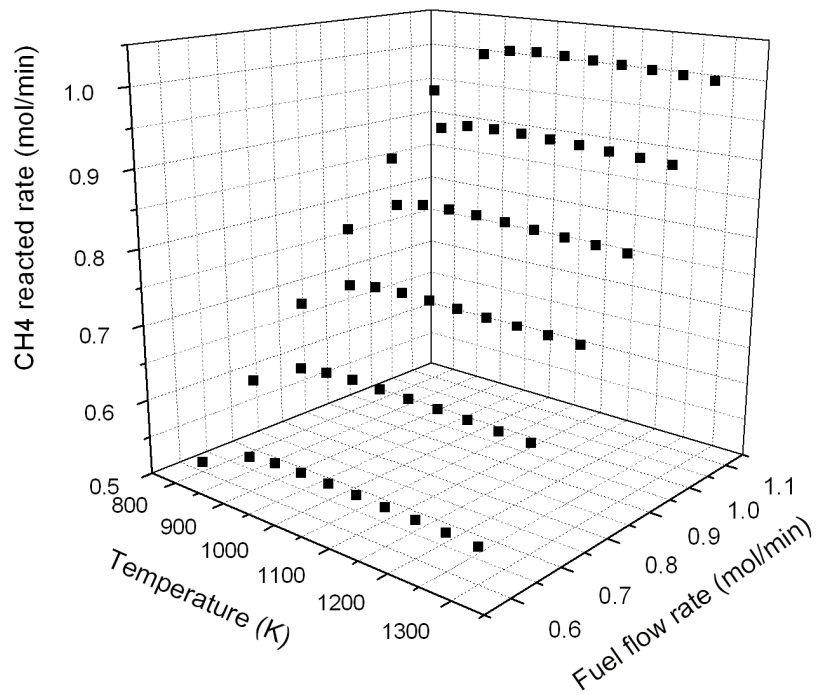


**Figure 2.3:** Methane reacted rate during reforming process

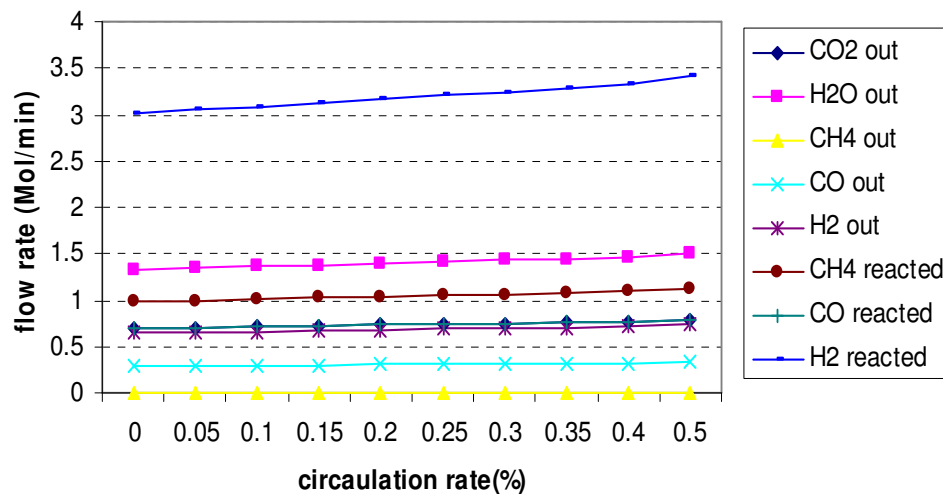


**Figure 2.4:** Reforming gas composition with circulation rate change

## 2.2.4 Modelling of flow, heat transfer and energy balance

To describe the thermal influence within the tubular SOFC stack two aspects, at least, need to be performed. One is the mass flow and heat transfer in the flow channels; another is variation of fuel cell potential field and current caused by electrochemical reaction at electrolyte and electrode. The electrochemical model for a single tubular SOFC has been illustrated in section 2.2.2. This section of modelling will concentrate on chemical reactions of species, heat transfer and energy conservation. To best discover the essence of electrochemical reactions and mass changes inside the fuel cell stack, a finite volume method is the most useful and apparent way to describe this process. The thermal modelling and simulation work in this section is conducted based on the computational fluid dynamics software Fluent®.

From the geometry parameters in table 2.1 and the operating flow speed of reactants of the 5 (kW) SOFC system, the Reynolds number anode flow and cathode flow can be calculated by equation (2.44) where  $u$  is flow velocity,  $\nu$  is fluid viscosity,  $d$  is hydrodynamic diameter of tubular flow channel. The calculation result shows that Reynolds number of anode flow and cathode flow is between 50-2700. It is commonly accepted that laminar flow is defined as those with Reynolds number under 2300 while turbulence flow is with Reynolds number of over 8000. So it is safe to assume flows within the SOFC anode and cathode is laminar flow.

$$Re = \frac{ud}{\nu} \quad (2.44)$$

The flows of reactant gas mixture go through the cathode and anode channel as indicated in figure 2.5. The governing equations for both flow streams are derived from conservation for mass, momentum, heat energy and species. These equations are based on universal laws of hydrodynamics.

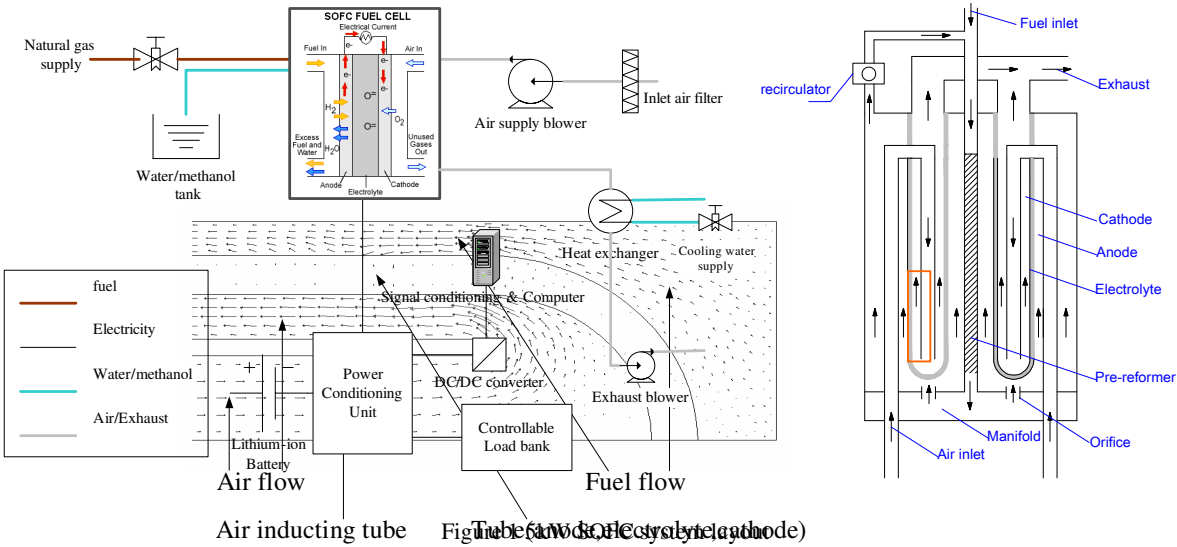


**Figure 2.5: Single tubular SOFC structure**

Mass conservation equation is written as equation (2.45).

$$\frac{\partial \rho}{\partial t} + \frac{\partial(\rho u)}{\partial x} + \frac{\partial(\rho v)}{\partial y} + \frac{\partial(\rho w)}{\partial z} = 0 \quad (2.45)$$

Where  $\rho$  is the density of flow,  $u$   $v$   $w$  are velocities vectors in directions of  $x$   $y$   $z$  coordinates. The conservation equations of flow momentum is shown as equation (2.46-2.48) if define  $\nabla$  as partial derivative for a vector quantity in Cartesian coordinates (Batchelor, 1967).

$$\frac{\partial(\rho u)}{\partial t} + \nabla \cdot (\rho u \vec{u}) = -\frac{\partial p}{\partial x} + \frac{\partial \bar{\tau}_{xx}}{\partial x} + \frac{\partial \bar{\tau}_{yx}}{\partial y} + \frac{\partial \bar{\tau}_{zx}}{\partial z} + F_x \quad (2.46)$$

$$\frac{\partial(\rho v)}{\partial t} + \nabla \cdot (\rho v \vec{u}) = -\frac{\partial p}{\partial y} + \frac{\partial \bar{\tau}_{xy}}{\partial x} + \frac{\partial \bar{\tau}_{yy}}{\partial y} + \frac{\partial \bar{\tau}_{zy}}{\partial z} + F_y \quad (2.47)$$

$$\frac{\partial(\rho w)}{\partial t} + \nabla \cdot (\rho w \vec{u}) = -\frac{\partial p}{\partial z} + \frac{\partial \bar{\tau}_{xz}}{\partial x} + \frac{\partial \bar{\tau}_{yz}}{\partial y} + \frac{\partial \bar{\tau}_{zz}}{\partial z} + F_z \quad (2.48)$$

Where  $p$  is static pressure at finite volume,  $\vec{u}$  is velocity vector,  $\bar{\tau}$  is stress tensor and  $F$  is the body forces.

According to the first law of thermodynamics, the increasing heat energy of a finite volume equals to heat flow plus work done by the body force and face force on the unit. This could lead to energy conservation equation with temperature as a variable quantity.

$$\frac{\partial(\rho T)}{\partial t} + \frac{\partial(\rho u T)}{\partial x} + \frac{\partial(\rho v T)}{\partial y} + \frac{\partial(\rho w T)}{\partial z} = \frac{\partial}{\partial x}\left(\frac{k}{c_p} \frac{\partial T}{\partial x}\right) + \frac{\partial}{\partial y}\left(\frac{k}{c_p} \frac{\partial T}{\partial y}\right) + \frac{\partial}{\partial z}\left(\frac{k}{c_p} \frac{\partial T}{\partial z}\right) + S_T \quad (2.49)$$

Where  $c_p$  is heat capacity,  $k$  is thermal conductivity and  $S_T$  represents the heat of chemical reaction and any other volumetric heat sources.

Species transport is applicable to governing equation (2.50), where  $Y_i$  means local mass fraction of each species.

$$\frac{\partial}{\partial t}(\rho Y_i) + \nabla \cdot (\rho \vec{u} Y_i) = -\nabla \cdot \vec{J}_i + R_i + S_i \quad (2.50)$$

In equation (2.50),  $R_i$  is the net rate of production of species  $i$  by chemical reaction,  $S_i$  is the rate of creation and  $\vec{J}_i$  indicates diffusion flux of species  $i$ .

In laminar flow,  $\vec{J}_i$  is approximately expressed as equation (2.51) during calculation in Fluent®.  $D_{i,m}$  is diffusion coefficient for species  $i$  in the mixture.

$$\vec{J}_i = -\rho D_{i,m} \nabla Y_i \quad (2.51)$$

The following section will introduce, in short, the simulation treatments based on Fluent®.

## Grid messing of flow channel

A single tubular SOFC is an axial symmetrical structure as shown in figure 2.5. If assuming the cross section along the axial bears uniform characteristics, a 2D mess grid with axial symmetry for a single tube is built according to the geometry parameters in table 2.1. There are totally 1500 grid units in axial direction and 64 grids in radial direction being allocated for messing.

## Treatment of tubular structure

From the introduction in section 1.2, the electrolyte is the media to transport the oxygen ion. The nature of the electrolyte is simulated as a porous material, which could let through the ion. The material properties of the anode, cathode, electrolyte and air guide tube are listed in table 2.3.

**Table 2.3: SOFC cell tube materials by layers**

Anode	Nickel cermet
Cathode	Lanthanum manganite
Electrolyte	Yttria stabilized zirconia
Air guide tube	Aluminum alloy
interconnection	Lanthanum chromite

## Settings of computational parameters

The temperature profile of the tubular SOFC model is expressed along an axial direction. The heat transfer within materials as well as heat exchange between solid structure and flows are involved in the modelling. During computation, chemical reaction of species is assumed to reach equilibrium according to the local temperature of each finite volume. It can also assume that the chemical reaction time is quicker than heat transfer time.

As for the tubular structure, the anode, electrolyte and cathode are bonded together. The electro-chemical reactions take place at the surface between electrode and electrolyte.

The ions are transported by high temperature electrolyte. To imitate these phenomena, the material property of the electrolyte membrane is regarded as ‘porous’ and the reaction type of anode and cathode reactions is looked at as ‘surface reaction’.

The temperature profile of the tubular SOFC is modelled according to the nature of the thermal electro-chemical reactions as explained in the above paragraphs. Figure 2.6 is one of the simulation results to describe the temperatures at different sections of the tube along the axial direction. The SOFC tube length is 1.5 metres overall. Where “0” position stands for the geometric symmetry centre of a single tubular SOFC; “0.75” position stands for the close end of the tube; and “- 0.75” stands for the open end of the tube. Some parameters used are listed in table 2.4.

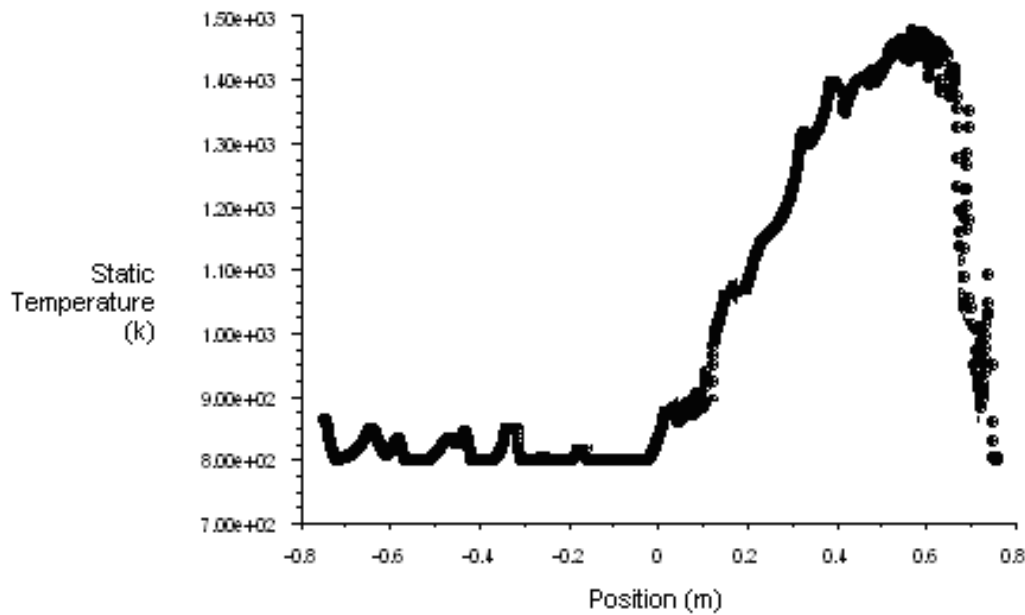


**Figure 2.6: Temperature profiles along the tube length (a)**

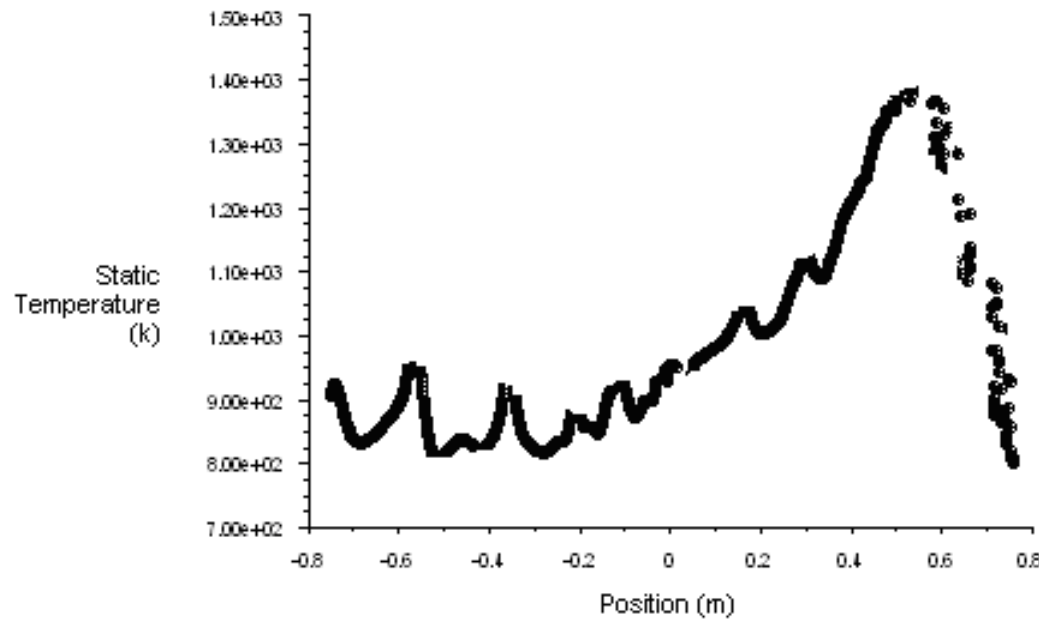


Figure 2.6: Temperature profiles along the tube length (b)

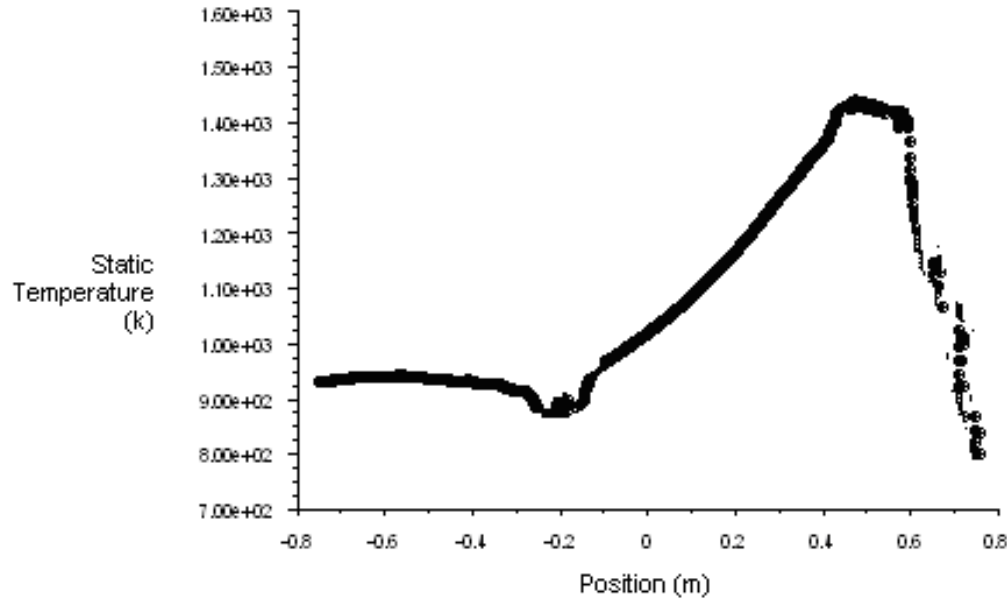


Figure 2.6: Temperature profiles along the tube length (c)

**Table 2.4: Main parameter settings for the computation of figure 2.6**

	Air inlet temp(K)	Air inlet mass flow rate(kg/s)	Fuel inlet temp(K)	Fuel inlet mass flow rate(kg/s)
a	1050	3e <sup>-4</sup>	823	3.5e <sup>-5</sup>
b	973	4e <sup>-4</sup>	973	1.2e <sup>-5</sup>
c	873	4.5e <sup>-4</sup>	1173	2.33e <sup>-6</sup>

From figure 2.6, it is obvious that the most severe temperature change happens at the closed end of the tube. The maximum temperature gradient is about 3500 ( $^{\circ}\text{C}/\text{m}$ ). This temperature gradient will make a large contribution to the thermal stress of the tube materials.

## 2.3 Auxiliary components models for SOFCs

The auxiliary is the most important part of the fuel cell system; its complexity is even higher than the fuel cell stack. The auxiliary subcomponent is also nominated as the balance of plant. In this section, the modelling methods of these subcomponents are introduced. The models are specially developed to reflect their influences on system characteristics.

### 2.3.1 Heat exchanger

A heat exchanger is used to collect the exhaust heat. The collected heat, stored in the form of hot water, takes up a large amount of system energy output. Heat recovery is calculated based on an energy conservation equation.

$$w_{water}c_{water}(T_{water}^{out} - T_{water}^{in}) = \eta_{HE}w_{exh}c_{exh}(T_{exh}^{out} - T_{exh}^{in}) \quad (2.52)$$

### 2.3.2 Burner

The burner is controlled to provide thermal input to heat the fuel cell stack to the operational temperature during start up and to maintain the temperature during system operation. The combustion of hydrogen and carbon monoxide from the exhaust mixture are also counted. It is reasonable to assume that sufficient oxygen is supplied. So, the combustor is simplified to contain two inlet streams from anode and cathode and one stream of exhaust. The reactions are shown as equation (2.53 and 2.55). Because of the diffusion of the burner wall and the condition of burning, the heat value of the reactant could not fully be transferred to useful heat energy. The effective burner, at present, could reach an efficiency of 99%. The burner used in the system is assumed to have an efficiency of 98%. The fuel of the burner is natural gas with a lower heat value of 49.182 (kJ/kg).



### 2.3.3 Battery Modelling

The battery used in the SOFC power system is a lithium-ion battery and is dedicated to continually provide BOP power. During start-up and shutdown of the fuel cell system, while the inverter is not operational, the battery system is charged by the internal battery charger. During inverter operation the battery charger is disabled and the batteries supply power to the BOP when the fuel cell power does not fully satisfy the inverter and BOP power requirements. Once the BOP power requirements have been fully satisfied

by the fuel cell, the batteries are re-charged by the inverter with the remainder of the available fuel cell power.

According to the studies from Paul Nelson et al (2003) a lithium-ion battery can be fitted to an equivalent circuit (figure 2.7) after various model tests. Where the open circuit voltage is conducted by correlating the data from hybrid pulse power characterisation tests and it can be display as equation (2.56).

$$OCV = ax^4 + bx^3 + cx^2 + dx + e \quad (2.56)$$

Where x=SOC% (status of charge); a=-6.052; b=12.554; c=-8.815; d=3.0565; e=3.1655

$$SOC = SOC_{Initial} - \int \frac{I}{C_{battery}} dt \quad (2.57)$$

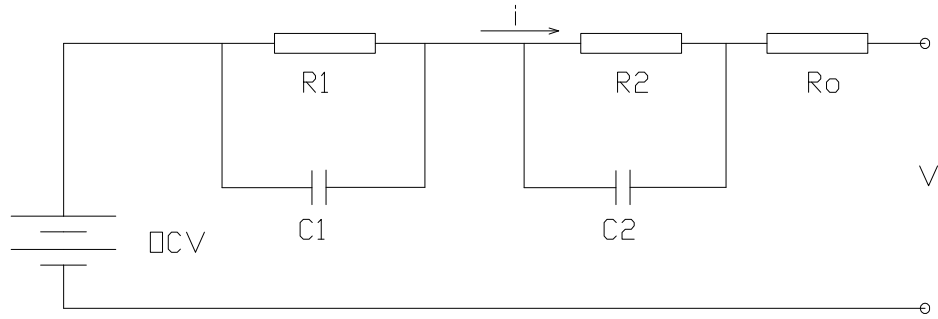


**Figure 2.7: Equivalent open voltage circuit of lithium-ion battery**

Based on the equivalent open voltage circuit diagram in figure 2.7, it is the time domain equation for the circuit is written as equation (2.58):

$$OCV - V = I(R_0 + \frac{R_1}{1+R_1C_1} + \frac{R_2}{1+R_2C_2}) \quad (2.58)$$

When  $I$  reaches the max and min value, the current through  $C_1$  and  $C_2$  is 0, so the limitation of fuel cell stack current is represented as equation (2.59)

$$I_{\min} = \frac{OCV - U_{\max}}{R_0 + R_1 + R_2}$$

$$I_{\max} = \frac{OCV - U_{\min}}{R_0 + R_1 + R_2} \quad (2.59)$$

The modelling of the battery is based on equation (2.56 to 2.59) and the capacity of the battery depends on the number and capacity of battery systems. The modelling details and block diagrams by using MATLAB SIMULINK software are shown in figure 2.8 as direct below.

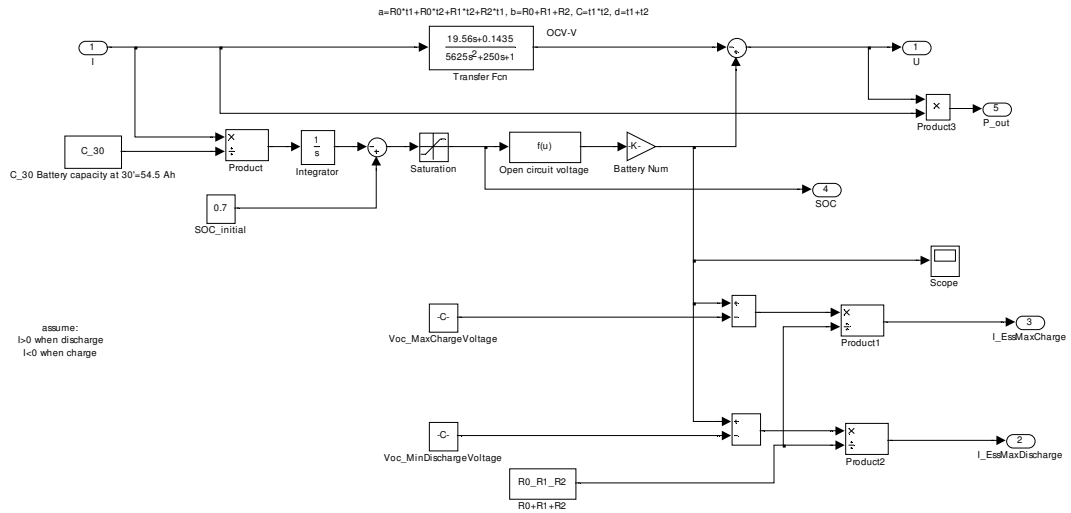


**Figure 2.8: MATLAB SIMULINK block diagram of battery modelling**

### 2.3.4 Power conditioning unit

The function of the power conditioner is to convert the electric energy supply from fuel cell and battery into desired current and voltage to feed the electric propulsion motor.

The power conditioning unit includes the battery and fuel cell power interface, Direct Current to Direct Current (DC/DC) booster, Direct Current to Alternative Current

(DC/AC) converter and control unit. The lithium ion battery and fuel cell electric output are connected in parallel to inverter as indicated in figure 2.1. In this section, the models of DC/DC booster and DC/AC inverter will be introduced.

The electrical output of the SOFC inverter may be connected either to a load or the utility grid. If the SOFC works alone as an AC voltage source, the default output frequency and voltage could be adjusted for the customer's requirements. While working in the grid-tie mode the inverter synchronises to the utility grid frequency and voltage and acts as an AC current source. The range of allowed voltage and frequency drift is limited by tolerance parameters. A control unit within the power conditioning system will be the watchdog of the operating parameters and adjust the output current set point.

The original output signal of the fuel cell stack is high current low voltage. Take the 5 (kW) SOFC for instance, the stack is made of two bundles with each having  $3 \times 8$  tube cells. The open voltage is the serial accumulation of eight times the single cell voltage output. The DC/DC booster is used to increase the voltage output. The circuit diagram of DC/DC boost chopper is shown in figure 2.9.

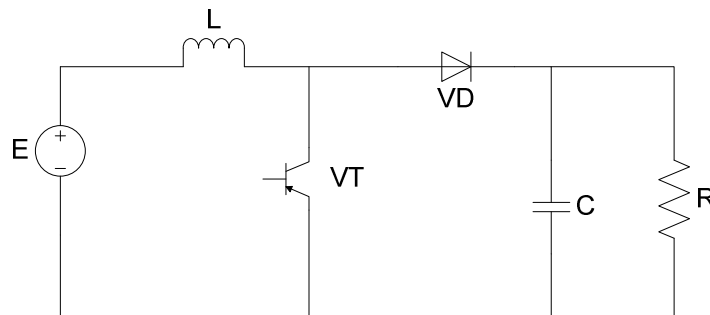


**Figure 2.9: Circuit diagram of DC/DC chopper**

A DC/AC converter is used to further change the DC power to AC power with the required voltage and frequency before parallel electric power to the grid. The principle of DC/AC converter is illustrated in figure 2.10. A Pulse Width Modulation (PWM) generator is used to trigger the Insulated Gate Bipolar Transistor (IGBT) of the universal bridge.

If only considering the steady state performance of the power conditioning unit, the controller's dynamics is neglected. Assuming the inverter works at a constant effective factor, the power output of DC/AC inverter is illustrated as equation (2.60).

$$P_{AC} = \eta_{cov} V_{DC} I_{DC} \quad (2.60)$$

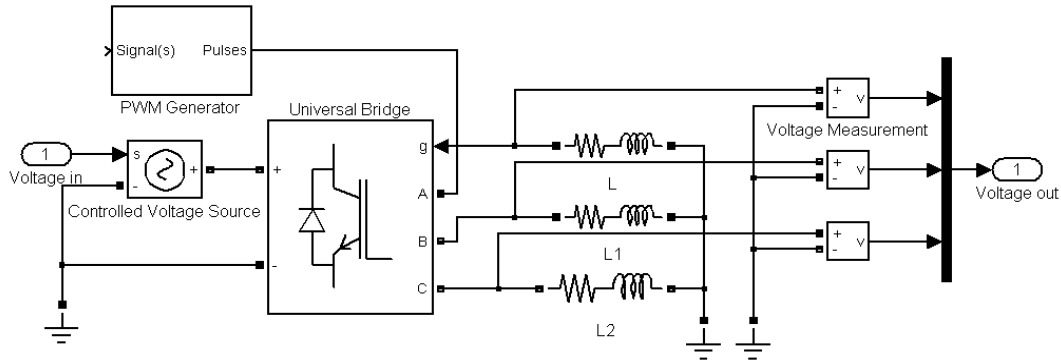


**Figure 2.10: Block model of DC/AC converter**

## 2.4 Modelling of system dynamic response

Quick dynamic response for transient operation of a power system is critical, for instance, a short starting time and quick system response. The response time of the whole system is influenced by not only the delay of reactions inside the fuel cell stack and its supply systems, but also the inertias of mechanical transmission, electrical transforming, chemical reaction, temperature tracking and system control. Previous research (Pukrushpan *et al*, 2005, Guzzella, 1999 and Pischinger *et al*, 2006) shows a response time of electrochemistry reaction of the fuel cell is rapid, in  $10^{-9}$  (seconds) order of magnitude, its influence can be neglected when calculating system time inertia. As seen from table 2.5 the fuel and air flow, mechanical transmission and cell temperature contribute most to the system dynamic inertia hence it should be included in simulation models.

**Table 2.5: Response time of subsystems**

Sub systems	Response time (seconds)
Electrochemistry	$10^{-9}$
Fuel and air manifold	$10^{-1}$
Mechanical and control transmission	$10^1$
Cell and stack temperature	$10^2$

The mechanical and control transmission delay is a constant period of time for a propulsion system and can be easily added to the simulation model. However the response time for manifolds and temperature depend on not only the SOFC structure but also the mass flow of gases. Therefore the modelling of manifold and temperature response will be explained in detail.

#### 2.4.1 Dynamic modelling of anode and cathode inlet manifold

The fuel inlet flows through the reformer and anode manifold as shown in figure 2.11. The pre-reformer is a catalysed reforming device. It could be regarded as a porous structure because the flow rate of natural gas is relatively slow. The flow can be regarded as a laminar flow. In a laminar flow through a porous media, the pressure drop is typically proportional to velocity. Ignoring convective acceleration and diffusion, the porous media model then reduces to Darcy's Law:

$$\frac{\partial p}{\partial x} \hat{i} + \frac{\partial p}{\partial y} \hat{j} + \frac{\partial p}{\partial z} \hat{k} = -\frac{\mu}{\alpha} \vec{v} \quad (2.61)$$

Assume the inlet pipe and reformer is symmetrical. Equation (2.61) could be transformed to equation (2.62) if only considering one direction of fuel flow.

$$\frac{\Delta p}{\Delta x} = -\frac{\mu}{\alpha} v \quad (2.62)$$

$$P_{manifold} - P_{in} = \frac{1}{k_{in}} w_{in} \quad (2.63)$$

Where  $v$  is velocity of fuel inlet and  $k$  is constant. Gas fuel flow rate is proportional to fuel velocity when the geometry of reformer flow channel is cylinder like. So, it is safe to change equation (2.62) to equation (2.63) where  $k_{in}$  is constant and  $w_{in}$  is flow rate of fuel inlet.

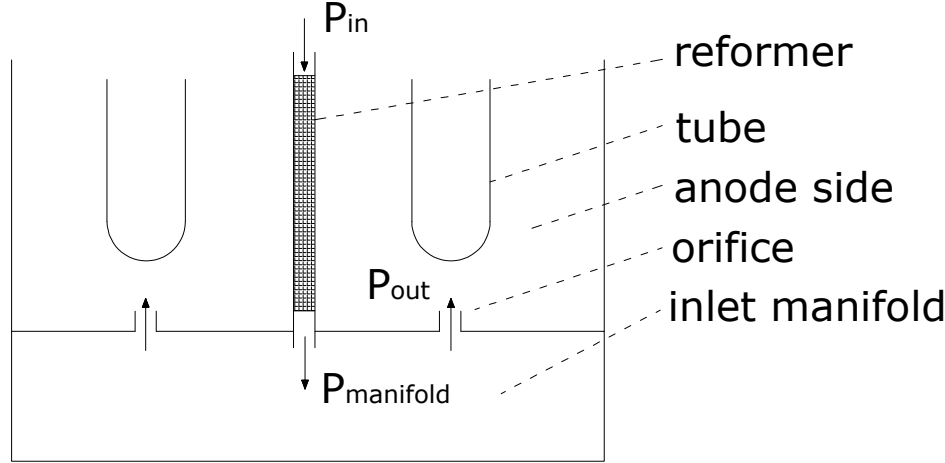


**Figure 2.11: Anode fuel flow diagram**

For any mass flow, the mass conservation is used although reforming reactions happen. If assume that the temperature in the manifold is constant at a certain period time, equation (2.64) is applied. Where  $w$  denotes the flow rate of fuel.

$$\frac{dm}{dt} = w_{in} - w_{out} \quad (2.64)$$

Among the manifold equation, Let  $C_{mix} = RT/V$  where  $V$  is volume of the manifold, then:

$$\frac{dp}{dt} = \frac{R_{mix} T}{V} (w_{in} - w_{out}) = C_{mix} \cdot (w_{in} - w_{out}) \quad (2.65)$$

Because the pressure differences between anode manifold and anode is small, flow rate is expressed linearly from nozzle flow equation as equation (2.66):

$$w_{out} = k_{out} (p_{manifold} - p_{out}) \quad (2.66)$$

From equation (2.64-2.66), we could produce equation (2.67).

$$\frac{1}{C_{mix}} \cdot \frac{dp_{manifold}}{dt} = (k_{out} + k_{in}) \cdot p_{manifold} - (k_{out} p_{out} + k_{in} p_{in}) \quad (2.67)$$

In order to simulate the dynamic response of the time delay in the manifold, transfer function method is applied. A transfer function is a mathematical representation of the relations between input and output of a linear time invariant system with zero initial conditions and zero-point equilibrium. Transfer function method is commonly used in the analysis of system with single input and single output.

According to equation 2.67, if assumes the input and output of the transfer function as:

*Input :*  $(k_{out} p_{out} + k_{in} p_{in})$

*output :*  $p_{manifold}$

Then laplace transform equation (2.67) gives equation (2.68).

$$\frac{1}{C_{mix}} \cdot sP(s) = (k_{out} + k_{in}) \cdot P(s) - I(s) \quad (2.68)$$

Where  $P(s)$  is the output of the transfer function and  $I(s)$  is the input of the transfer function. So, transfer function of anode flow throw reformer and manifold could be represented as equation (2.69)

$$\frac{P(s)}{I(s)} = \frac{-1}{\frac{1}{C_{mix}} \cdot S - (k_{out} + k_{in})} = \frac{\frac{1}{k_{out} + k_{in}}}{\frac{-1}{C_{mix} \cdot (k_{out} + k_{in})} \cdot S + 1} \quad (2.69)$$

Equation (2.69) is a typical first-order response system with time constant  $\tau$ .

$$\tau_{manifold} = \frac{-1}{C_{mix} \cdot (k_{out} + k_{in})} = \frac{-V}{R_{mix} T (k_{out} + k_{in})} \quad (2.70)$$

If considering a 5% error difference to the final value, then the time to reach this limitation of 95% of its desired control value is 3 times  $\tau_{manifold}$ . The time domain response for a step input change of this reformer and manifold flow channel is shown as figure 2.12. As can be seen from equation (2.70) the time constant for manifold will be different with temperature changes of gases flowing through the manifold channel.

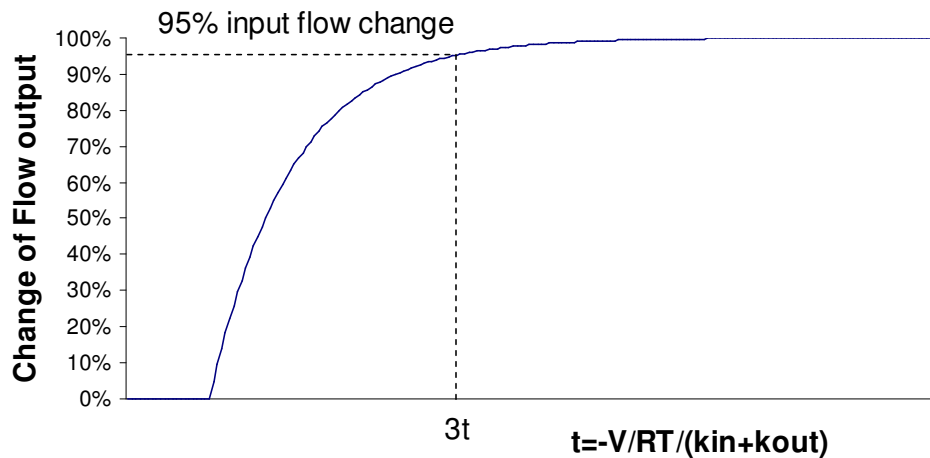


**Figure 2.12: Output flow rate change of reformer and manifold after an input step change**

#### 2.4.2 Temperature response time of fuel cell stack

As discussed in section 2.4, cell and stack temperature change take the largest share of system response time. The thermal capacity of fuel cell stack would affect the time delay of system power output. This section will explain how to simulate this influence.

In practice, temperatures at different parts of the stack are not identical. However, it is applicable to assume an identical stack temperature  $T_{stack}$  if feedback control is applied during the modelling of the stack temperature response. Because the feedback controller could compensate the accuracy problem during real time control. The block diagram of stack temperature model is shown in figure 2.13 while the feedback control is discussed in chapter 5.

As indicated in figure 2.13, the fuel inlet and air inlet, after passing through manifolds, will bring an amount of heat to the SOFC stack respectively. The reactions taking place in the stack will also release heat into the SOFC stack. On the other hand, exhaust gases and ambient media would take away a certain amount of heat from the stack.

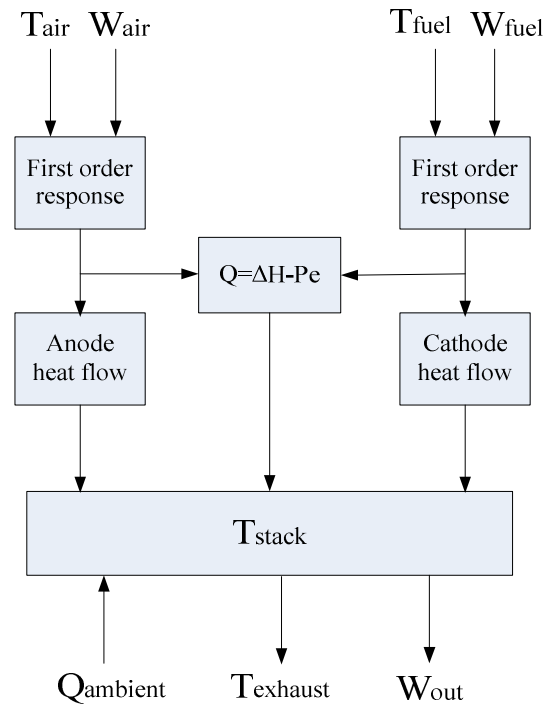


**Figure 2.13: Block diagram of stack temperature control**

According to energy conservation, equation (2.71) represents the energy balance of the fuel cell stack, where  $C$  is the thermal capacity of elements inside the fuel cell stack, like air, fuel and stack structure. Where  $c$  represent the specific heat capacity of each elements.  $H_{react}$  denotes enthalpy change of chemical reaction and  $P_e$  is the stack electricity output.  $T_{air}$   $T_{fuel}$   $T_{stack}$   $T_{exhaust}$  means temperatures at the air inlet, fuel inlet, stack and exhaust respectively.

$$(C_{fuel} + C_{air} + C_{stack}) \frac{dT_{stack}}{dt} = Q_{air} + Q_{fuel} + Q_{react} + Q_{ambient} + Q_{exhaust} \quad (2.71)$$

$$Q_{air} = w_{air} c_{air} (T_{air} - T_{stack}) \quad (2.72)$$

$$Q_{fuel} = w_{fuel} c_{fuel} (T_{fuel} - T_{stack}) \quad (2.73)$$

$$Q_{react} = \Delta H_{react} - P_e \quad (2.74)$$

$$Q_{exhaust} = w_{out} c_{exhaust} (T_{stack} - T_{exhaust}) \quad (2.75)$$

$$C_{fuel} = m_{fuel} \cdot c_{fuel} \quad (2.76)$$

$$C_{air} = m_{air} \cdot c_{air} \quad (2.77)$$

$$C_{stack} = m_{tube} \cdot n_{cell} \cdot c_{cell} \quad (2.78)$$

If  $C_{SOFC} = C_{fuel} + C_{air} + C_{stack}$ , then equation (2.71) is changed to equation (2.79), which could illustrate the dynamic thermal state of the fuel cell stack.

$$\begin{aligned} C_{SOFC} \frac{dT_{stack}}{dt} &= (w_{out} c_{exhaust} - w_{air} c_{air} - w_{fuel} c_{fuel}) T_{stack} \\ &+ w_{air} c_{air} T_{air} + w_{fuel} c_{fuel} T_{fuel} - w_{out} c_{exhaust} T_{exhaust} + Q_{react} + Q_{ambient} \end{aligned} \quad (2.79)$$

If using the state space method to describe control relationships, the state space form of the model is re-written as equation (2.80-2.86)

$$\begin{aligned}\dot{X} &= AX + Bu \\ y &= CX + Du\end{aligned}\tag{2.80}$$

$$\begin{aligned}\dot{X} &= \frac{dT_{stack}}{dt} \\ X &= T_{stack}\end{aligned}\tag{2.81}$$

$$u = \begin{bmatrix} T_{air} \cdot w_{air} \\ T_{fuel} \cdot w_{fuel} \\ T_{exhaust} \cdot w_{out} \\ Q_{react} \\ Q_{ambient} \end{bmatrix}\tag{2.82}$$

$$A = \frac{w_{out}C_{exhaust} - w_{air}C_{air} - w_{fuel}C_{fuel}}{C_{SOFC}} \text{ (negative value)}\tag{2.83}$$

$$B = \begin{bmatrix} \frac{c_{air}}{C_{SOFC}} & \frac{c_{fuel}}{C_{SOFC}} & \frac{c_{exhaust}}{C_{SOFC}} & \frac{1}{C_{SOFC}} & \frac{1}{C_{SOFC}} \end{bmatrix}\tag{2.84}$$

$$C = 1\tag{2.85}$$

$$D = [0 \ 0 \ 0 \ 0 \ 0]\tag{2.86}$$

So, the combined control block diagram is shown in figure 2.14.

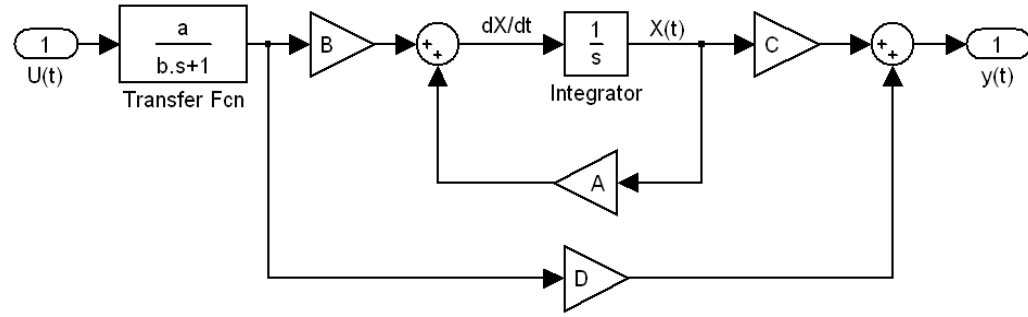


**Figure 2.14: Control block diagram of fuel cell stack thermal model**

If transferring state space system to transfer function by analysis, equation (2.87) is used.

$$Y(s) = C(sI - A)^{-1} B U(s) \quad (2.87)$$

Considered fuel flow rate input has a step change then the time constant for stack temperature change is:

$$\tau_{Stack} = \frac{1}{A} = \frac{C_{SOFC}}{w_{out}c_{exhaust} - w_{air}c_{air} - w_{fuel}c_{fuel}} \quad (2.88)$$

According to figure 2.11, the combined system response model is a multi-input and single output system if we looked at  $T_{stack}$  as a state variable as well as output. When we assume the system response is under single input change, then the system can be transferred to a second order system. The transfer function could be written in the following form, as equation (2.89). Hence, the time delays of temperature response and manifold response could be expressed in this model if  $\tau_{stack}$  and  $\tau_{manifold}$  are identified.

$$\frac{Output}{Input} = \frac{G_{manifold}}{\tau_{manifold} \cdot s + 1} \cdot \frac{G_{stack}}{\tau_{stack} \cdot s + 1} \quad (2.89)$$

Beside the influence of stack temperature response, the limitation of temperature gradient for tubular structure also needs to be addressed, because the material for

tubular structure could only withstand certain temperature differences. The tubular fuel cell in this system is a cathode supported type. The strength of tube structure has a strong relationship with thermal stress caused by temperature difference at local sections along the tube structure. The discussion of the temperature gradient along the tube structure has been expressed in section 2.2.4. The simulation results will be used as limiting conditions for calculating the temperature response time of the whole system, especially when ascertaining the starting time for the SOFC system.

## 2.5 Summary and conclusion

Modelling of whole SOFC power system is a complicated issue. The accuracy of system simulation depends on the precise modelling of subcomponents within the system. Modelling of subcomponents in the SOFC system was introduced in this chapter. The stack was modelled according to the thermodynamic reactions taking place within a single cell. The reforming and pre-reforming processes of methane rich natural gas was described with an assumption that reforming reactions reach equilibrium. The mass flow and heat transfer model was built up based on CFD theory. The computation work of mass flow and heat transfer were done in advance and the results used directly in the follow up system simulation because the computation of the CFD model is time consuming.

To imitate the dynamic response of the SOFC power system, control theory is implemented to describe the response time of the combined system model. The response time of the stack temperature and mass flow contribute most to system time inertia. Thus, these two phenomena are modelled in detail.

After interpretation of subcomponents' modelling within the SOFC system, the development of the combined model for the whole SOFC power system will be presented in the next chapter.

## Chapter 3 SOFC marine power system and its modelling strategy

### 3.1 Introduction

To simulate a marine SOFC power system, either for ship propulsion or electricity generation, the influence of electric and mechanical load has to be incorporated. This includes modelling works for ship hull resistance, propeller, electric motor and electric load where applicable.

In this chapter, modelling of a ship propulsion system is proposed first. The second part of this chapter will emphasise on the simulations of the SOFC power control unit and electric output distribution. The layout of a marine SOFC power system control strategy will also be explained.

### 3.2 Modelling of ship propulsion systems and driving chain

#### 3.2.1 Propulsion and ship resistance modelling

A typical marine electrical propulsion assembly consists of motor, hull resistance, and propeller. If only considering horizontal movement of the ship and the rotation of rotors, then:

$$2\pi I \frac{dn}{dt} = T_e - T_p - T_f \quad (3.1)$$

$$m \frac{dV_s}{dt} = P - R_t \quad (3.2)$$

Where  $I$  is the rotation inertia of motor, shaft gear and propeller;  $T_e$  is the driving torque of motor;  $T_p$  is the resistant torque from propeller and hydrodynamic force;  $T_f$  represent the friction torque from transmission system;  $m$  is the mass of ship;  $P$  is the propeller driving force;  $R_t$  is the hull resistant.

According to the operation principle of propeller,  $T_p$  and  $P$  are illustrated as equation (3.3 and 3.4) (Harvld, 1983). Where  $D$  is the diameter of the proper:

$$T_p = K_q \rho n^2 D^5 \quad (3.3)$$

$$P = K_t \rho n^2 D^4 (1-t) \quad (3.4)$$

$t$  is the propulsion force deduction factor

$K_t$ ,  $K_q$  and  $\eta$  are displayed over  $J$ , which are obtained from the curves of open water test of propeller series. The advance number  $J$  is defined as:

$$J = \frac{V_A}{nD} = \frac{V_s(1-\omega)}{nD} \quad (3.5)$$

$V_A$  is the average inflow speed,  $V_s$  is ship speed,  $\omega$  is wake fraction.

In order to calculate the ship speed in equation (3.2) the numerical values of  $P$  and  $R_t$  need to be confirmed in real time. The propeller driving force  $P$  is a function of shaft rotation as indicated in equation (3.4).  $R_t$  is related to ship speed. Consequently, if electric motor torque is confirmed then the ship speed can be deducted accordingly.

### 3.2.2 Electric motor drive chain

Electricity output of the fuel cell is direct current. As indicated in figure 2.1, the fuel cell electric power output is connected to the power conditioning unit which is used to change the form of electric power to either AC or DC current. The converted electricity is consumed by various electric loads e.g. propulsion motor. Generally, the propulsion motor could be either a DC machine or an AC machine. Therefore, models for two typical electric motors/machines are introduced in this section, one is a separately excited DC machine and the other is a permanent magnet synchronous AC machine. The control model of the electric machine will also be discussed.

### 3.2.2.1 Separately excited DC machine

A typical model of a separately excited DC machine includes import and export interfaces of field, armature and torque terminals.

The armature circuit of a DC machine consists of an inductor  $L_a$  and resistor  $R_a$  in series and a Counter-Electromotive Force (CEMF); while the field circuit could be represented by an RL circuit.

The CEMF is proportional to the machine rotate speed.

$$CEMF = K_E \cdot \omega_e \quad (3.6)$$

$K_E$  is the voltage constant and  $\omega_e$  is the motor rotation speed.

In a separately excited DC machine model, the voltage constant  $K_E$  is proportional to the field current  $I_f$ :

$$K_E = L_{af} \cdot I_f \quad (3.7)$$

where  $L_{af}$  is the field-armature mutual inductance.

The electromechanical torque developed by the DC machine is proportional to the armature current  $I_a$ .

$$T_e = K_T \cdot I_a \quad (3.8)$$

where  $K_T$  is the torque constant.

The torque constant is equal to the voltage constant.

$$K_T = K_E \quad (3.9)$$

The mechanical parts of DC machine is represented by the equation

$$J_e \frac{d\omega}{dt} = T_e - T_L - B_m \omega - T_f \quad (3.10)$$

where  $J_e$  = inertia,  $T_L$  = torque applied to the shaft,  $B_m$  = viscous friction coefficient, and  $T_f$  = Coulomb friction torque.(Permanent magnet synchronous machine, 2008)

### 3.2.2.2 Permanent Magnet Synchronous Machine

The Permanent Magnet Synchronous Machine model is derived from a second-order state-space model. It is assumed that the flux established by the permanent magnets in the stator is sinusoidal, which implies that the electromotive forces are sinusoidal.

The following equations are implemented for a sinusoidal model as explained above. These equations are expressed in the rotor reference frame, where all quantities in the rotor reference frame are referred to the stator.

$$\frac{d}{dt}i_d = \frac{1}{L_d}v_d - \frac{R}{L_d}i_d + \frac{L_q}{L_d}p\omega_r i_q \quad (3.11)$$

$$\frac{d}{dt}i_q = \frac{1}{L_q}v_q - \frac{R}{L_q}i_q - \frac{L_d}{L_q}p\omega_r i_d - \frac{\lambda p\omega_r}{L_q} \quad (3.12)$$

$$T_e = 1.5p[\lambda i_q + (L_d - L_q)i_d i_q] \quad (3.13)$$

$L_q$ ,  $L_d$  refer to q and d axis inductances;  $R$  is resistance of the stator windings;  $i_q$ ,  $i_d$  are q and d axis currents;  $v_q$ ,  $v_d$  represent q and d axis voltages;  $\omega_r$  is angular velocity of the rotor;  $\lambda$  means amplitude of the flux induced by the permanent magnets of the rotor in the stator phases;  $p$  is number of pole pairs;  $T_e$  means electromagnetic torque.

The  $L_q$  and  $L_d$  inductances represent the relation between the phase inductance and the rotor position due to the saliency of the rotor.

The mechanical principle of permanent magnet synchronous machine is illustrated by equation (3.14)

$$J_e \frac{d\omega}{dt} = T_e - F\omega - T_m \quad (3.14)$$

$T_m$  is shaft mechanical torque and  $F$  is combined viscous friction of rotor and load.

### 3.2.2.3 Drive chain and motor control

It can be seen (from equation 3.10 and 3.14) that the mechanical principle of electric motor is similar both for DC and AC machines. The motor rotation speed can be deduced if the shaft torque and electromagnetic torque is confirmed. The shaft mechanical torque comes from loads of propeller and propulsion shaft, while electromagnetic torque is decided by power supply of electric motor.

Generally, electric motor speed and torque are controlled by altering voltage, current and frequency or a combination of them depending on type of motor. The following is an explanation of control of AC permanent magnet synchronous motor as indicated in figure 3.1.

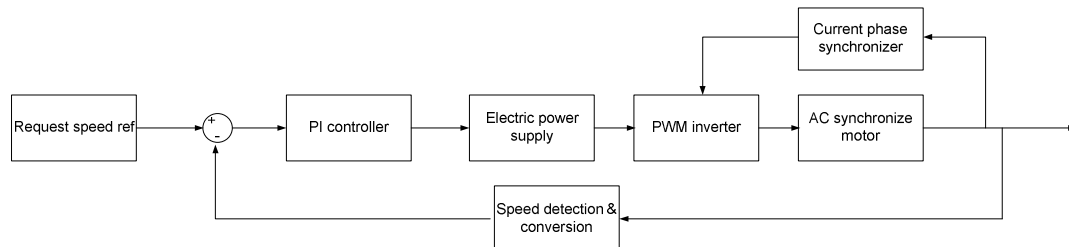


**Figure 3.1: Control diagram of AC permanent magnet synchronous motor**

The Permanent Magnet Synchronous Machine is controlled with a closed loop control system. A PWM inverter is used to convert the DC electric power supply from fuel cells to AC current to feed the synchronize motor. Two feedback controls are used; the inner loop synchronizes the pulses of the PWM converter with the electromotive forces, and the outer feedback control loop regulates the motor's speed, by varying the voltage of DC power bus supply.

As shown in figure 3.1, when a ship speed command is accepted, the required ship speed is translated as a certain amount of voltage accordingly. The reference speed is compared with the feedback from motor shaft and then implemented by Proportional-Integral (PI) feedback control to adjust the electric power distribution for the motor. The inner loop feedback control is to synchronize the current phase by monitoring the electric rotor angle and stator current.

Further, the electric motor is connected with the propulsion device. The calculation of ship speed is indicated as figure 3.2. The equations used for calculations are introduced in section 3.2.1.

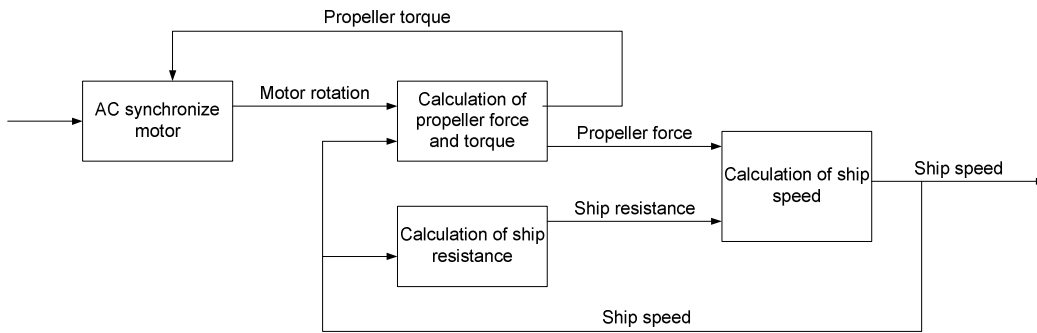


**Figure 3.2: Block diagram of drive chain for propulsion**

### 3.3 Grid bus modelling and power distribution

In a SOFC power system, the fuel cell stack and battery are employed to jointly provide electric power to a grid bus to feed electric load. Fuel cells, battery and power consuming devices are all connected to a main grid bus. Hence, the voltages of fuel cell, battery and power output are the same. The electric power produced by each device is comparative to the electric currency respectively. When the power supplied by the fuel cell stack meets the electric energy consumption, the grid bus will supply enough energy to the electric load and simultaneously charge the battery. Conversely, the grid bus will absorb the electric energy from both the fuel cell and battery to power the electric load when the energy consumption of the power system overtops the capacity of the fuel cell stack.

In addition, the maximum output of the grid bus should be limited by the Status Of Charge (SOC) of the battery. The battery discharges only when its SOC is bigger than the lower limit which is represented as SOC\_min. So, the maximum and minimum power provided can be confined by the following conditions:

$$P_{bus}^{\max} = V_{bus} (I_{FC}^{\max} + I_{disch \arg e}^{\max}) \quad \text{when (SOC>SOC\_min)} \quad (3.15)$$

$$P_{bus}^{\max} = V_{bus} \cdot I_{FC}^{\max} \quad \text{when (SOC=SOC\_min)} \quad (3.16)$$

$$P_{bus}^{\min} = V_{bus} \cdot I_{ch \arg e}^{\max} \quad \text{when (SOC<SOC\_max)} \quad (3.17)$$

$$P_{bus}^{\min} = 0 \quad \text{when (SOC=SOC\_max)} \quad (3.18)$$

According to the above explanation regarding integrating control strategy and limiting conditions, the logic topology of current distribution strategy for the grid bus is expressed by diagram figure 3.3.

As seen from the diagram, the total current of power consumption is monitored in real time and the battery charging status is also identified. The status and output of fuel cell and battery will be controlled based on the grid bus control strategy.

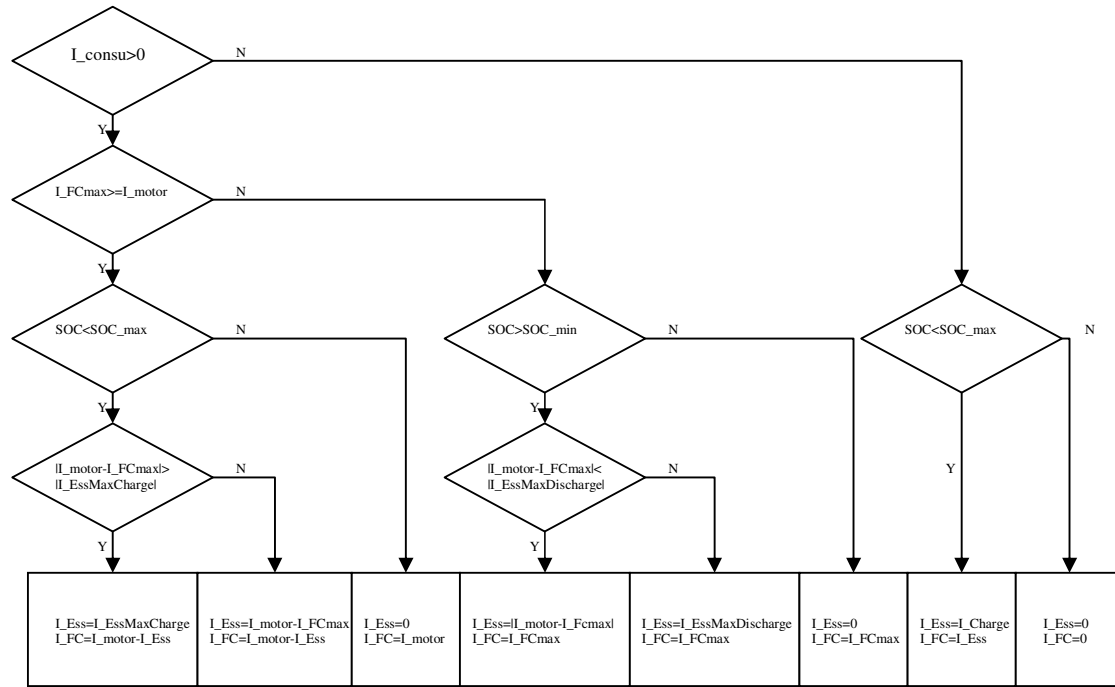


**Figure 3.3: Current distribution strategy of power bus**

### 3.4 SOFC power system modelling strategy

SOFC power system modelling is an integration process to combine subcomponent models by complying with a certain strategy. The integration approach can be roughly divided into the following steps.

- Analysis of system requirement: End user's expectations for system performance including characters of power system, control accuracy, steady and dynamic response, environmental conditions and load limit etc. These aspects should comply with relevant ship rules and regulations where applicable.
- System design and configuration: Based on the requirement in (a), a detailed simulation system is designed by choosing appropriate subcomponent models. The configuration of each subcomponent model needs to also be aligned with the operation

requirements. Simulation time also needs to be optimized. This is fulfilled by choosing some simplified subcomponents while not touching the bottom line of system accuracy.

- c) Testing of subcomponent models: Before reaching system integration, the performance of the subcomponent model shall be tested. This includes the limits and requirements for each model and dynamic response test of the fuel cell stack.
- d) Design of control strategy: To mimic the fuel cell power system the logical control relations and interactions among subcomponents should be well considered. Control flow charts are used to document control relations within the power system.
- e) System integration and simulation test: Combine the subcomponent models according to the designed control logic. Run the simulation system under steady and dynamic conditions. During testing, the requirements and limits for the system objectives, as mentioned in (a), should be covered.

As mentioned in section 3.4 (b), SOFC power system modelling is an integration of subcomponent models with a desired system control strategy. Generally speaking, detailed analytical models, either 2D or 3D, show better simulation results than simplified models. However it is also obvious that a complex model takes more computational time than does a simple one. So, it is unwise and impossible to combine all detailed models of subcomponents as a whole especially when trying to discover system operational aspects. Consequently, some subcomponents of the system are detailed, such as reactions within the cell, mass flow, heat transfer and reforming process; while some auxiliary subcomponents are simplified. The compromise of system complexity is based on the discretions of the system designer and his prospect of computational outcomes.

In the following chapters, simulation of the SOFC power system is performed under different operating scenarios. To achieve the best simulation results, some subcomponent models are simplified and some subcomponents are detailed. The configurations of system models are listed in table 3.1.

**Table 3.1: Composition of integrated SOFC power system**

	Stack steady	Stack starting	Stack dynamic	SOFC power system	SOFC propulsion system
SOFC stack	Detailed	Simplified	Detailed	Detailed	Detailed
Reforming process	Detailed	Simplified	Simplified	Simplified	Simplified
Heat exchanger & burner	Detailed	Simplified	Simplified	Simplified	Simplified
Heat transfer & energy balance	Detailed	Detailed	Simplified	Simplified	Simplified
Manifold	Simplified	Detailed	Detailed	Detailed	Detailed
battery	N/A	N/A	N/A	Detailed	Detailed
Power conditioning	N/A	N/A	N/A	Detailed	Simplified
Propulsion train	N/A	N/A	N/A	N/A	Detailed
Control system	N/A	N/A	N/A	Detailed	Detailed

### 3.5 Summary and conclusion

In a SOFC power system, the SOFC and battery are the sources where electric power is generated. The generated power output is then accumulated to feed electricity consumption devices via a grid bus. The electricity consumption can be a simple electric load or a complicated electric propulsion system. Following the introduction of the SOFC stack model in chapter 2, this chapter proposes modelling methods for the simulation of a ship propulsion system and grid bus.

With all the subcomponent models in hand, it is possible to finally construct a system model for a SOFC power system. The integration work of system models needs to be optimized to obtain the best perspective results. This process depends highly on the strategy of system configuration and the complexity of models. Consequently, the principle for SOFC power system integration has been concluded by different application scenarios.

By applying the system modelling strategy as explained in section 3.4, simulation examples for SOFC power systems under both steady state and dynamic state will be presented in the following chapters.

## Chapter 4 Modeling of a 5 (kW) SOFC at steady state

The modelling process for a SOFC power system was introduced in chapter 2 and 3. In this chapter an example of a 5 (kW) SOFC power system is simulated by using the methods mentioned in chapter 3. The target 5 (kW) SOFC systems will be introduced first, followed by configuration of subcomponents and integration of the system model. The simulation system will be run at steady state to discover how the system alone would perform under different loads. With the intention of marine application, the simulation results are analysed to identify compliance with marine ship rules.

### 4.1 The 5 (kW) SOFC power system

A fuel cell marine power system is a novel innovation without much experience from traditional marine power systems. The components of marine fuel cell systems are coupled both electrically and mechanically. The main purposes for marine fuel cell systems are to drive ship propulsion and supply electric power for auxiliary consumption. In the simulation example, a 5 (kW)/ 2.6 (kWe) SOFC is used as the target system for electricity generation purposes.

The prototype 5 (kW) SOFC is produced by a FCT Alfa system. The system layout and appearance are illustrated as figure 4.1 and 4.2.

The FCT 5 (kW) SOFC is a type of high temperature fuel cell operating at 700 to 1000 ( $^{\circ}\text{C}$ ). Fuel is pre-reformed internally by a catalysed reformer before entering the stack. The pre-reformed fuel then goes into the anode which is at the outer side of a SOFC tube. At the other end, air is pumped into the SOFC stack from the bottom side and heated up while the air travels towards the air manifold at the top of the stack. The heated air then enters the inner side of SOFC tube which is a cathode. After reaction, the high temperature exhaust gas from both the anode and cathode is used to heat up the SOFC stack and let off the system. The exhaust gas heat is further collected by a heat exchanger.

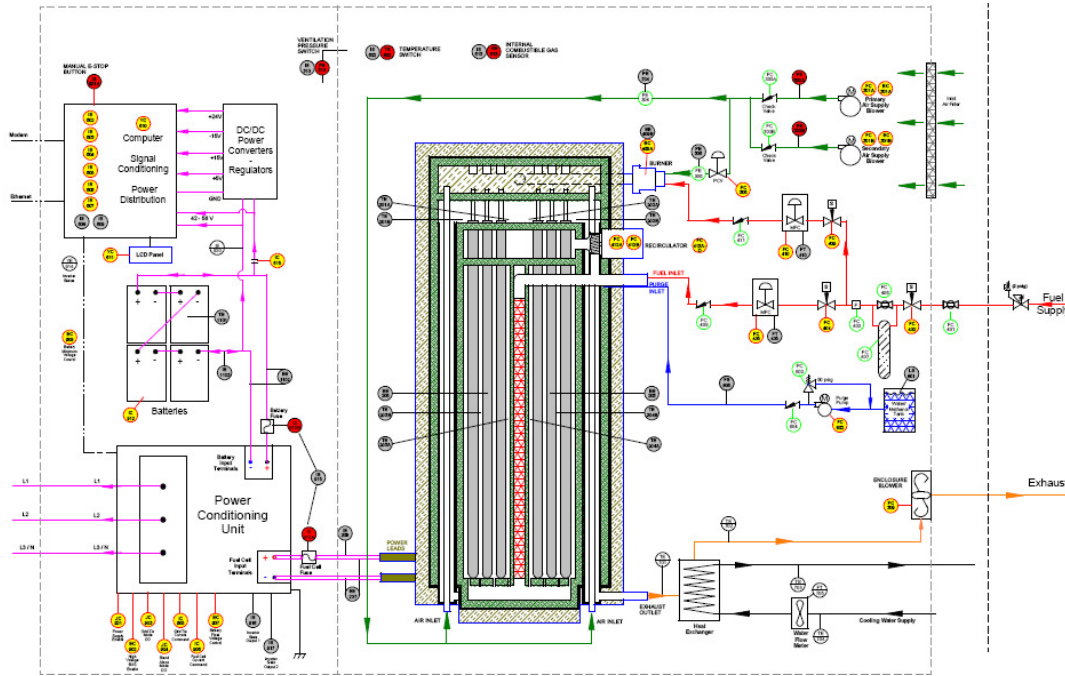


Figure 4.1: 5 (kW) SOFC lay out

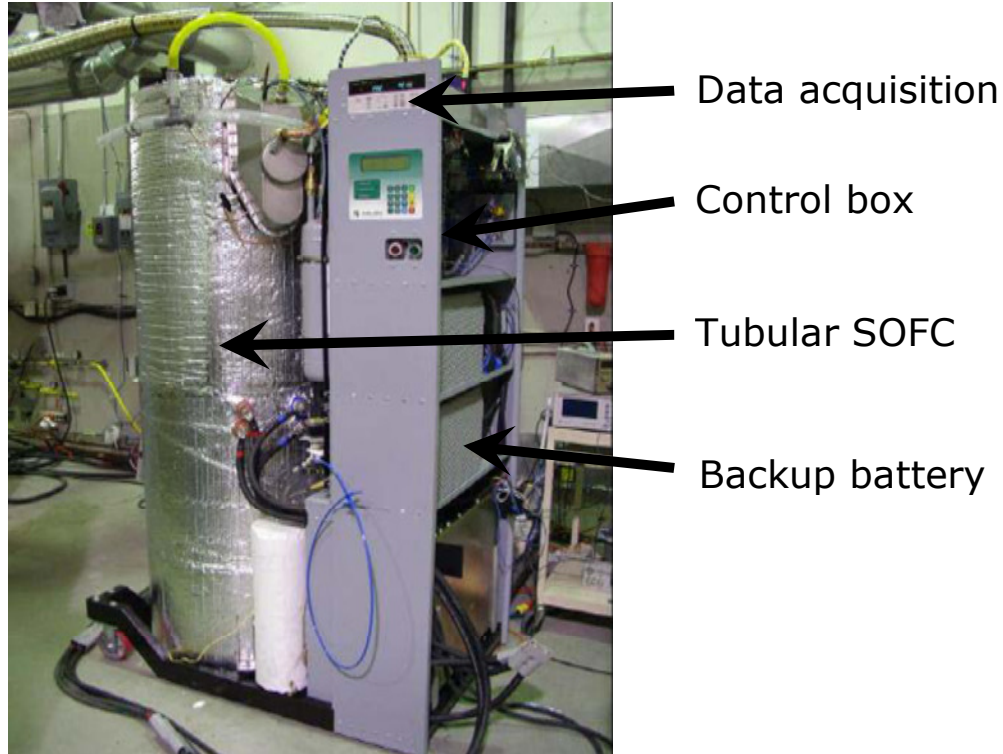


Figure 4.2: FCT 5 (kW) SOFC system outlook

FCT has produced two generations of 5 (kW) system. The first delivery of FCT 5 (kW) Alpha system started in May 2003. The current FCT Beta system was first manufactured at the end of 2004. The main technical data of the 5 (kW) Beta unit is as table 4.1 (Operation and maintenance manual Beta 5 kW SOFC system, 2005).

**Table 4.1: Characteristics of the 5 (kW) SOFC Beta system**

Nominal Electrical Power Output:		2.6 (kWe), 120(Volts) AC, Split Phase, 60 (Hz) (100V, 50Hz, & 3-Phase output optional)
Nominal Thermal Output:		2.8 (kW)
Input Fuel:	Type:	Natural Gas
	Consumption:	1.2 (m <sup>3</sup> /h)
	Supply Pressure:	14 to 34 (kPa)
Air/Exhaust:	Flow Rate:	200 to 1200 (l/min)
	Exhaust Gases:	O <sub>2</sub> (5%), CO <sub>2</sub> (2.5%), NO <sub>x</sub> (< 0.2 ppm), CO (<1 ppm), SO <sub>4</sub> (< 3 ppb), Balance N <sub>2</sub> & H <sub>2</sub> O
	Ventilation Air Flow Rate:	7000 (l/min)
Coolant:	Pressure:	Maximum 375 (kPa)
	Temperature:	Maximum 90 (°C)
	Flow Rate:	3 to 10 (l/min)
	Medium:	Clean Water (less than 5 micron particle size)
Dimensions:	Width:	1253 (mm)
	Depth:	821(mm)
	Height:	2210 (mm)
Weight:		1110 (kg)
Operating temperature ambient:		-5 to +40 (°C)
Warming up time		16 (hours)

## 4.2 Configuration of subcomponent models

As explained in section 3.4, to model the SOFC performance at a steady state, the fuel cell stack model, reforming process and energy balance have to be considered in detail.

a) Fuel cell stack: the 5 (kW) SOFC comprises two bundles of tubular SOFCs. The tubular cell is standard Siemens tube and each bundle has  $3 \times 8$  tubular cells. Two bundles of tubes are placed in parallel with 48 cells in total. The modelling equations used for SOFC stack is explained in section 2.2.2. Stack voltage is calculated as the equation (2.4-2.22). The inputs for stack voltage calculation are net current density  $i$  and stack temperature  $T_{stack}$ . Factors and coefficients used are listed in table 4.2. Other relevant configurations are expressed in the context of section 2.2.2

**Table 4.2: Parameter settings for 5 (kW) SOFC stack**

Type of SOFC	Siemens standard tubular SOFC
No. of bundles	2
No. of tubes/bundle	$3 \times 8$
Working pressure	2.0 (MPa)
R	8.314 (J/mol K)
F	96485 (C/mol)
$L_{anode}$	$1 \times 10^{-4}$ (m)
$L_{cathode}$	$2.2 \times 10^{-3}$ (m)
$L_{electrolyte}$	$4 \times 10^{-5}$ (m)
$L_{interconnect}$	$8.5 \times 10^{-5}$ (m)
$A_{anode}$	0.10367247 ( $m^2$ )
$A_{cathode}$	0.102353 ( $m^2$ )
$A_{electrolyte}$	0.10273 ( $m^2$ )
$A_{interconnect}$	0.0128 ( $m^2$ )
$\rho$	See equation(2.10-2.13)

A <sub>act</sub>	0.002
i <sub>0</sub>	10 (mA/cm <sup>2</sup> )
m	0.0001
n	0.008

b) Fuel: fuel for the 5(kW) SOFC is methane rich natural gas; the percentage of methane may vary in practice. The natural gas composition used for simulation is listed in table 4.3 assuming only methane is considered during reforming reactions.

**Table 4.3: Natural gas composition**

Methane	89.25 (% mol)
Ethane	6.79 (% mol)
Propane	2.60 (% mol)
Butane	0.95 (% mol)
Heavier hydrocarbons	0.06 (% mol)
Nitrogen	0.23 (% mol)
LHV	49.248 (MJ/kg)
Density at 111K	465 (kg/m <sup>3</sup> )

The pre-reforming and reforming process for tubular SOFC is explained in section 2.2.3. Simulation results of the reforming process were also illustrated. From figure 2.3 and 2.4, the composition of reformed gas could be confirmed if knowing the temperature and fuel flow rate at certain parts of SOFC. However, the calculation of gas composition in real time is time consuming. So, during SOFC system simulation, the reforming process has been calculated beforehand at all temperature ranges and flow rates. These results are then embedded in the SOFC system model via look up tables. For instance, a certain input temperature and fuel flow rate will be matched to a certain gas composition after reforming reaction.

### 4.3 Integration of SOFC stack model

The integration of the SOFC stack model is illustrated as figure 4.3. It can be seen, if looking at the integration model as a black box, the inputs of stack model are stack temperature T and stack current density i while the output of stack model is stack voltage. On zooming into the stack model, the fuel flow rate and reactant gases composition are also resulted via the simulation process. With fuel flow, stack current and voltage in hand, the calculation of stack power and stack efficiency are also straight forward.

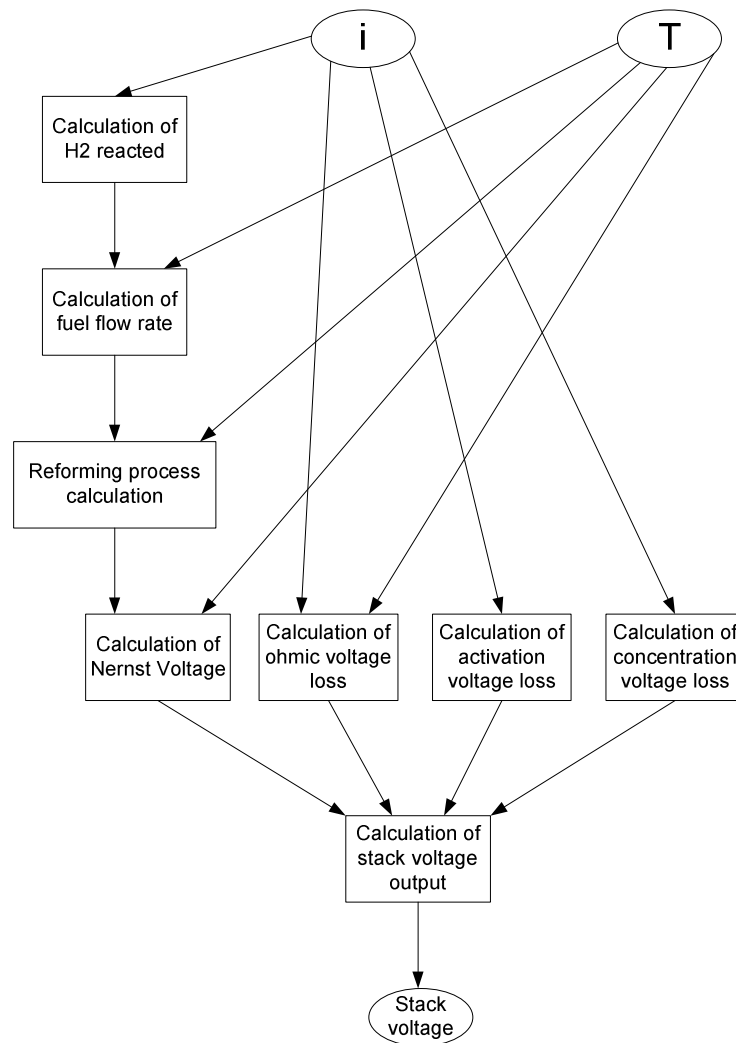


**Figure 4.3: Diagram of SOFC stack model integration**

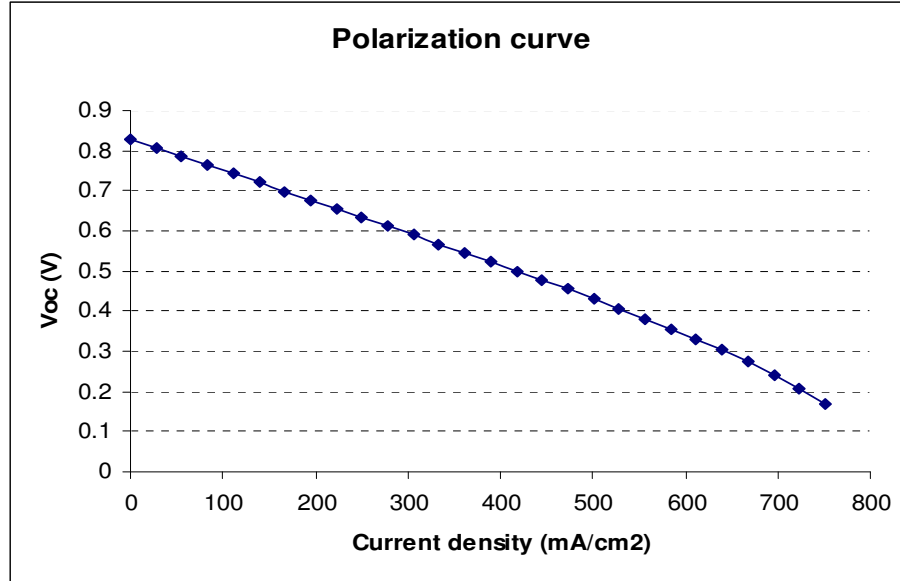
#### 4.4 Steady state simulation results and analysis

By using the SOFC model as described previously, the general simulation results at steady state are shown in table 4.4 when assuming working temperature is 847 ( $^{\circ}\text{C}$ ). The result shows a very similar output of the real system based on laboratory testing report (Allen, 2004).

**Table 4.4: Simulation result at steady state for 5 (kW) tubular SOFC model**

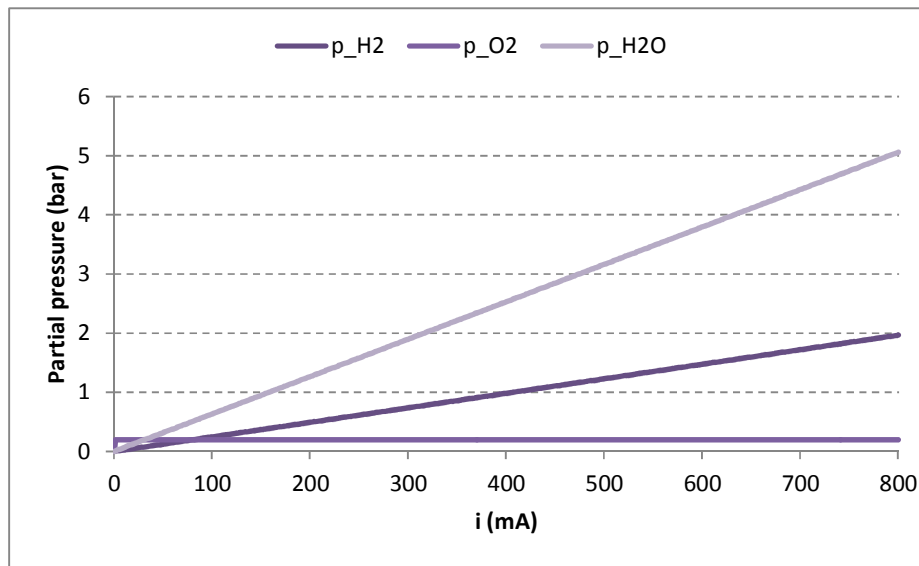
System		Calculation process	Simulation results
DC/AC converter  (Net power output)	DC/AC converter output (W)		1979
	Efficiency	DC/AC output / fuel energy	43.8%
DC/DC converter	DC/DC converter Power output (W)		2328
	Efficiency	DC/DC output / fuel energy	51.5%
stack	Stack Power output(W)		2616
	Efficiency	Stack Power output / fuel energy	58%
Heat recovery	Hot Water (W)		1403
	Efficiency	Hot water energy / fuel energy	31.1%
Fuel energy	W (LHV)		4513
Overall System Efficiency (include heat recovery)		Net power output + Heat recovery	74.9%

Figure 4.4 plots the open voltage of a single cell with increasing current density, which is often called the polarization curve. It shows that the polarization curve of the fuel cell is quite linear. This character indicates that the SOFC stack is ideal for system control.



**Figure 4.4: Polarisation curve of the fuel cell**

To watch the reforming process, partial pressures of reforming reactants have been simulated with increasing current density, which also represents the fuel flow rate. The simulation results are shown as figure 4.5



**Figure 4.5: Partial pressure of reforming reactants**

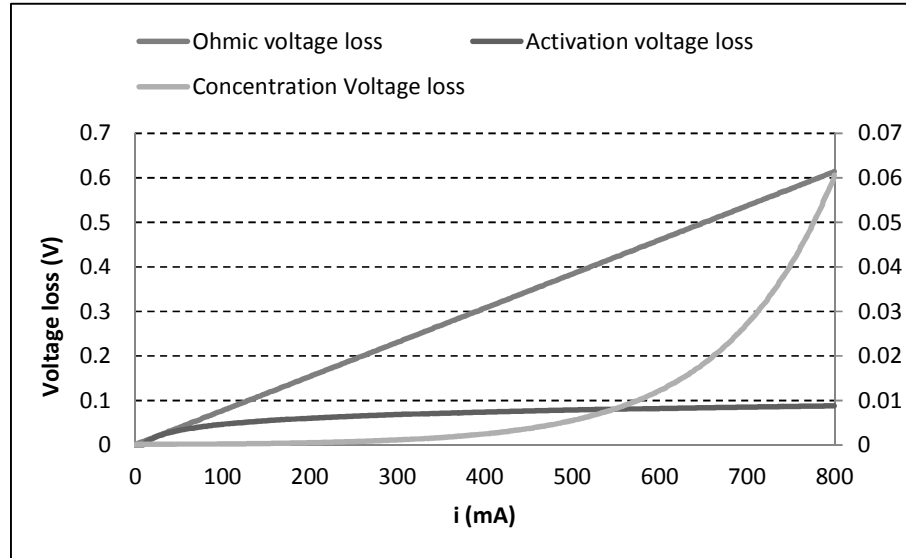


**Figure 4.6: Simulation results of stack voltage drop**

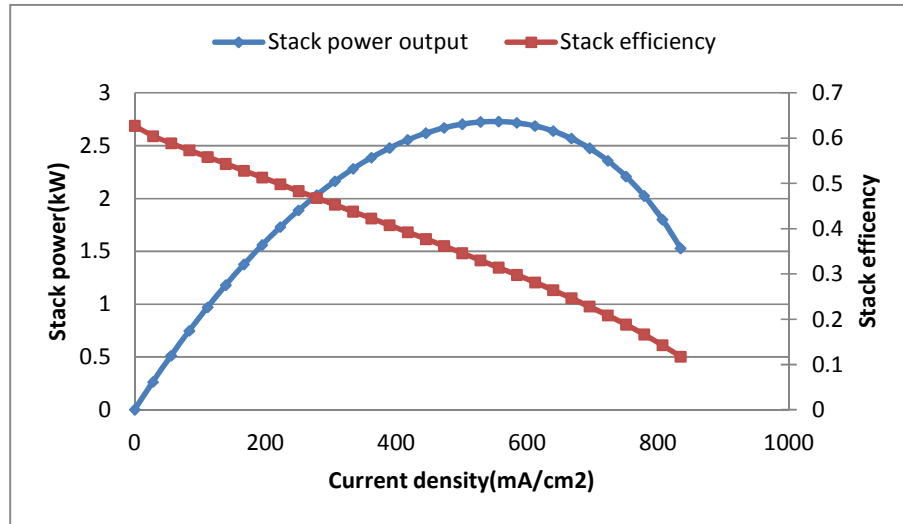


**Figure 4.7: Stack power and efficiency at different current density**

Calculation results of ohmic, activation and concentration voltage losses are expressed as figure 4.6. It can be seen that the ohmic voltage loss takes a large share of stack voltage drop especially when current density is below 600 (mA).

For the intention of marine application, the SOFC stack is examined according to ship rules and regulations. Consequently, the SOFC stack power range, stack power efficiency and overload capacity are simulated. If considering the overall power output, electricity and thermal output, the 5 (kW) SOFC stack power and its efficiency is shown in figure 4.7. Low heat value of natural gas is taken in terms of efficiency calculation. There is definitely an optimised power output when current density is around 550 ( $\text{mA/cm}^2$ ). The efficiency of fuel cell decreases with increase of current density.

## 4.5 Conclusion

Simulation of a 5 (kW) SOFC was executed under a steady state based on modelling methods described in chapter 2. The results in table 4.4 show that the outcomes of simulation results are very reasonable. The simulation results compare with laboratory test results will be discussed later in chapter 7.

Beside the whole stack characters, the reforming process and stack voltage losses were simulated at various stack currents.

Stack power simulation result indicate that the electric power output of the stack can reach up to 2.7 (kW). However, the efficiency for stack, in terms of heat energy utilisation decreased with the rising stack current. Consequently, concerning marine application, the intended electric load of SOFC needs to be limited so that the fuel cell can work at its optimum running conditions. Take the 5 (kW) SOFC stack for instance, the maximum continual electric power output should below 2.4 (kW) to leave a 10% over loading safety factor as required by ship rules.

After steady state simulation, the validation of the 5 (kW) SOFC at dynamic load change will be discussed in chapter 5.

## Chapter 5 Dynamic simulation of a 5 (kW) SOFC power system

The SOFC stack model has been run at steady state in chapter 4. It is proved that the SOFC is an effective power source and the power output could be controlled ideally. However, in practice the electric load of the SOFC is randomly changed. The character of dynamic response for SOFC is a more critical issue. In this section of the thesis, dynamic simulation for the 5 (kW) SOFC system will be performed.

### 5.1 Configuration of dynamic system

As explained in section 2.4, the time delay of system response mainly comes from the time inertia of mass flow change and stack temperature change. The time inertias of stack temperature and flow change are represented by  $\tau_{stack}$  and  $\tau_{manifold}$  respectively.

According to section 2.4.2, the stake temperature dynamic response is related to the time constant as indicated below.

$$\tau_{stack} = \frac{1}{A} = \frac{C_{SOFC}}{w_{out}C_{exhaust} - w_{air}C_{air} - w_{fuel}C_{fuel}} \quad (5.1)$$

$$C_{SOFC} = C_{fuel} + C_{air} + C_{stack} \quad (5.2)$$

According to CFD analysis in section 2.2.4, the heat transfer between frame structure of stack and reacting gases is much slower than the heat transfer between gases. Supposing the wall structure inside the stack is adiabatic during dynamic response then equation (5.2) could be changed to equation (5.3):

$$C_{SOFC} = C_{fuel} + C_{air} + C_{cells} \quad (5.3)$$

For the 5 (kW) SOFC, the relative setting value is assuming at:

$$C_{SOFC}=0.2125 \text{ (kJ/K)}$$

$$C_{air}= 1.012 \text{ (kJ/kg.K)}$$

$$C_{fuel}=2.19 \text{ (kJ/kg.K)}$$

$$C_{exhaust}=1.081 \text{ (kJ/kg.K)}$$

$$w_{air}=1.117 \text{ (e}^{-2} \text{ kg/s)}$$

$$w_{fuel}=2.39 \text{ (e}^{-4} \text{ kg/s)}$$

$$W_{out}=W_{air}+W_{fuel}$$

So  $\tau_{Stack}$  is estimated to be:

$$\tau_{Stack} = \frac{1}{A} = \frac{C_{SOFC}}{w_{out}C_{exhaust} - w_{air}C_{air} - w_{fuel}C_{fuel}} = 425(s)$$

For a stack temperature step change, the dynamic response time to reach a control error limit of 5% is around 1275 (seconds), which is three times  $\tau_{Stack}$ , based on the analysis method introduced in 2.4.1.

In accordance with the requirements of the International Association of Classification Societies (IACS) (M50 Programme for type testing of non-mass produced I.C. engines, Unified Requirement, 2013), Chinese Classification Society (CCS) Rules and Lloyd's Register (LR) engine test specification (Test specification Number 4 for internal combustion engines, 2012), "engine governing system should drive engine to return to the limit of less than  $\pm 10\%$  of requested power when load is suddenly changed." By using the same methods as in section 2.4.1, the dynamic response time for stack temperature change is around (1100) seconds.

This illustrates that the temperature change is very slow if considering the heat exchange effect caused by the variation of reactant gases flows. In other words, the dynamic change of fuel cell power output has very little influence on stack temperature for a short period.

This conclusion is similar with the result of Kandepua *et al* (2007). His results are shown in figure 5.1. The SOFC temperature only decreases less than 0.1 degree when load is suddenly taken off.

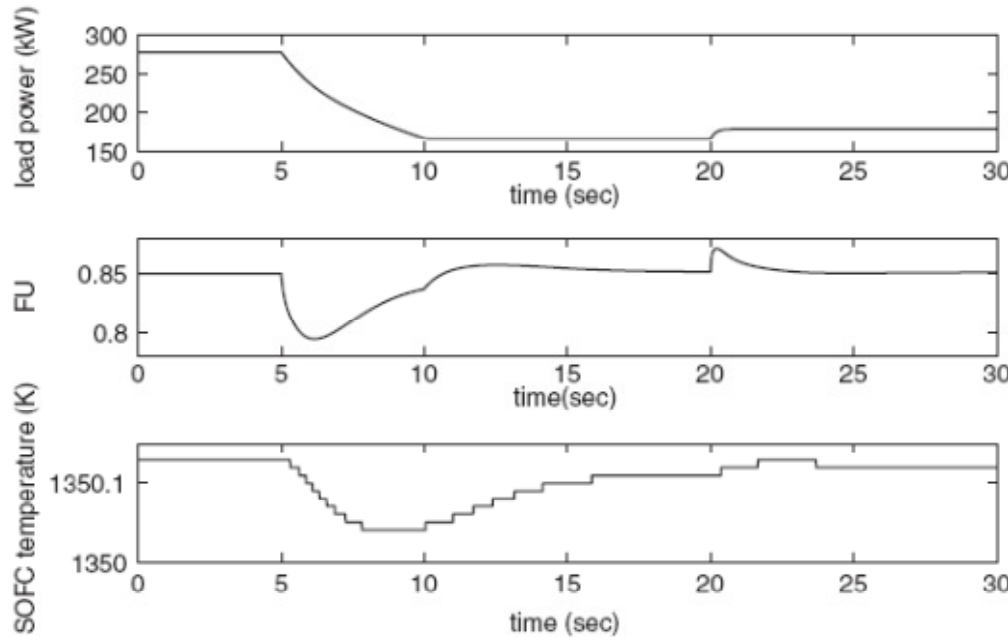


**Figure 5.1: SOFC temperature change with load change**

Consequently, it is safe to make the hypothesis that the effect of stack temperature on dynamic power response is not considered. However, in terms of simulation of system start-up, when the stack temperature is heated slowly, its influence is included and discussed later, in section 5.2.1.

Taking a look at the dynamic response of SOFC manifold, working out the time constant for fuel cell manifolds, assuming the air manifold and fuel manifold for the 5kW SOFC are as follows:

$V_{\text{manifold air}} = 0.3 \text{ (m}^3)$ , the combined space includes the volume of pipes from compressor to fuel cell stack, internal flow channel of pre-heater and burning chamber volume.

$V_{\text{manifold fuel}} = 0.2 \text{ (m}^3)$ , the combined space includes the volume of pipes from fuel inlet control valve to fuel cell stack, catalysed reformer and the space before entering the reaction chamber.

If taking:

$$R_{\text{fuel}}=518 \text{ (J/kg.K)}$$

$$R_{\text{air}}=286.9 \text{ (J/kg.K)}$$

$$k_{\text{out}}=2.25 \text{ e}^{-6} \text{ (kg/s.Pa)}$$

$$k_{\text{in}}=2.25 \text{ e}^{-6} \text{ (kg/s.Pa)}$$

$$T_{\text{stack}}=1100 \text{ (K)}$$

The time constants for air manifold and fuel manifold are calculated as:

$$\tau_{\text{air\_manifold}} = \frac{V}{R_{\text{mix}} T (k_{\text{out}} + k_{\text{in}})} = 0.211(s)$$

$$\tau_{\text{fuel\_manifold}} = \frac{V}{R_{\text{mix}} T (k_{\text{out}} + k_{\text{in}})} = 0.078(s)$$

Hence:

$$3\tau_{air\_manifold} = 0.633(s)$$

$$3\tau_{fuel\_manifold} = 0.234(s)$$

In practice the flow changes for air and fuel are controlled simultaneously. This operation is executed by the stack controller as indicated in figure 4.1.

As the whole fuel cell system is not mechanically coupled, the system is controlled by electric signals, so the time delay by the controller should also be counted in dynamic response. It is assumed that the time delay caused by controller and electric signal transfer is 0.1 second.

## 5.2 Execution of simulation

The simulation execution is based on the 5kW tubular SOFC system with controllable inductive load. To identify the 5kW SOFC system dynamic response, three types of simulation test have been arranged in the following sections. One simulation is to observe the SOFC stack starting process. The second one is to simulate the SOFC under dynamic load without the combination of a battery. The third simulation is the SOFC stack plus battery mode that fuel cell and battery output are paralleled together.

### 5.2.1 Starting up of SOFC

The operating temperature of the SOFC stack is around 927 ( $^{\circ}\text{C}$ ). A burner is used to heat the inlet air. The heated air runs throughout the entire stack and warms up the SOFC stack. So, during heating process, the input variables of the system are air flow rate and inlet air temperature. The inlet air temperature is controlled by burner which is assumed to be a fast response feedback control device. The control strategy of the burner is based on the calculation of thermal stress at utmost situation and the

consideration of durability of cell material. Assume that  $T_{\text{lim\_startup}}$  is the limitation of controlled temperature difference between stack and air inlet during starting. When the SOFC system is heating up, it means no heat is released from the chemical reactant. The configuration of starting control model is set as follows:

$$Q_{\text{react}} = 0$$

If  $|T_{\text{air}} - T_{\text{stack}}| \leq T_{\text{lim\_startup}}$  then  $T_{\text{air}}(t+1) = T_{\text{air}}(t) + \Delta T$

If  $|T_{\text{air}} - T_{\text{stack}}| > T_{\text{lim\_startup}}$  then  $T_{\text{air}}(t+1) = T_{\text{air}}(t)$

$T_{\text{air}}(t)$  means the temperature of inlet air at certain time

$T_{\text{air}}(t+1)$  means the temperature of inlet air at next time step

$\Delta T$  is the temperature step change from certain moment

$T_{\text{lim\_startup}}$  is the controlled temperature limitation between stack and inlet air temperature. The value of  $T_{\text{lim\_startup}}$  should be between 0 to  $\Delta T$ .

The temperature step change  $\Delta T$  is strictly limited to avoid causing severe thermal stress to the stack structure. This value can be resulted from the previous modelling of heat flow and transfer in section 2.2.4

According to the analytical outcome of CFD calculation the extreme temperature gradient takes place at the closed end of tubular structure. This extreme temperature gradient is about 3500 ( $^{\circ}\text{C}/\text{m}$ ) along longitudinal direction of fuel cell tube. Take a safety factor of 2 for the considerations of dynamic load change affection, durability operation and material performance at different temperature range. The revised maximum temperature gradient of the tube material is 7 ( $^{\circ}\text{C}/\text{mm}$ ).

As specified in table 2.1 of section 2.2.2, the thickness of the SOFC tube is 2.34 (mm) if combining three layers of anode, cathode and electrolyte material. So, the maximum temperature difference between the anode and cathode sides is estimated around 16.38 ( $^{\circ}\text{C}$ ). Concerning the most brittle parts of materials subject to thermal shock within the SOFC system are at the closed end of the tubular structure, it is therefore reasonable to assume  $\Delta T$  equals 16.38 ( $^{\circ}\text{C}$ ).

According to the previous calculation, the simulation of SOFC cold start is simulated by estimating  $\tau_{Stack} = 425(\text{s})$  and  $\Delta T=16.38 (^{\circ}\text{C})$ .

If assuming:

$$T_{\text{lim\_startup}} = 5\% \times |T_{\text{air}} - T_{\text{stack}}| \quad (5.4)$$

Then, the simulation results of SOFC stack temperature changes are shown as figure 5.2 and 5.3.

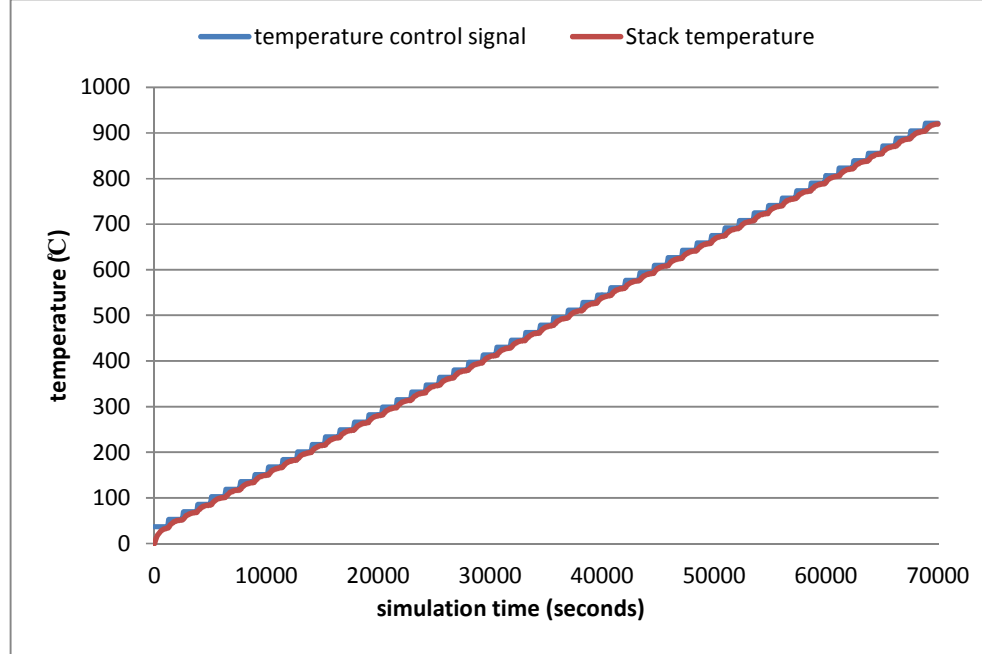
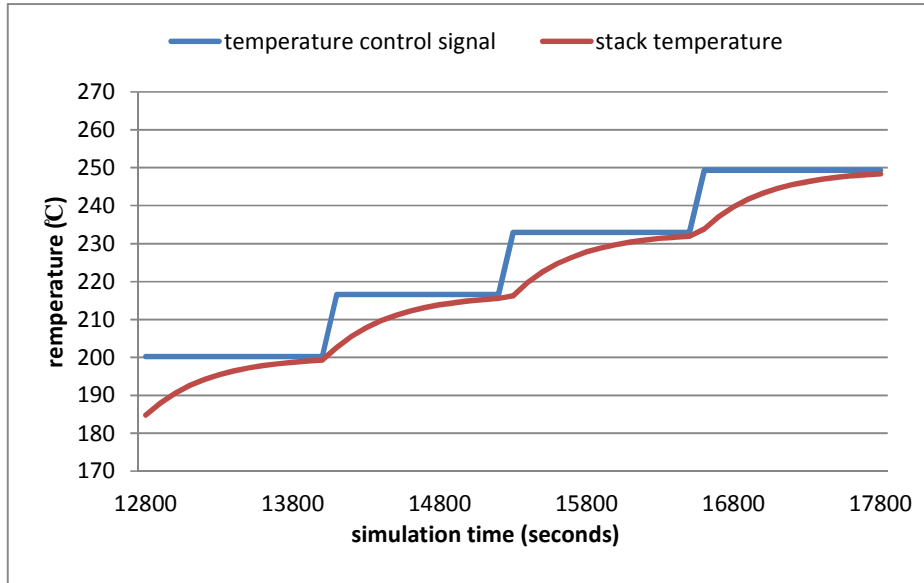


Figure 5.2: Stack temperature during starting process if equation (5.4) is applied



**Figure 5.3: Amplified figure of 5.2**

If assuming

$$T_{\text{lim\_startup}} = 50\% \times |T_{\text{air}} - T_{\text{stack}}| \quad (5.5)$$

Then, the simulation results of stack temperature changes are shown as figure 5.4 and figure 5.5

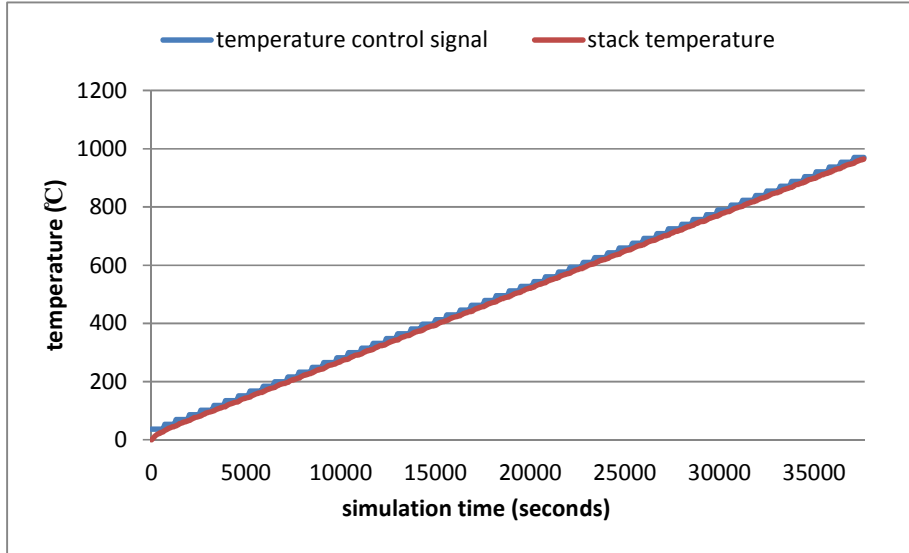


**Figure 5.4: Stack temperature during starting process if equation (5.5) is applied**

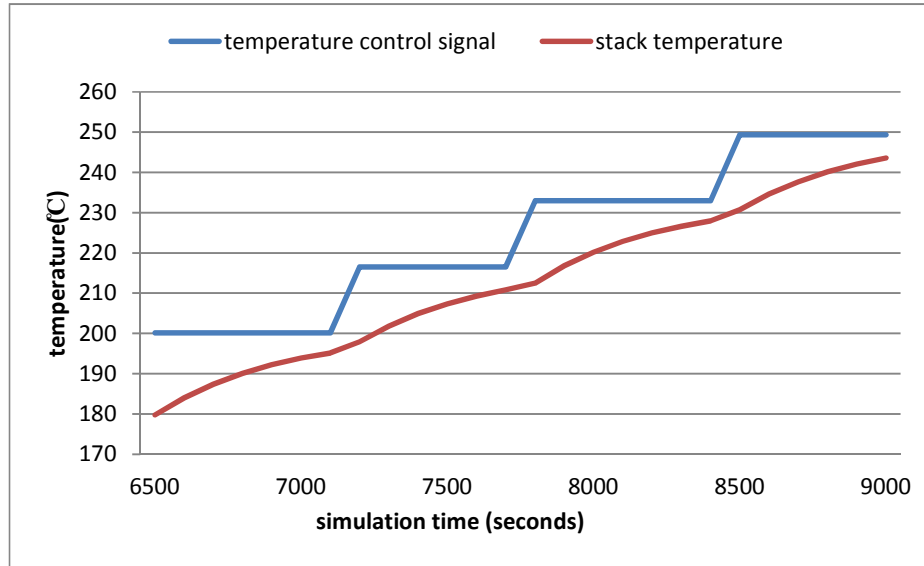


**Figure 5.5: Amplified figure of 5.4**

It can be seen by comparing figure 5.2 and figure 5.4 that the starting time of SOFC stack can be dramatically reduced by using different starting control limitations.

If optimise the starting simulation by using feedback control to smooth the control signal, then the temperature control signal is adjusted according to the real time stack temperature to ensure that the temperature difference between stack and temperature control signal is always at its utmost value of 16.38K. The feedback control of the stack starting process is illustrated as figure 5.6.

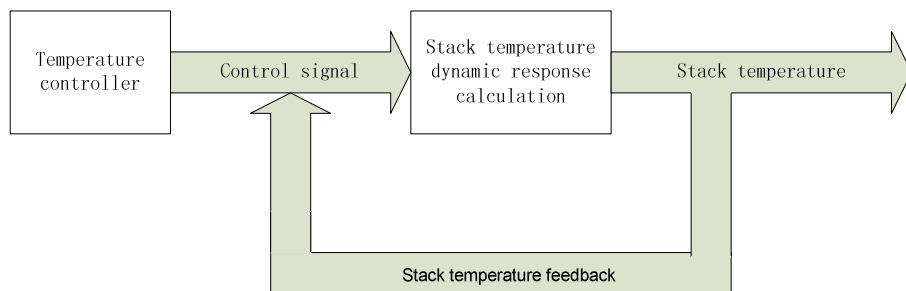


**Figure 5.6: Feedback control of SOFC stack starting process**

The stack temperature is monitored in real time. This recorded stack temperature refers to when the controller adjusts the control signal to control inlet air temperature. The optimised starting process is shown as figure 5.7 and figure 5.8.

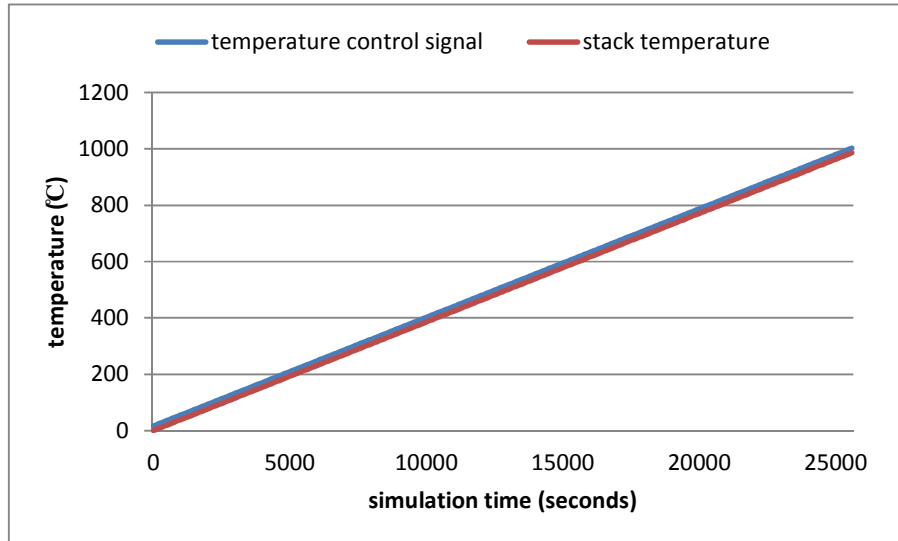


**Figure 5.7: Stack temperature change under optimised control process**

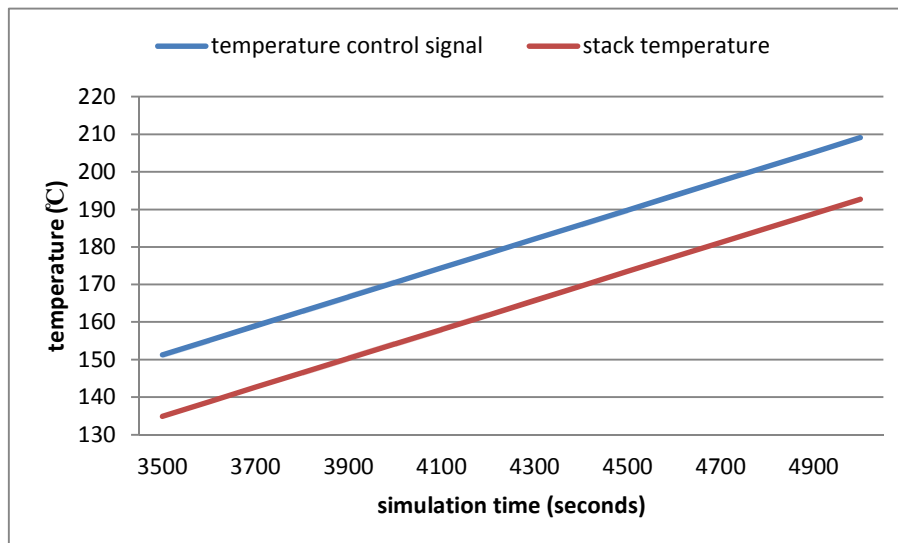


**Figure 5.8: Amplified figure of 5.7**

According to the simulation result of figure 5.7, the warming up time (starting time) of the 5 (kW) SOFC could be reduced to 25000 seconds (6.94 hours) if the warming up process is controlled smoothly. Compared with the instructed starting time of 16 hours

(Operation and maintenance manual Beta 5kW SOFC system, 2005), there is still plenty of space to decrease the SOFC warming up time.

### 5.2.2 5kW SOFC dynamic simulation result

The electric load for SOFC marine application is a randomly changing signal. This is required as the SOFC needs to quickly follow the dynamic change of load and provide the desired power output. To simulate the dynamic character of the 5 (kW) SOFC, a testing plan needs to be set beforehand.

As the SOFC is intended for marine application, the control signal of the electric load change is set to comply with “the requirement of diesel engine using for marine test program” of the LR Type Approval System (Test specification Number 4 for internal combustion engines, 2012), the transient load point is programmed as figure 5.9. Electric load changes happen at 25%, 50%, 75%, 90%, 100% and 110% of the SOFC Max Continuous Rated Power (MCR) respectively. The overload of 110% MCR is running at short period.

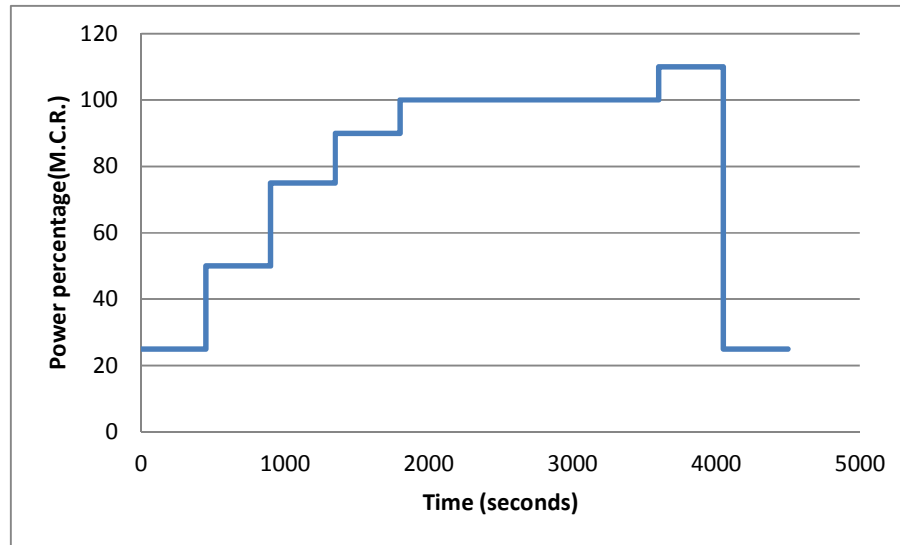


**Figure 5.9: Programmed electric load change for dynamic simulation**

The configuration of dynamic SOFC model was explained in section 5.1. Based on the required electric load, responses of 5 (kW) SOFC output are plotted as figure 5.10, figure 5.11 and figure 5.12.

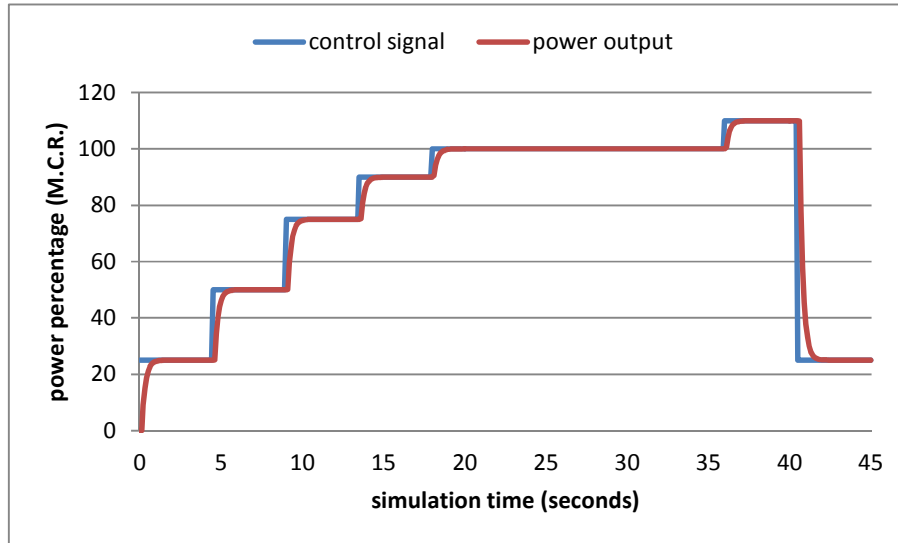


**Figure 5.10: Dynamic simulation of SOFC with load changes**

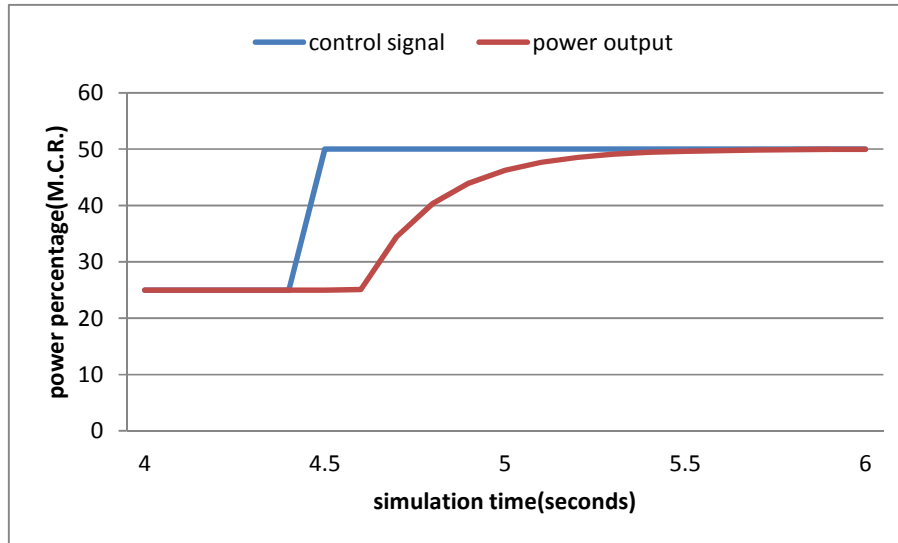


**Figure 5.11: Response of step load change at 4-6 seconds**

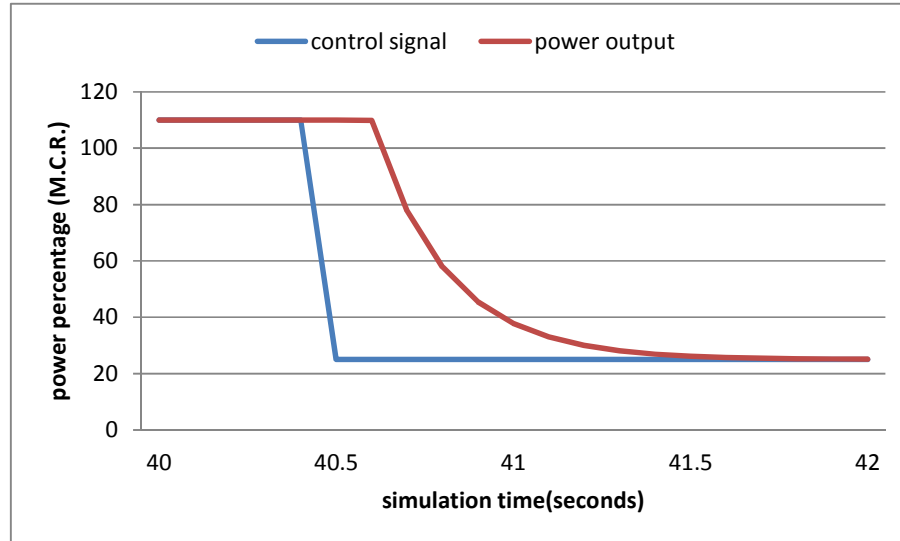


**Figure 5.12: Response of step load change at 40-42 seconds**

As per ship rules, an error difference of 10% of requested load change is permitted for dynamic response of marine machinery. The ship rules request a response time of dynamic load to be less than 5 seconds.

It can be seen from figure 5.11 and figure 5.12 that the response time of a required load change is around 1.1 seconds if the control error permission is 10% of the requested power change. This time inertia results from both the delay of flow manifold and the delay of control signal.

### 5.2.3 SOFC simulation with the use of battery

From previous simulation results, the operating character of the SOFC can meet the requirements of ship rules and regulations. It is capable for marine application both under steady state and dynamic state. However, these simulations are based on the extreme operating situation to maximise the usage of SOFC. In practice, the maintenance, safety and optimisation issues of the SOFC are also considered. Therefore, most of the SOFC power systems are equipped with batteries to offset the power output deficiency during operating. By paralleling SOFC and batteries output together, the

transient load could be absorbed by battery while SOFC produces continuous and steady power output. Consequently, the smooth running of SOFC could level off the operating stack temperature which reduces the thermal stress of cell structure.

In this section a 5 (kW) SOFC power system together with battery will be simulated at dynamic load changes. Figure 5.13 shows the layout of the 5 (kW) SOFC electric power plant system. The system includes a fuel cell generator, batter, power conditioners, grid bus, electric load and secondary bus.

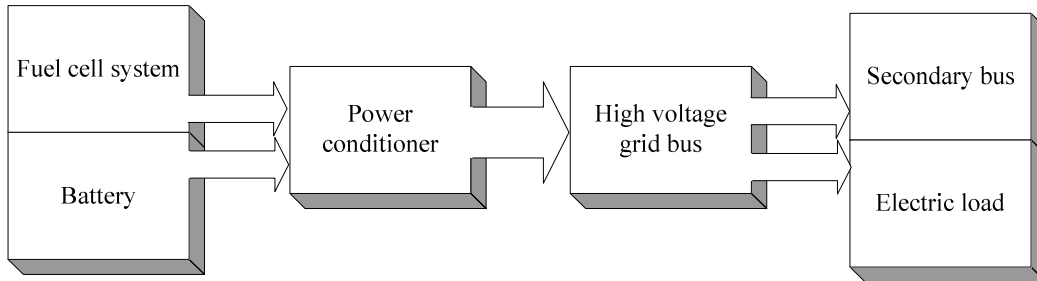


**Figure 5.13: Structure of fuel cell power system**

The power output of the fuel cell and battery are paralleled to connect to the grid bus via a power conditioner. A power conditioner can be made of a DC/DC converter and DC/AC inverter to adjust the output of fuel cell and battery to a desired voltage and frequency. The adjusted electric power after power conditioner is then fed to the grid bus to be consumed by electric consumers. The electric consumer can be an electric motor, electric load or a secondary switch board.

The modelling and configuration of the 5 (kW) SOFC is the same as with previous sections. The battery model is defined in section 2.3.2. Data for a combined parameter model of lithium-ion battery are based on a stabilised manganese spinel-graphite system with a 0.5 (kWh) electric energy storage capacity. The battery charging or discharging status is controlled by SOC.

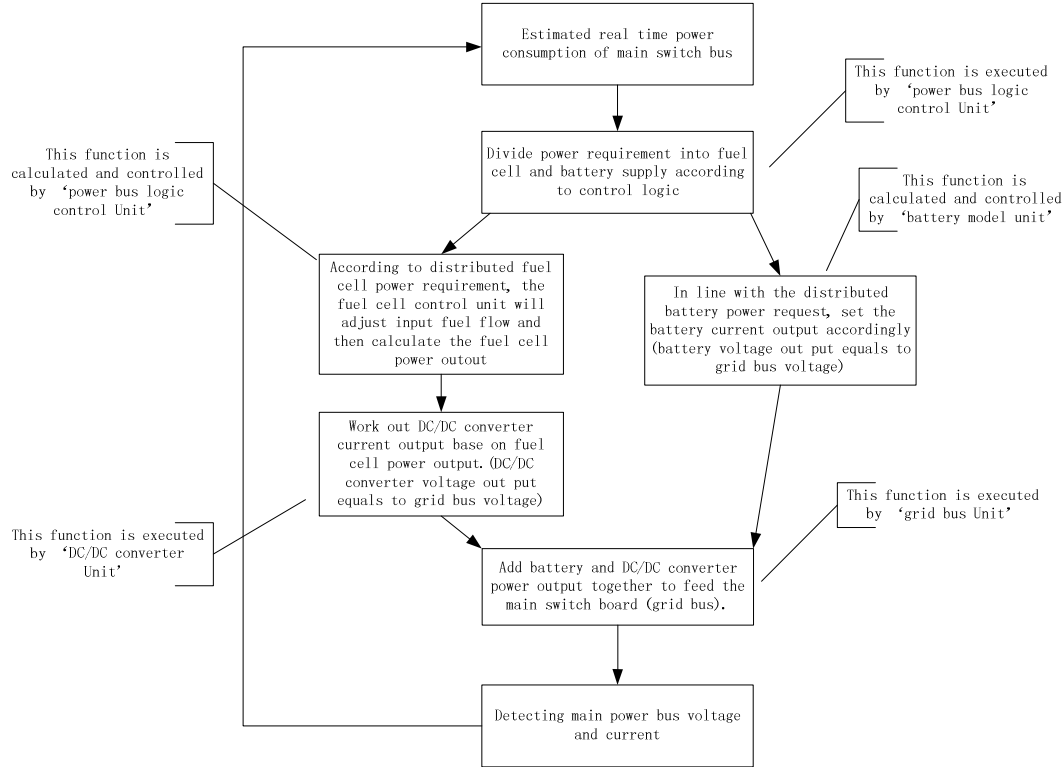


**Figure 5.14: Control scheme of power distribution**

The power distribution scheme of the SOFC and battery is illustrated as figure 5.14. Grid bus voltage and current are recorded and fed back to the controller. The power requirement is then calculated. The grid bus controller will decide how much power is distributed to the battery and SOFC based on the operating status of the battery and SOFC. According to the allocated power requirements, the SOFC control unit will adjust the flow rate of fuel and air inputs. At the last stage, the power output of the SOFC and battery are regulated by the power conditioner and feed to the grid bus. This process is looked as a close loop feedback control.

The simulation program is validated by Matlab Simulink®. In order to simulate the maximum electric output of the SOFC system, the load is set to reach its maximum power from the beginning. The range for the original SOC of the battery is from 0.7 to 0.3. The simulation results for a duration of one hour are presented in figure 5.15 and figure 5.16. The battery would provide some 300 to 500 (W) backup power when load requests a higher power demand. This would help the SOFC power system to work at

up to 120% overload. The battery could continually produce backup power until the SOC reaches a threshold of 0.3. This period is expressed at figure 5.15 from start to 3200 seconds. Afterward, the fuel cell stack produces power alone. Figure 5.16 illustrates the relationship between battery SOC and power output.

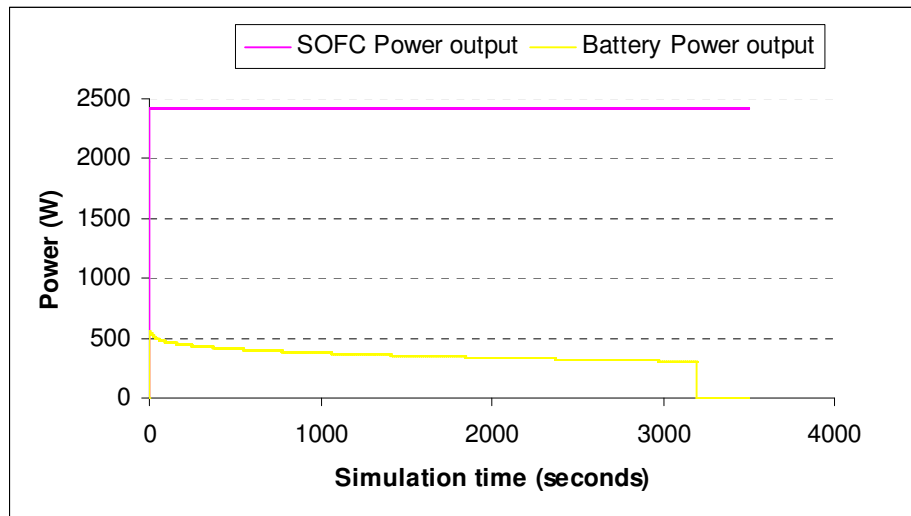


**Figure 5.15: SOFC and battery output at full load**

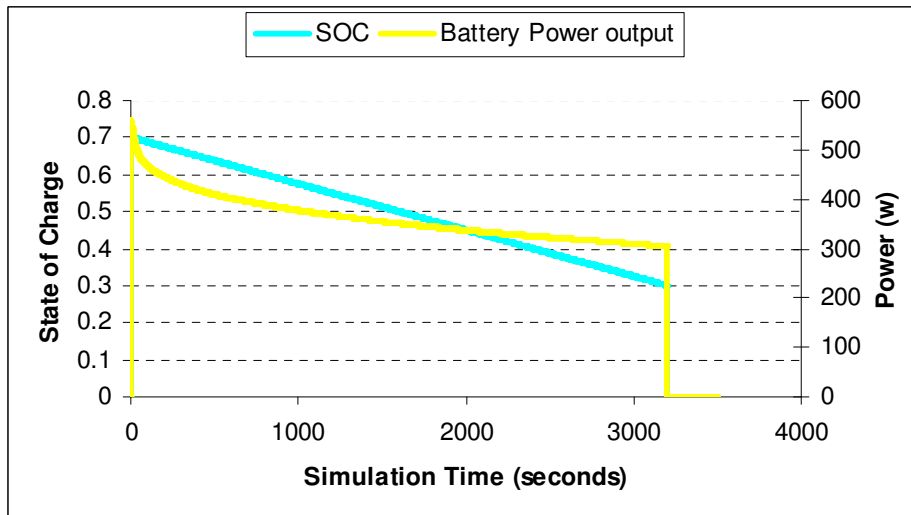


**Figure 5.16: Battery discharge status at full load**

To test the system at sudden load change, a power request is set as the blue line in figure 5.17. The SOFC power output could not follow the power request instantly due to slow time inertia of the system as discussed in section 5.2.2. The battery is paralleled with the grid bus, hence this deficiency of power will be covered by the backup battery as shown in figure 5.18. On the other hand, extra power from the stack power could be saved in the battery when the load is decreasing sharply.

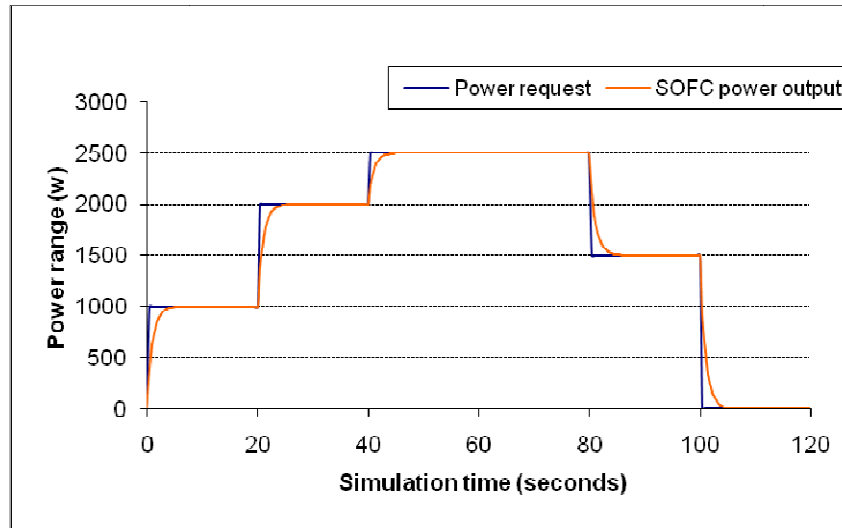


**Figure 5.17: SOFC output responses at different load changes**

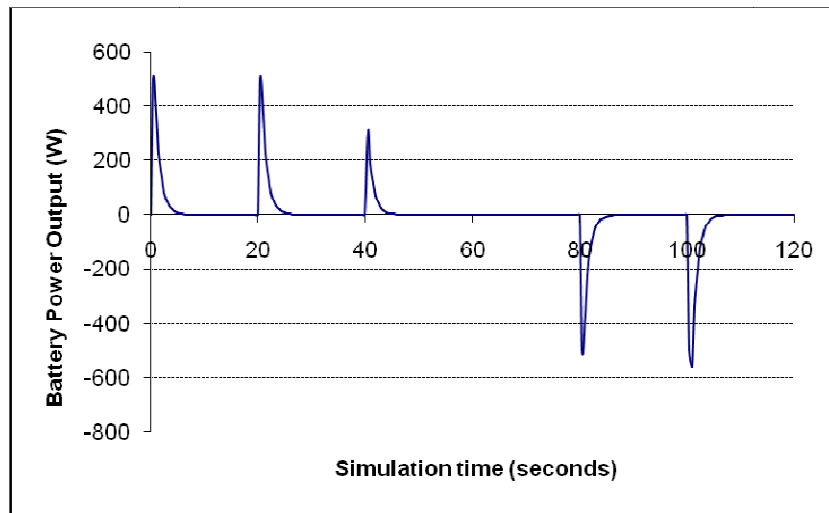


**Figure 5.18: Battery output responses at different load changes**

### 5.3 Conclusion

In this chapter dynamic simulation of the 5 (kW) SOFC was performed in three different working scenarios, namely starting up, standalone mode and battery parallel mode. The dynamic character of the SOFC is largely determined by two time constants  $\tau_{stack}$  and  $\tau_{namifola}$ .

According to simulation results:

The starting time of the 5 (kW) SOFC can be reduced to within 7 hours by optimising starting control logic.

A dynamic response time of 5 (kW) SOFC at step load change is around 1.1 seconds, which complies with the requirement of less than 5 seconds to return to  $\pm 10\%$  error of nominated power as required by ship rules.

With the use of a backup battery, the overload capacity of SOFC power system is increased and the operating status of the SOFC is more stable than standalone mode.

## Chapter 6 Marine SOFC system installation, risks and conceptual design

Fuel cell technology has been proposed as an efficient and clean alternative to internal combustion engines. While promising to revolutionise marine power generation in the longer term, the relative immaturity of the technology makes the technology currently unsuitable for the provision of power on large internationally trading vessels. However, if look forward 10 years, commercially viable fuel cell products can be expected to generate megawatt-strength power. The fuel cell marine power system will find its niche market, e.g. for vessels which spend significant operating time in coastal areas. In recent years, another notable trend for the marine power industry is the shifting of oil fuel to gas fuel with low flash point (<60 °C) driven by the increasingly stringent emission and environmental regulation. For example natural gas and methanol, are seriously considered by owners as a bunker fuel option thanks to their emissions reduction benefit. In fact, many existing ships are currently powered by low flash point fuels and more under construction. Whilst the new emissions limits for both NO<sub>x</sub> and SO<sub>x</sub> contained in MARPOL Annex VI are coming into force in a few years time. Finding clean and efficient alternative solution to power ship will be a impending task for marine industry. SOFC will rightly join this trend thank to its high efficiency and the capability to use various low flash point gas as fuels.

In this chapter, the topic of SOFC marinisation will be discussed. Firstly, risk and safety issues for using fuel cells onboard commercial ships are identified. Then Ship Rules and Regulations relevant to the SOFC system and its on board installation will be discussed from all perspectives in relation to ship machinery systems. Then, a conceptual design for SOFC marine systems are presented in the later part of the chapter.

### 6.1 Fuels for fuel cells marine installation

Depending on the types of fuel cells and electrochemical reaction mechanisms, hydrogen rich gas or hydrocarbon rich gas are preferred to be the direct fuels for fuel cells. By chemical reaction and production, various other types of fuels can be used to fuel the fuel cells after chemical conversion. Therefore, the source of fuels for fuel cells

can range from traditional fossil fuel to renewable fuels. To better illustrate the pathway for fuelling fuel cells, figure 6.1 is plotted to indicate various fuels for fuel cells.

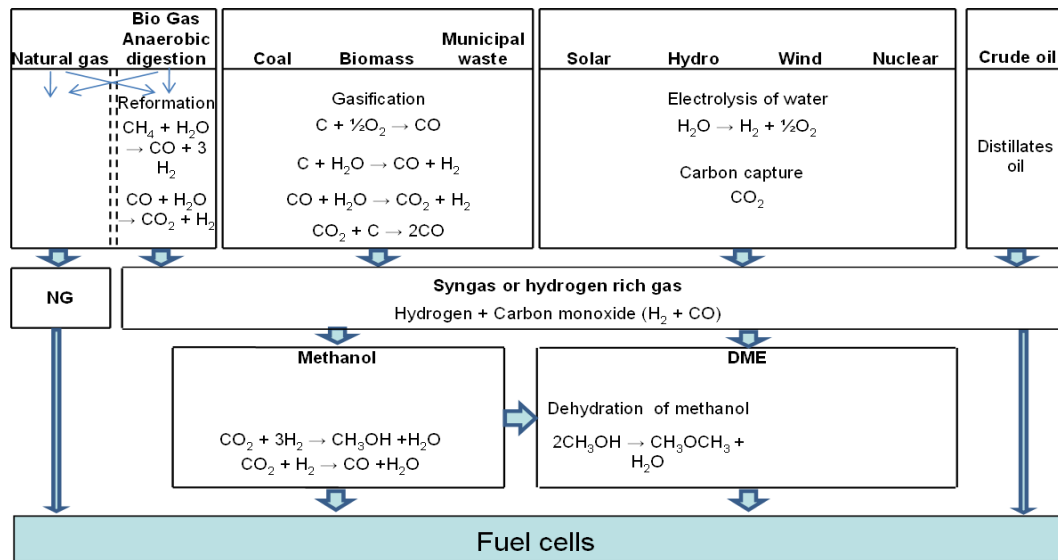


**Figure 6.1: Fuels for fuel cells**

It can be seen from figure 6.1 that the primary sources of fuels will be transformed to low flash point fuels (<60 °C), most of which are gaseous phase, before feeding into fuel cells. The direct fuels for fuel cells can be pure hydrogen, Synthesis Gas, natural gas, methanol or Dimethyl Ether (DME). The properties for the fuels are listed in table 6.1.

**Table 6.1: List of fuel properties**

	Hydrogen	Carbon monoxide	Methane	n-Butane	Methanol	DME
Flammable range (in air)	4 – 74%	12.5-74.2%	5 - 15%	1.5 – 9%	6 – 36%	3.4-14.5%
Flash point (°C)	-253	-191	-175	-60	12	-45
Self-Ignition temperature (°C)	500	605°C	595 °C	365 °C	470 °C	160
Minimum ignition energy (mJ)	0.02	0.3	0.25	0.2	0.14	0.19
Vapour density (air = 1)	0.07	0.97	0.55	2.1	1.1	1.62
Boiling point at atmospheric pressure (°C)	-259	-191.5	-162	-0.5	65	34

## 6.2 Risks for SOFC marine installation

### 6.2.1 Risks management procedures and methodology

The objective of risk management process used during the development of SOFC system and its ship installation is to ensure that any risks derived from the SOFC system onboard installation should be controlled and managed in systematic manner such that any residual risk are no greater than those normally associated with conventional diesel engine installation. In accordance with risk management best practice, the process will employ a number of recognised risk management techniques intended to identify hazards resulting from a variety of sources including inappropriate design, components and system failure, human error, abnormal operation etc. Due to the novelty of SOFC system and the absence of quantitative safety and reliability data, particularly with regard to marine fuel cell installations and natural gas or other low flash point gas as a marine fuel, the risk management methodology makes use of qualitative risk assessment techniques relying heavily on the judgement of technical experts. The objective of the risk management process is to eliminate or mitigate the risks to the ships personnel and to the environment to an acceptable level. The methodology and process used for risk assessment is aiming to:

- Identify hazards to the ships personnel and the environment
- Evaluate the associated risk
- Determine the tolerability of the associated risk
- Eliminate or reduce the risk of harm to an acceptable level
- Record results and recommendations

For merchant shipping, the ship design and installation is mainly governed by statutory requirements published by IMO and Flag States, and Class requirements published by Classification Societies to which the ship is registered. These requirements and standards are descriptive rules which does not regulating on the risk assessment method and procedures used. In the absence of descriptive standard for marine fuel cells

installations, risk based approaches is to be developed based on the best practice of system engineering. For example, Lloyd's Registers system engineering requirements as specified in the "Lloyd's Register Rules for the Engineering System of Unconventional Design" would be a good base for the risk assessment of SOFC marine installations.

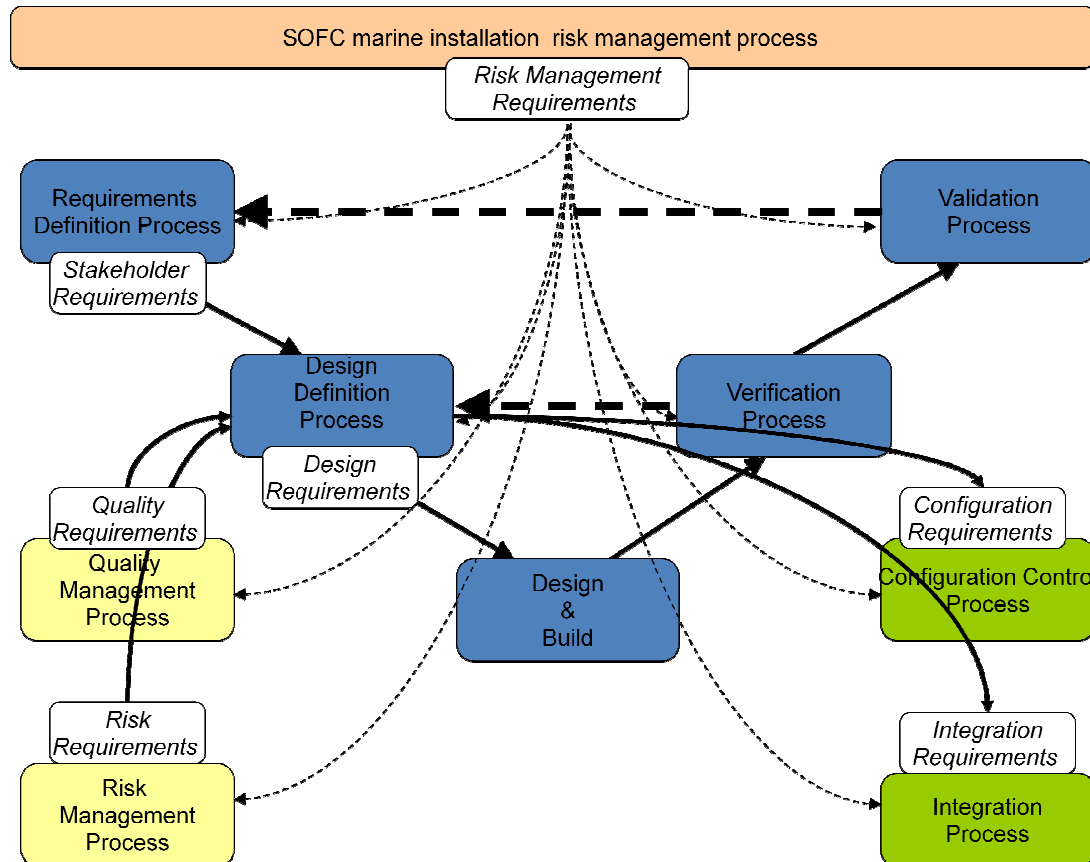


**Figure: 6.2: Lloyd's Register risk management process for unconventional design**

The "Lloyd's Register Rules for Engineering Systems of Unconventional Design" is aims to align with the IMO guidelines on formal safety assessment adopted at IMO Marine Safety Committee circular number 1023. The general risk management process is illustrated as figure 6.2. It can be seen from figure 6.2, the stakeholder's requirement and design definition should be well placed ahead of the design and construction. These definitions will serve as the objectives of the SOFC risk assessment and quality management process. Then various risk assessment procedures should be undertaken to

identify the risks and mitigate the risks in the design and construction process. Once the production design and ship installations begin, all the risks identified beforehand must be verified. The stakeholder's requirement will also be validated at last to ensure the design and risk management meet the aims and objectives set up at the first stage.

As explained above, in addition to compliance with the applicable requirements of LR's Rules and Regulations, the SOFC installation risk management process would employ several risk analysis techniques, focused on both the SOFC unit itself and also the SOFC shipboard installation system as a whole. Take METHAPU project (METHAPU project, 2010) as an example, the following studies were carried out for the SOFC system installation:

At sub-system level:

- Potential Problems Analysis (PPA) – Fuel Cell Unit
- Preliminary Hazard List (PHL) – Fuel Cell Unit
- Failure Mode Effect and Criticality Analysis (FMECA) – Fuel Cell Unit
- Hazard and Operability analysis (HAZOP) – Fuel Cell Unit

At system level:

- Hazard Identification (HAZID) - System
- Hazard and Operability analysis (HAZOP) - System

In combination with procedures as introduced, the overall risk assessment and governance process of the SOFC marine installation can be summarized at figure 6.3.

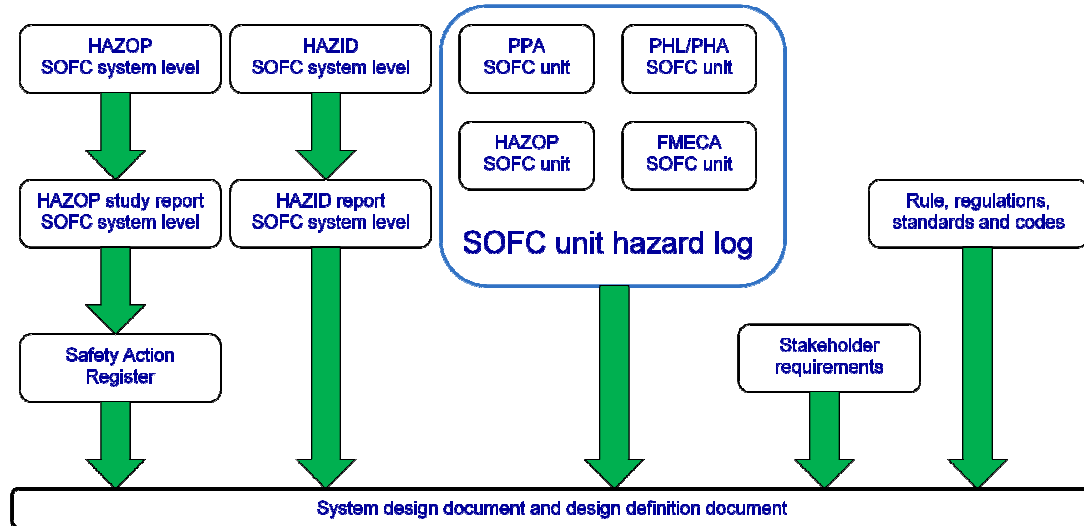


**Figure 6.3: Risk assessment and governance process of the SOFC marine installation**

At sub-system level, the PPA, PHL and PHA studies were carried out at early design stage of SOFC unit development. These preliminary hazard studies are brainstorming practices which can be further analysed at preliminary risk mitigation stage. FMECA is applied to both components as well as SOFC unit partial system level. The effect of the local failure and system failure, probability of failure occurrence is to be found and documented in particular to analyse the SOFC start-up and shutdown procedures. The HAZID and HAZOP study apply to both subsystem level and system level. These two systematic methods are for examine the complex system and process to identify potential hazardous at both design and operation of the SOFC system. The systematic HAZID and HAZOP should cover all the SOFC marine installations including SOFC unit, fuel cell room, gas fuel bunkering, gas fuel storage, and gas fuel supply system. The operating error, external effect, integrity failure, material defects, emergency and maintenance factors must also be taken into consideration. Each of the risk item identified must be logged. The probability and the severity of each risk item also need to be estimated. The probability and severity of risk estimation should be based on a predefined a risk assessment matrix.

### 6.2.2 Risks associated with SOFC unit

Fuel cells are formed of an integrated system comprising of subcomponents and subsystems. However, if excluding the risks from fuel, the risk control objective for the SOFC unit itself mainly aims to provide a level of safety and reliability equivalent to that associated with conventional oil-fuelled propulsion and auxiliary machinery. The Following are some thoughts regarding the risk of SOFC units.

- a) The malfunction of SOFC may come from the failure of any part of the system. Most of the commercially available fuel cells are automatically controlled and designed for “fail-safe”. Fuel cells would also be automatically shut down in the event of abnormal operation or failure.
- b) The risks arising from marine environments are to be specially considered by manufacturers and system integrators. For example, ship vibration would require resilient mounting and flexible couplings, the highly humid and saline air of marine environments need to be dehumidified and filtered before feeding into fuel cell stacks for the purpose of corrosion protection.
- c) The marine engine is designed to have a life time of approximately 25 years. However the reliability of fuel cells for marine use has not been proven.
- d) Depending on type, the performance of fuel cells can deteriorate after years of running. This has to be accommodated in the initial ship design allowing for some marginal power to be sacrificed.
- e) Ideally, fuel cells are to be placed in engine rooms, which mean the fuel cells unit has to be gas safe. To achieve this, fuel cells unit may need to be self-enclosed with forced ventilation and gas detection. Inside the fuel cells unit, the components may also need to be separated, e.g. place electrical equipment and ignition source away from gas dangerous zones.

- f) Starting characters for fuel cells are different from diesel engines. Some high temperature fuel cells take hours to start and restart (B. San, 2010). Traditional requirements on starting capacity and starting control procedure need to be justified.
- g) The transit load change of fuel cells is to be compensated by other sources of power either from the existing ship grid or backup battery. The scale of power used for compensation needs to be carefully selected.

All the above mentioned risk concerns are mainly to the responsibility of the manufacturers for the best practice of risk and safety management. However third party inspectors, e.g. classification society, should verify and monitor the whole risk and safety management activities. The whole system safety managements should include at least the considerations of reliability, safety and quality of the fuel cells. Due to the lack of technical standards for fuel cells and reliable data for fuel cell installation in marine environments, a risk based approach to safety assessment should be used to carry out the examination of the fuel cells. Suitable risk management methodology should be carefully selected based on the judgment of technical experts as explained in section 6.2.1.

### 6.2.3 Risks associated with low flash point fuels

For marine installation of fuel cells systems, a large proportion of the risk and hazards is attributed to the fuels it uses.

- a) The fire and explosion risk arise from a combination of fuel characters such as its flashpoint, minimum ignition energy, self-ignition temperature, vapour density and flammable range. Specifically considering ship environments, unprotected hot surfaces, poor ventilation conditions and ship vibration will add to the fire hazard. The relatively high expansion ratio for liquid low flash point fuel can yield a large amount of gas if leaked.

- b) When fuel is stored in its liquid phase, the cryogenic hazard is crucial for containment systems as well as ship structure. Brittle fracture occurs if stressed carbon steel is subjected to very low temperatures, due to spillage of liquid nitrogen, liquid hydrogen, LNG or similar cryogenic liquids. Also, when some liquefied gas, e.g. LNG, is in contact with water, explosive forces can occur due to the different temperature profiles, this is known as rapid phase transition. When the temperature of one liquid is greater than 1.1 times the boiling point of the cooler liquid, a rapid rise in temperature is initiated such that the surface layer temperature can exceed the spontaneous nucleation temperature and bubbles appear. In some situations this superheated liquid vaporises within a minute producing vapour at an explosive rate.
- c) While low flash point gas fuels are stored in liquid phase, the storage tank vapour pressure will rise naturally due to the heat being absorbed from the environment. Excessive pressure generated by the vaporization of gas fuels will need to be managed in whole life cycle without venting to atmosphere.
- d) Humans accidentally in contact with low temperature liquid fuel may suffer cryogenic burns, an effect on the skin similar to that of a high temperature burn. Many low flash point fuels, such as methanol, are also toxic to humans.

#### 6.2.4 System level risks

System level risk integration and management for fuel cell installations is critical. It is also closely related to the fuel cell unit characters and fuel properties. The arrangement of systems needs to be in line with the principles for ship design and the existing ship rules and regulations. Based on the previous discussion, the principal risks are:

##### a) Fuel storage

To optimise the volume for fuel storage, fuels are preferred to be stored in liquid phase or compressed gaseous phase. If fuel is stored as compressed gas, it has to be in an independent tank. Limited by tank design pressure, this has significant disadvantages

for maximising storage space. The cost of pressure vessels and the availability of large volume compressed tanks also make the option of compressed gas less favourable for large ships. Confirmation with the relevant national administration should be sought to allow the storage of compressed gas tanks below deck (San and Bradshaw, 2012). For gas fuel stored in its liquid phase, specially constructed tanks are needed in line with relevant international standards. Continuous monitoring of the tank pressure is needed as the thermal insulation of storage tanks cannot totally isolate thermal transfer and prevent the build-up of gas pressure. A secondary barrier is also required to prevent spillage should the primary barrier fail. The main risk for fuel storage is leakage and damage to fuel tanks.

b) Location and arrangement

As explained earlier, most types of fuels for fuel cells are more hazardous than traditional marine fuels. The traditional arrangement of fuel oil tanks is not suitable for fuels with a low flash point. Most low flash point fuels being considered are flammable gas at ambient temperature and pressure. The location and arrangement of systems should be engineered to mitigate or minimise the risks such as leakage or damage of tanks containing low flash point fuel. The preferred location of low flash fuel tanks is on open deck for leakage risk and in the middle of the ship to avoid collision. However this combination will leave less flexibility for ship design and may reduce the commercial attractiveness of fuel cell systems. In terms of tank damage prevention, the distance from the location of fuel tank to the ship's hull is the key figure to prevent collision damage. Collision and grounding data originating from a research project GOALDS (GOALDS, European Commission funded research project on Goal Based Damage Stability, 2012) indicates that a distance from the side shell of 20% of ship's breadth ( $B/5$ ) would not lead to tank damage in 60% of all cases. A value of 15% of breadth covers 50% of all collisions and even a distance of 5% of  $B$  covers 30% of all collisions. Therefore, the arrangement of tank location itself cannot eliminate the risks arising from collision damage. Trade off has to be made to an acceptable level of tolerance on fuel tank damage and mitigating possible consequences so as to ensure ship safety.

c) Piping

The risk for piping systems comes from the leakage of fuels. Depending on the properties of fuels, e.g. temperature, pressure and phase, the piping may need to be thermally insulated and double walled. The materials for pipe construction also need to take account of fuels being transmitted and prevent erosion. For double wall piping with gas fuel running inside, all piping systems including connections are to be seamless and butt welded. Double wall pipes are to have a gas tight secondary barrier construction with either inert gas or continuous ventilation in between two pipes.

d) Ventilation and gas detection

Any spaces where flammable gases can accumulate from the release or leakage of fuels must be suitably ventilated to mitigate the risk of a stoichiometric fuel/air mixture forming. Where practicable there should be both flammable gas and toxic gas detection systems fitted in such spaces. The location of gas detector shall take in to account the gas property especially gas heavier than air. The heavier gas could be trapped or go into machinery piping system.

e) Fire protection

Hazardous area zoning for areas containing fuel tanks and other systems containing low flash point fuels is to meet the requirements of IEC 60079-10. This defines hazardous areas and splits them into three zones according to the likelihood of a flammable atmosphere existing: Zone 0, which has the highest risk, Zone 1 and Zone 2. Electrical equipment located in these areas must be approved for use in specific zones.

### 6.3 Classification regulations for marine SOFC application

For most of the machinery systems to be installed onboard ship, the design and installation procedure need to be approved and surveyed according to rules and codes issued by regulation organisations. The definition and requirements for traditional

mechanical devices have been covered by rules and regulations based on years of shipping experience. However, almost no relative regulations can be found for fuel cell installations onboard merchant seagoing ships, because the issue of ship rules depends highly on statistics and experience of seagoing performance. This experience is what the fuel cell industry lacks so far. The performance of unconventional materials and components used within fuel cell systems needs to be verified during long term seagoing circumstances. Ship classification organisations and bodies are in the very early stages of trying to provide tentative guidance on definition of marine fuel cell systems. Germanischer Lloyd and Bureau Veritas issued their first guidance on fuel cell marine application in 2003 and 2009 respectively. This guidance includes the definition of the fuel cell system and its associated components, materials used, protective devices and trials of systems. Conversely Lloyds Register is cautious to roll out requirements on fuel cell, believing that the technology of fuel cell is in its very early maturity and may not be wise to set regulations with the changing of techniques at this stage. Apart from fuel cells itself, the examination of auxiliary components of fuel cell systems could be applied by following some similar rules defined by current ship machinery regulations. Hence, Lloyd's Register tends to creatively use current marine rules and regulations to assess this novel machinery, e.g. by applying Requirements for Machinery and Engineering Systems of Unconventional Design (Requirements for Machinery and Engineering Systems of Unconventional Design, 2012), FMECA (IEC 60812: Failure mode and effective analysis, 2006) and HAZOP (IEC 61882: International Standard for HAZOP studies, 2006) methods to verify system performance in addition to some parts of fuel cell systems which could not be assessed by certain clauses in currently available rules. In terms of fuel cell stack approval, ISO, IEC and National standards for fuel cells are applied.

Generally for a fuel cell power system to be installed onboard ship, measurements need to be provided to protect ship and personnel in case of hazard, e.g. leakage, fire or explosion, due to failure or malfunction of the fuel cell system. The arrangement of the fuel cell system is to be such that currently available power or electrical systems are capable of being sustained in the event of failure of fuel cell systems and vice versa.

Consequently, the assessment of marine fuel cell system installation will focus on safety hazards associated with operation or failure of the system. The dependability of equipment providing essential or safety critical services will also need to be evaluated.

In the Appendix 1, an analysis of marine rules which could be apply to SOFC will be presented in line with regulations issued by LR, International Maritime Organization (IMO), IACS and British Standards Institution (BSI).

## 6.4 Improvement and modification of the SOFC marine system

At present, the SOFC is not a mature type of power system for ship use. As explained in section 6.2 and 6.3 there are many items to check and improve for a SOFC system to be installed onboard ship. Some modifications are needed according to the requirements of ship rules and regulations, while some improvements are needed to facilitate the marine environment. These improvements are explained as follows.

### a) Operational environment

The marine SOFC system is expected to be designed for a machinery space environment with specifications as generally addressed with unrestricted seagoing use. Factors such as temperature, pressure, humidity, air salinity, vibrations and even wind pose challenges to the systems installed on board. Also, conventional engine exhaust and possible contamination of air is an issue to consider with SOFC units, as well as availability of specific auxiliary systems on board.

The operational environment temperature for enclosed spaces is defined as 0 to 45 ( $^{\circ}\text{C}$ ). The inclination requirements, as defined in the Classification Societies' Rules, are 15 degrees for athwart-ship and 5 degrees for fore-and-aft at static situation, and 22.5 degrees for athwart-ship and 7.5 degrees for for-and-aft at dynamic situation.

Particle filtering and demisting are common in machinery space solutions for inlet air. Salt in particle form is removed with these solutions. However, humidity from the inlet

air is not removed by these. Air humidity may be an issue with electrical equipment that has additional cooling in way of water-to-air, as the moisture in the air condenses easily on the cooler surfaces. Salinity and humidity together pose a corrosive environment. This is possible to address with an air dehumidifier. Precautions are to be taken in order to prevent air intake from clogging, especially in dusty environments. Air dehumidifier specifications are to meet the temperature, flow rate and dew point requirements of a SOFC system. As to the nature of the air in machinery spaces in general, the intake air to SOFC system may require filtering from particles of a certain size. For some non-pressurised SOFC systems, pressure drop for air filters is to be considered also.

A SOFC in itself generates close to no vibrations as it has very few moving parts such as fluid pumps and air blowers. The vibration generation of a pump or a blower is minimal and does not affect the operating environment. The main and auxiliary engines' vibration from the ship are the main vibration sources that may influence the structure and components of the SOFC unit. Vibration damping, e.g. flexible mounting, is possible to address the problem. Flexible piping, such as hoses and bellows, may also be used to deal with the inter-component movement to compensate the vibration and thermal expansion from both outside and inside the SOFC system.

### b) Volume density

Almost all pre-commercialised SOFCs are built for stationary application where space limitation is not an issue. This makes it difficult to install an SOFC on a ship when the power demand is high. For instance, the specific volume of new type of dual fuel diesel engine is about 20 (l/kW), while the specific volume of SFC-200 125 (kW) SOFC is 978 (l/kW). However, the SOFC is not volume optimised and the BOP system takes a large amount of space. If only the volume of fuel cell stack is accounted, the specific volume is 17-30 (l/kW). Planner SOFC is a more compactable type compared with tubular SOFCs. Some specialists estimated specific volume of SOFC after optimization as 45-112 (l/kW), which is 2-5 times more than that of a dual fuel diesel engine.

### c) Power range

The power range of a current tubular SOFC unit is less than 500 (kW). The maximum rated electric power of a commercially available SOFC unit is 250 (kWe). Theoretically, a higher power demand could be met by parallel connection of a group of SOFC units. But each single unit has its own BOP and control system. A parallel connection of units could cause a large waste of system components and volume. Hence a fuel cell module with higher power output is required by the marine power generation market.

### d) Durability and maintenance

More than 20,000 running hours of land based SOFCs testing has been carried out. This record is not comparable with the marine diesel engine of 400,000 hours life time. The reliability and safety of running is another problem when fuel cells operate at seagoing conditions. A fuel cell system is more likely to fail and needs more regular maintenance checks. Consequently, the life time of a fuel cell system is a major obstacle to prevent it from onboard installation.

### e) Power conditioning

After electrical conversion and inversion, the electric power output of the fuel cell system is in the form of low voltage alternative current. Normally the voltage output is less than 1kV. It could be connected to the low voltage switchboard widely used in conventional low voltage systems. However, some ships like the newly built LNG carriers of large cargo capacity are more likely to use a high voltage main switchboard. A suitable power conditioning unit is needed to convert the low voltage and high current electricity output from fuel cells into a high voltage and low current system. Normally a SOFC power conversion is conducted in two stages. A DC/DC conversion is used to raise the voltage obtained from the fuel cells to a level suitable for the DC/AC inverter and for DC loads in the fuel cell system. Then an inverter generates a three phase sinusoidal AC-current that is fed into the ship grid. The inverter is required to tolerate expectable voltage and frequency variations and transients on the ship's grid.

An isolation transformer may sometimes be included at the inverter output to comply with leakage current, isolation strength and emergency requirements.

#### **f) Fuel cell housing**

Based on the rules of classification society, e.g. LR and DNV, fuel cell systems should be installed separately from traditional engine room systems. Fuel cell systems could be either accommodated in an enclosed space by means of a bulkhead in the engine room or deployed in an open deck area. To operate fuel cell systems safely, the layout of the engine room and deck arrangement needs to be adjusted accordingly to avoid hazards. All these changes should be done based on the principles of keeping the original hull division and maintaining cargo hold volume.

#### **g) Heat recovery system**

The exhaust heat of gas mixture released by the fuel cell is very high, e.g. 0.8 to 1 (kW/kWe) at temperatures of around 800 ( $^{\circ}\text{C}$ ). Exhaust temperatures of this level are good for producing high quality steam with steam temperatures of over 500 ( $^{\circ}\text{C}$ ). This steam is suitable for a Rankine cycle. So, for large power SOFC installation, exhaust gas from the fuel cell system is to be sent to the exhaust boiler to produce steam, which could feed to a steam turbine generator.

#### **h) Fuel supply system**

Depending on the type of fuel used, the fuel supply system including storage tank, piping, pumps and valves is to be independent of the existing ship system used for conventional engines. Details of the requirements are discussed in section 7.3.

#### **i) Start-up system**

Due to the fact that the SOFC operates at a very high temperature, a start-up or warm up process may need additional devices to be installed, such as start-up gas and start-up water. Take the SOFC system used in the METHAPU project, for example. The SOFC

system requires reducing purge gas during heating-up to prevent oxidation of fuel cell catalyst layer. This is achieved by using a hydrogen nitrogen mixture. A number of gas bottles for hydrogen-nitrogen mixture with a small amount of hydrogen have been used in the installation.

## 6.5 Conceptual design of 750 (kW) SOFC power system on LNG carrier

### 6.5.1 Introduction and assumptions

Following previous simulation result and discussion on installation issues, it is concluded that SOFC could meet both the stable load and transient load requirement of ships. In this section a conceptual design to install a 750 (kW) SOFC power system onboard a 12,000 ( $m^3$ ) LNG carrier to provide an auxiliary power supply are proposed for SOFC marine application. In order to analysis the design concept, certain assumptions need to be made to quantify the technical and economic justifications behind the decisions taken.

The mother ship being used for the conceptual design is chosen as a 12,000 ( $m^3$ ) LNG ship as show in figure 6.4. It is understood SOFC is preferred to use gas as fuel. Compare with other types of ships, LNG ship have LNG cargo on ship all the time if assuming the ship will carry a certain amount of heel LNG cargo to maintain the cold condition of the cargo tank. This will make it easier for SOFC to access to the available gas fuels. On top of that, LNG cargo while being transported will generate large amount of Boil Off Gas (BOG) due to the heat absorption from environment. SOFC power plant will help to manage BOG by consuming gas as fuel. Economic wise, natural gas is the cheapest available fuels for SOFC compare with other gas fuels such as hydrogen. The price of natural gas is also lower diesel oil fuels. An overall CAPEX and OPEX in comparison to the conventional diesel generator plant will be discussed later.

The mother ship was originally design for regional LNG distribution with a service speed of around 17 knots at design draft. The LNG ship is derived from an existing

LNG carrier recently delivered by AVIC Dingheng shipbuilding Ltd in 2011. The ship's LNG cargo system is comprised of two 6,000 ( $m^3$ ) type C tanks. The design pressure of the cargo tanks is 4 (barg). The main parameters of this carrier are as follows:

- Length over all: 152.30 (m)
- Length between perpendiculars: 142.36 (m)
- Breadth moulded: 19.50 (m)
- Depth to main deck: 11.50 (m)
- Design draught: 6.7 (m)
- Dead weight: 8,200 (ton)
- Cargo tank capacity (100%): 12,120 ( $m^3$ )
- Speed: 17 (kn)
- Propulsion machinery: MAN 6546 MC-C8 at 8,280 (kW)
- Propeller type: 4 blades controllable pitch propeller
- Bow thrusters: El.-Hydraulic driven CPP at 400 (kW)
- Main engine shaft generator maximum output: 1,200 (kWe)
- Auxiliary engines: 3 Caterpillar C3208 at 994 (kW)



**Figure 6.4: 12,000 ( $\text{m}^3$ ) LNG ship Bahrain Vision (Bahrain Vision, 2013 )**

To replace the diesel auxiliary generation plant of the LNG ship with SOFC power generation system, the operating modes and the electric load of the ship needs to be looked in details. The electricity load of the reference LNG ship at different operate modes is summarized in table 6.2 directly below.

**Table 6.2: Load distribution at different operation modes**

	<i>Loaded voyage (kW)</i>	<i>Ballast voyage (kW)</i>	<i>Manoeuvring (kW)</i>	<i>Harbour (kW)</i>
Propulsion	7,000	6,500	1,600	0
Service load	350	350	350	300
Bow thruster	0	0	400	0
Compressor	590	0	0	0
Cargo pump	0	0	0	400
Total	7,940	6,850	2,350	700

It can be seen from table 6.2 that the service load during loaded voyage is 350 (kW). The service load plus bow thrusters electricity demand is around 750 (kW). The electricity used for harbour operation is 700 (kW) in total. These figures can conclude that a 750 (kWe) electricity auxiliary plant is big enough to cover all the requirements for ship operation. Therefore to replace the current diesel generating plant, the designed SOFC power plant is to have 750 (kWe) electricity output in total.

The SOFC modules used in this design are chosen to have three 250 (kW) SOFC units. A summary of assumed performance of the 250 (kW) SOFC units are given in table 6.3. This information is derived from publications of Siemens Power Generation Co (Siemens Stationary fuel cell performance, 2010). The original outlook of the 250 (kW) SOFC power system is indicated at figure 6.5. On paper, the weight of the three 250 (kW) units is 90 tons in total, which is more heavy than the original diesel engines generating plant of around 5 tons in total (Caterpillar 3208 specification). However the additional weight added to the ship is relatively small compare with the 8,200 (tons) dead weight of the ship. The location of the SOFC rooms is on the open deck just above the second cargo tank and symmetrical along the longitudinal centre line of the ship . Consider the fact that the cargo loading and unloading conditions are already included while calculating the ship stability. The additional weight of SOFC system on top of cargo tank two can be equally seen as an additional cargo loading weight and will be within the loading margin tolerance. Therefore the impact of the SOFC weight on ship dimension and stability will be tiny and not be discussed in details.

**Table 6.3: Characteristics of 250 (kW) SOFC (Veyo, 2003)**

SOFC type	Seimens CHP250
Number of tubular cells	2292
Power output (Max)	250 (kWe)
Working pressure	Atmospheric
Thermal output	Up to 200 (kW)
Electrical output efficiency	45-50% (typical 47%)
Over all system effectiveness	80%

Operation mode	Unattended automation
Cooling	Air cooled
Exhaust Gases composition	No measurable SO <sub>x</sub> , CO, VOCs, <0.5 ppm NO <sub>x</sub> , No particulate emissions
Start time	<18 hours
Maintenance	Annual inspection and maintenance
Duration	>20,000 hours tested land base
Dimension	9.5 × 3.6 × 3.6 cubic meters (L×D×H)
Weight	30 (tons)

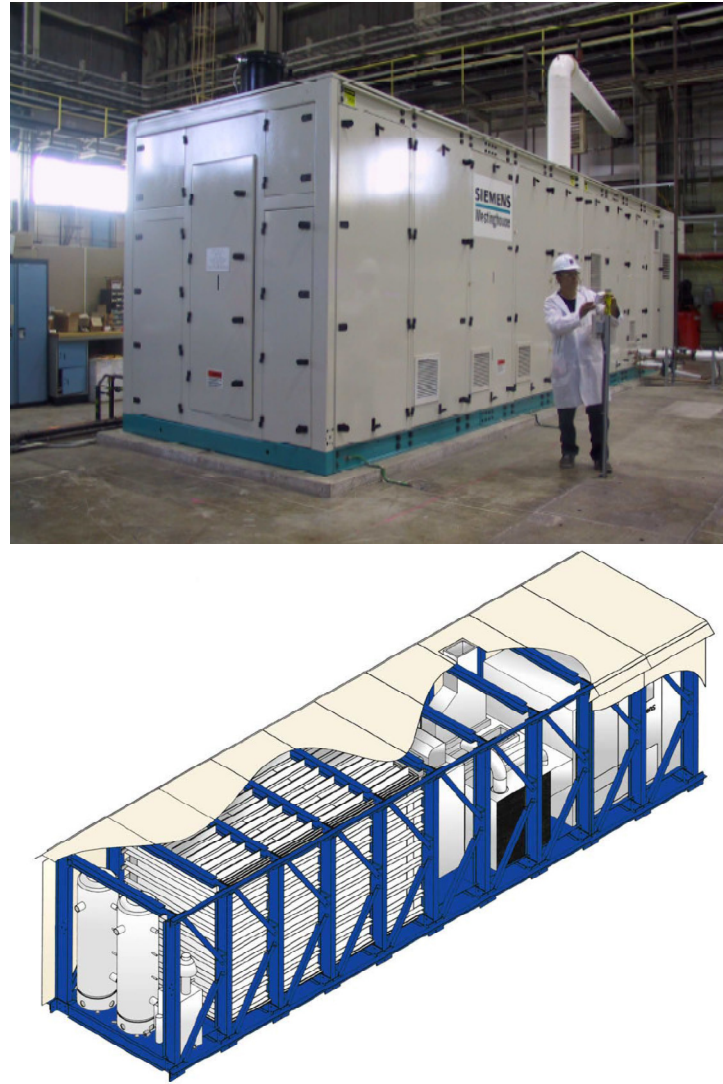


**Figure 6.5: 250 (kW) SOFC power system**

### 6.5.2 System arrangement

As explained before, the 750 (kW) SOFC plant will use natural BOG from the cargo tank as fuel. This arrangement will have both technical and economic advantages. The SOFC requires nearly pure methane as fuel. BOG vaporized from LNG will contain near 100% methane which can be directly feed to SOFC without treatment. The using of

BOG also saved capital cost of fuel storage facilities for LNG since the LNG cargo tank has a well equipped pressure management and alarming system.

### **General system arrangement:**

The main propulsion system of the 12,000 m<sup>3</sup> LNG ship is a mechanical drive system. One MAN 6546 MC-C8 diesel engine is to provide the propulsion power. For auxiliary electricity generation, one shaft generator and three 250 (kWe) SOFC units are combined to provide all electric service demands.

The machinery configuration of the conceptual LNG Ship with SOFCs includes:

- One main engine, MAN 6546 MC-C8 at 8,280 (kW)
- One main engine shaft generator, maximum output 1,200 (kWe)
- 3×250 (kW) SOFC, electric power output: 3×250=750 (kWe)
- One emergency generator, output approximately 150 (kWe)

The three 250 (kW) SOFC units are proposed to be installed inside a dedicated fuel cell room placed on the deck of cargo area and supply auxiliary electric power for ship operation. The allocated space for the fuel cell room is just in front of compressor room as indicated in figure 6.6 where the red circles highlighted. In the original mother ship design, this particular area was an empty space left for future retrofit of reliquefaction plant and not being used at the moment. The space is around 11 metre long, 13 metre wide and 6 metre high which is big enough to be converted into a fuel cell room. The fuel cell room will be a separate room with enclosure of an A-60 bulkhead and is located at the deck of cargo area which is arranged next to compressor room. This arrangement will make it convenient for natural gas supply and ventilation as well as minimise the effect of fire risk comparing with an engine room installation.

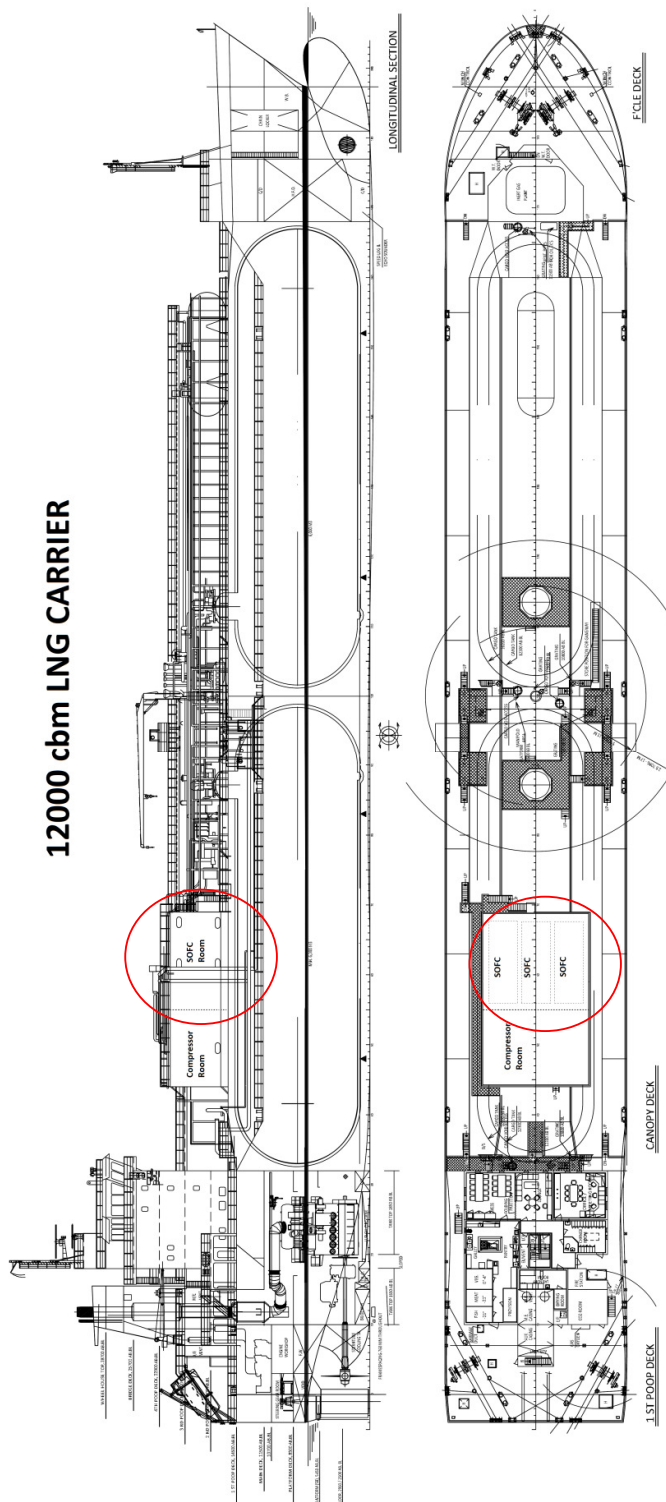


**Figure 6.6: 12,000 (m<sup>3</sup>) LNG Ship general arrangement plan**

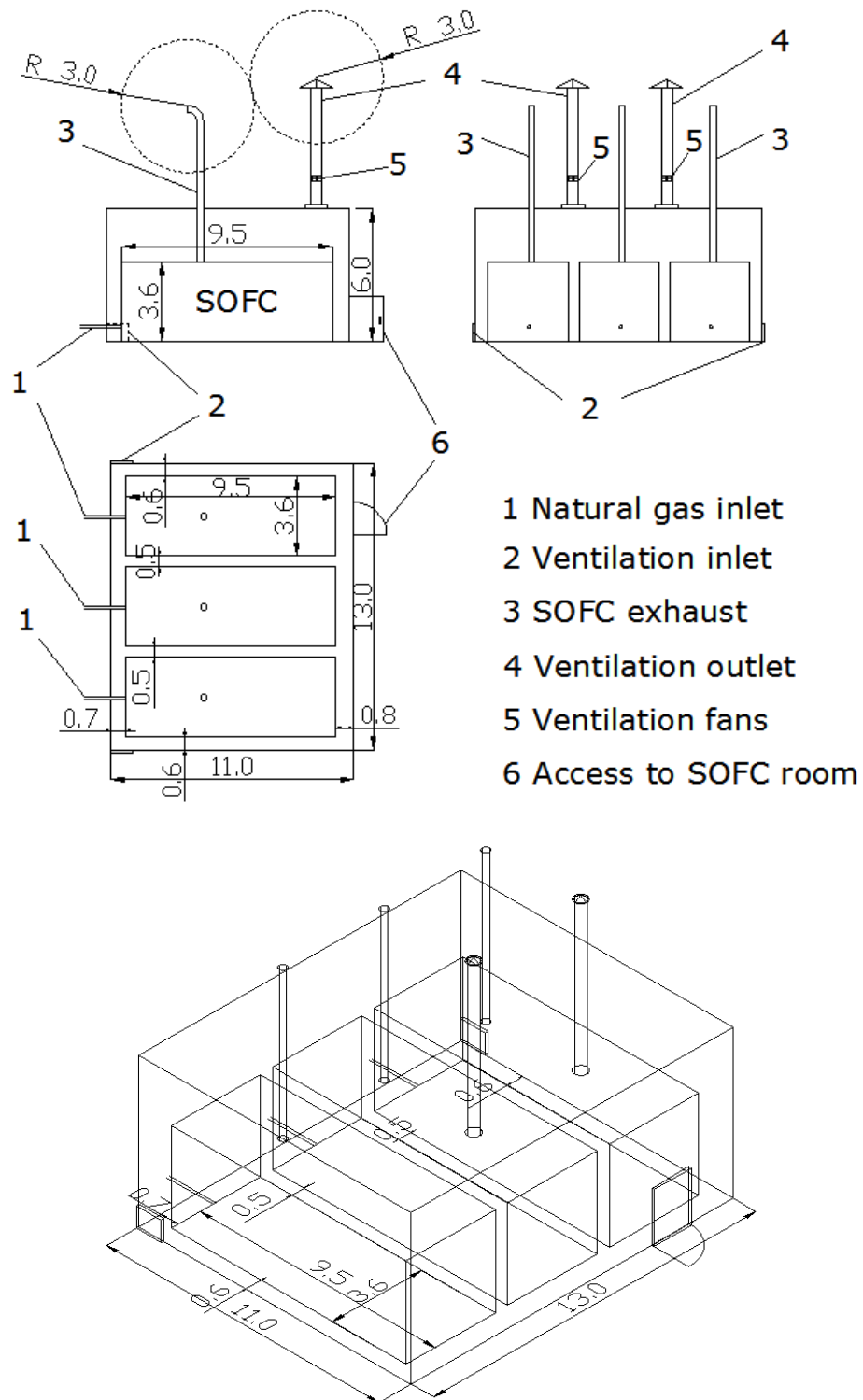


**Figure 6.7: SOFC room arrangement plan (unit in meters)**

As can be seen from figure 6.7, the fuel cell room has a dimension of 11×13×6 (L×W×H) cubic meters which makes enough clearance space between fuel cell modules and walls of the SOFC room. The three SOFC units are self enclosed. The gas inlet pipes (number 1 in figure 6.7) will penetrate the bullhead of the SOFC room and lead to the compressor room which is located directly next to SOFC room. The exhaust pipes are positioned at the roof of SOFC units all the way penetrating the SOFC room roof and lead to the open air. The ventilation system is arranged to have two inlets (number 2 in figure 6.7) and two outlets (number 4 in figure 6.7) in case one of them failed. The ventilation outlet is approximately 6 meters away from the SOFC exhaust pipe outlet (number 3 in figure 6.7). This arrangement will ensure the potential ignition sources are away from the possible methane gas mixture.

The SOFC is very sensitive to gas composition. Mole percentage of methane in natural gas will dominate the performance of the fuel cell. For a specific composition of natural gas, the SOFC system configuration needs to be adjusted to provide best performance. Incorrect settings of systems, e.g. re-circulator and controller, may cause damage or failure of the systems. Even though the SOFC is using BOG as fuel which contains near pure methane, a gas composition monitor device, such as gas analyser or gas chromatograph, is to be installed.

### **SOFC typical working condition:**

The typical working conditions for the Siemens SOFC are summarized as figure 6.8. The data is extracted from the public release of Siemens CHP250 type SOFC (*Siemens tubular SOFC*, 2013). Both the air inlet and the natural gas fuel inlet are around atmospheric pressure. The inlet air is preheated by heat exchanger to 594 °C before enter into the SOFC stack. The reactions inside SOFC stack is already explained in section 2.2 and there as not repeated here.

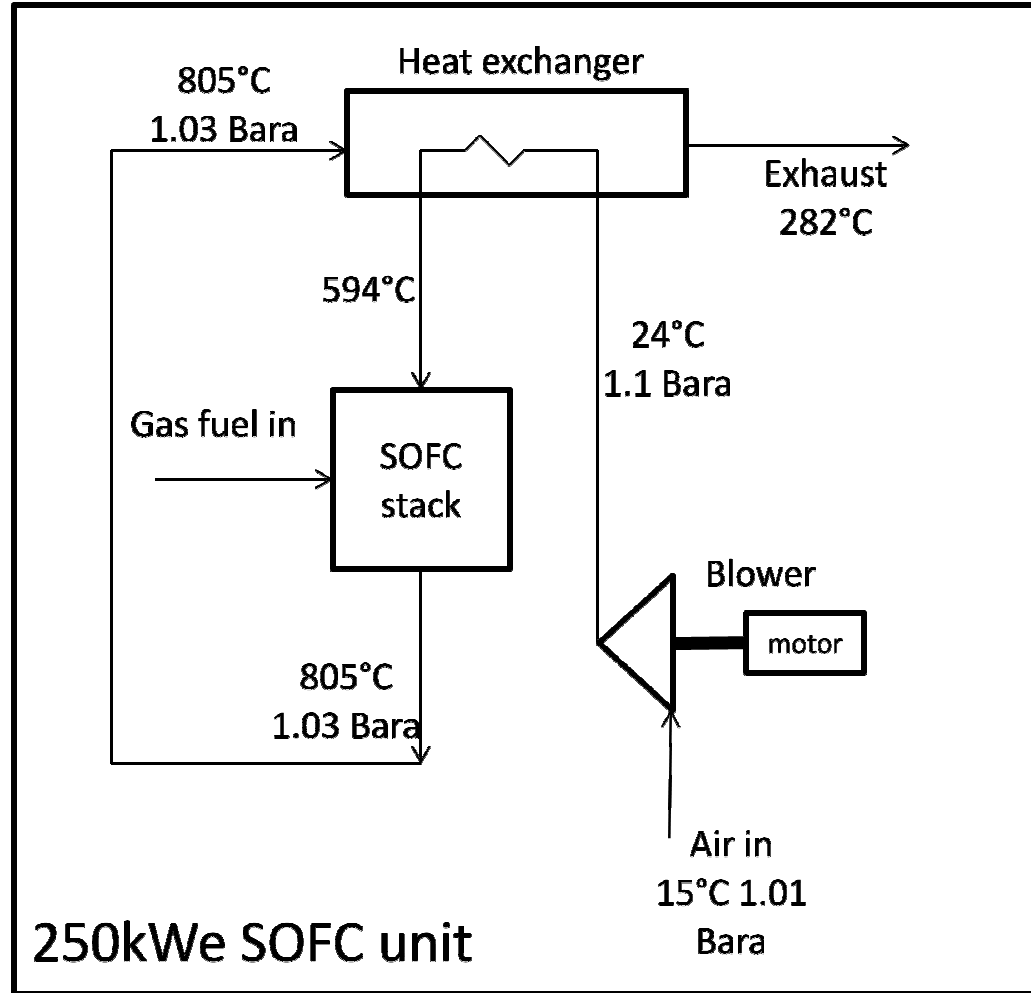


**Figure 6.8:** Typical working conditions for the Siemens CHP250 SOFC unit

### Gas supply system for SOFC:

The conceptual design of gas fuel supply system for SOFC is illustrated in figure 6.9 (a) and 6.9 (b) where “M” means main pump, “S” means spray pump, “HD” means high duty compressor, “LD” means low duty compressor and “IG” means inert gas. The system is designed to use the existing ship cargo system onboard the mother ship to supply BOG to SOFC at near atmospheric pressure. As indicated in figure 6.8 (a) when BOG generated is enough to feed SOFC, the relatively low temperature natural gas

vapour is collected in the gas dome at the top of cargo tank. Low duty compressor is used to feed the BOG to a gas heater to bring the natural gas to a desirable temperature and pressure for SOFC. In some special occasions, such as loading and unloading operations, where the natural generated BOG is not enough for SOFC consumption, spray pump is used to pump out a certain amount of cold LNG and send to forcing vaporizer to vaporize LNG to gas phase and then further feed the gas to low duty gas compressor and gas heater before finally feed to SOFC. This process is illustrated in figure 6.8 (b).

Gas supply pressure is also important for fuel cell systems, normally 138-344 (mbarg) for this non-pressurized SOFC system. Consequently, the gas supply of a fuel cell system needs to be monitored in real time, especially when an LNG ship is loading and unloading at a terminal when the changes of gas pressure and composition may occur. A gas control device is therefore needed to monitor composition of gas supply in real time.

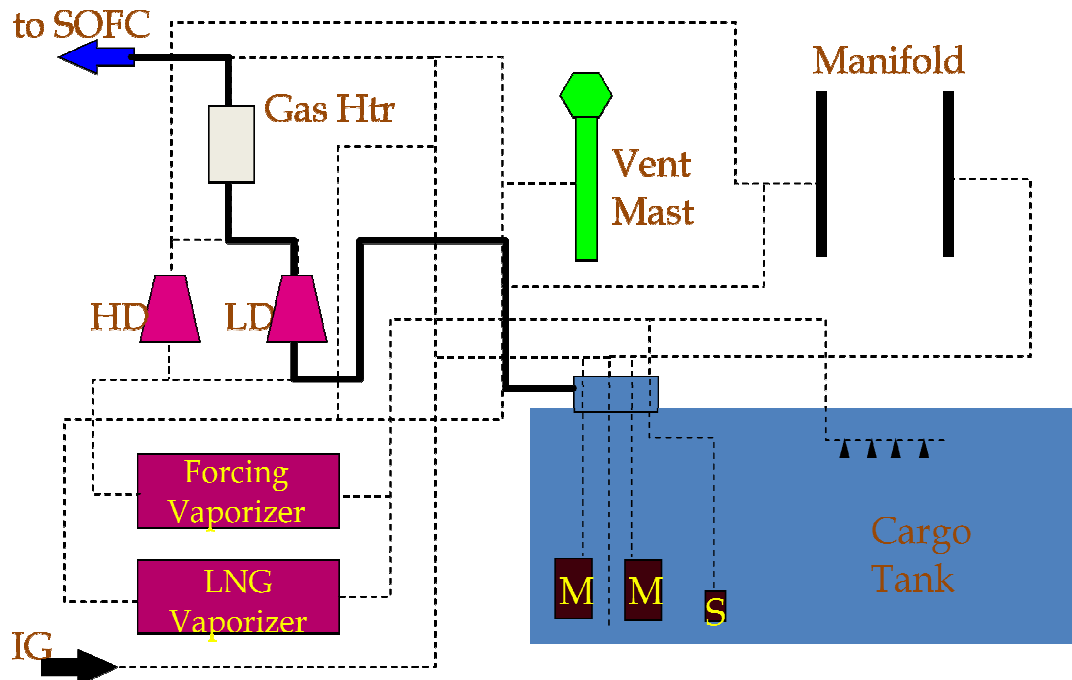


Figure 6.9 (a): Natural boil off gas fuel supply to SOFC

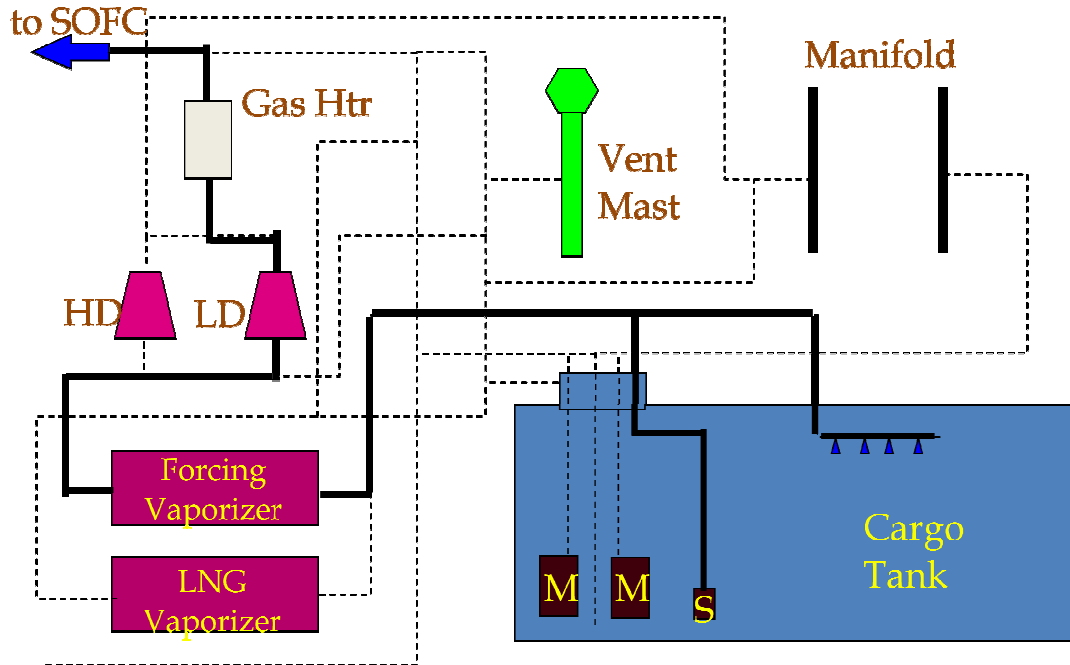


Figure 6.9 (b): Forced boil off gas supply to SOFC

#### BOG rate calculation:

The BOG is supplied during both the laden voyage and the ballast voyage. During ballast voyage, an amount of cargo heel is to be maintained to keep the cargo tank cool before reloading and also provide fuel gas for SOFC. The BOG generating rate for the LNG ship is around 0.35% per day which is equivalent to 1.75 ( $\text{m}^3/\text{h}$ ). If assuming the LNG is vaporized at neat atmospheric pressure and -160 ( $^\circ\text{C}$ ) then the BOG generating rate is equivalent to 734 ( $\text{kg}/\text{h}$ ).

#### SOFC gas fuel consumption:

The SOFC system (Siemens CHP250) have a typical electrical output efficiency of 47% calculating on the lower heating value of 50 (MJ/kg) for methane. It gives a methane consumption rate of 114.9 (kg/h).

The BOG generated (734 kg/h) is far more than the amount being consumed by the SOFC consumption (114.9 kg/h) in normal design conditions. The excessive BOG will be either contained within the cargo tank by allowing the gas phase pressure to rise inside the tank or burned at a combustion unit. When allowing the gas pressure to rise in the cargo tank, the pressure inside the LNG cargo tank will normally take over 50 days to reach the design pressure of 4 (barg) given a mean K-value tank insulation rate of 0.121 (W/m<sup>2</sup>K). This 50 days buffer range will be longer enough for regional LNG distribution purpose. Therefore no additional reliquefaction plant or other BOG management means are needed for this conceptual design.

### **SOFc room ventilation arrangement and calculation:**

There are two ventilation inlets and two ventilation outlets. The ventilation inlets (number 2 in figure 6.7) are placed at the lower corners of the SOFC room close to the gas inlet pipes where gas leaks are likely to happen. The ventilation outlets (number 4 in figure 6.7) are placed at the roof of the SOFC room and away from the SOFC exhaust pipes outlets. Each ventilation outlet duct is equipped with a ventilation extract fan driven by electric motor (number 5 in figure 6.7).

The SOFC room ventilation is required to have a minimum 30 air changes per hour according to the ship rules (Appendix 1.4). The calculation of ventilation rate is indicated as equation 6.1 assuming the ventilation space is the SOFC room volume deduces three SOFC units' volume.

$$(13 \times 11 \times 6 - 9.5 \times 3.6 \times 3.6 \times 3) \times 30 = 14659 \text{ m}^3 / \text{hour} = 4.07 (\text{m}^3 / \text{sec}) \quad (6.1)$$

It is also considered that the air inlet needed for the three SOFC units are calculated as equation 6.2 assuming the air inlet ratio for the Siemens CHP250 SOFC is around 0.002 (kg/kW·s) and the air density is about 1.13kg/m<sup>3</sup>.

$$\frac{250 \times 3 \times 0.002}{1.13} = 1.32 (\text{m}^3/\text{sec}) \quad (6.2)$$

Therefore the overall ventilation rate required for the SOFC room is 5.39 (4.07+1.32) ( $\text{m}^3/\text{second}$ ).

It is also noted that air flow velocity in ventilation ducts should be kept within certain limits to avoid noise and friction loss and energy consumption. If assuming the recommended ventilation flow velocity inside the ventilation duct is 10 meters/second (Recommended air velocities in ducts, 2013, *The engineering Tool Box*) for low pressure duct system, then the total ventilation inlet duct cross section area is to be  $0.539 (\text{m}^2)$  and the ventilation outlet duct cross section area is to be  $0.407 (\text{m}^2)$ .

As can be seen in figure 6.7 there are two ventilation inlet ducts and two outlet ducts. Therefore the cross section area for each ventilation inlet duct is about  $0.27(\text{m}^2)$  and the cross section area for each ventilation outlet duct is about  $0.204 (\text{m}^2)$ .

As indicated in figure 6.7, the ventilation outlet is to be at least 3 metres away from any source of ignition. The exhaust outlet is also to have a 3 metres clearance from source of ignition.

### 6.5.3 Operating strategy

Considering the electric load demand as summarized in table 6.2, the 750 (kW) SOFC system will run continuously to cover service load and hotel load at all time. The main engine shaft generator will help to generate extra electricity when the main engine is running at laden voyage. The BOG generated form cargo tank is used as primary gas fuel for SOFC. Exhaust gas heat from both main engines and SOFC is recovered in exhaust gas boiler to generate steam. Shaft generator and SOFC will feed the electric consumers from the main switchboard.

The operational strategy of the power plant is summarized as table 6.4:

**Table 6.4: Operation strategy of designed power system**

	<i>Main Diesel (kW)</i>	<i>Shaft Generator (kWe)</i>	<i>SOFC (kWe)</i>
Laden voyage	7,000	790	3×50
ballast voyage	6,500	N/A	1×250 2×50
Manoeuvre	1600	N/A	3×250
Cargo discharge	N/A	N/A	3×250
Harbour stay	N/A	N/A	1×200 2×50

While at laden voyage, the main engine will provide the propulsion power and also drive the shaft generator to provide service electric load. The shaft generator will cover the all the electrical power load during laden voyage. The Three SOFCs can run at a very low idle load around 50 (kWe) each to keep the SOFC system warm and ready.

While at ballast voyage when the service electrical load is mainly from the service load of around 350 (kWe), three SOFC unites are running with one SOFC providing 250 (kWe) output while two SOFC operating at low load approximately 50 (kWe) each. SOFC electric output feed into the main switchboard. The main switchboard supplies all electric consumers. The LNG ship's cargo tank should leave enough heel cargo to maintain the cold condition of cargo tank and also to feed SOFC as gas fuel.

While the ship is at manoeuvring, the bow thrusters will require 400 (kWe) in addition to the 350 (kWe) service load. The three SOFC units will all running at full load providing a combined output of 750 (kWe).

While the ship is at harbour, three SOFC are running at full load to provide electricity used for all service load as well the cargo pump electrical consumption.

While the ship is stayed at harbour without cargo operation, three SOFC unites are running with one SOFC providing 250 (kWe) output while two SOFC operating at low load approximately 50 (kWe) each.

#### 6.5.4 Economical analysis

In this section, a high level comparison of the proposed 750 (kW) SOFC plant to ordinal diesel generating plant will be analysed from both economical and environmental perspectives (The reason for only comparing SOFC with diesel generating plan is that the currently available and reliable dual fuel engines do not cover this small power range). To make the comparison sensible, certain assumption shall be made beforehand to estimate the CAPEX and OPEX.

As a quite mature market, the CAPEX of traditional marine diesel engine generating plant can be easily quoted from the manufactures. Therefore it is assumed that a 750 (kW) diesel generating plant including three 250 (kW) diesel engines and three electric generators will cost 640,000 (USD) including the commissioning cost. For CAPEX of SOFC, James and etc. (2012) estimated in their report that the cost of SOFC will be around 402 to 532 (USD/kW) depends on the mass production rate of the system. So if adopting a relatively higher estimation of 532 (USD/kW) plus some margins for profit and uncertainty, it is safe to assume a 800 (USD/kW) for estimation of the SOFC on its own. Then it works out around 600,000 (USD) for the 750 (kW) SOFC system. If auxiliary equipment, installation cost, and mariniation cost (including Class approval) are included, it is safe to assume a 1,500,000 (USD) to put a 750 (kW) SOFC system onboard and up-running.

Whiles OPEX of a generating plant involve in various items such as maintenance cost, repairs, spare parts, fuel cost and etc, but the cost of fuel will obvious prevail among all the factors. It is therefore to use fuel cost to compare the OPEX. The bunker fuel market is a very volatile and the industry quotes from many different sources of fuel cost depends on the source that best suits the application. For clarification, table 6.5 summarized the assumptions for the prices of marine bunker fuel and LNG bunker price based on the latest market resource published by Bunker world (2013) and Platts (2013). It is to be noted, at the moment there is no LNG bunker price available. The LNG

bunker priced used in table 6.5 is based on the assumption the reliquefaction cost for converting pipeline gas to LNG is around 1.5 US dollars per MMBtu.

**Table 6.5: Fuel oil bunker price versus LNG bunker price at July 2013**

\$US/MMBtu	IFO380	MGO	NG	LNG
Tokyo	15	23	N/A	15.65
Houston	14	23.2	3.6	5.1
Rotterdam	13.6	20.8	10.4	11.9
Singapore	14.3	22.4	N/A	15.25

The difference in fuel cost between oil fuel and LNG varies depending upon the source of LNG and also the fuel oil used for diesel engine. It is clearly for diesel engine of a few hundred kilowatts range, heavy fuel oil cannot be used. Also based on the fact that the price difference for MGO (Marine Gas Oil), MDO (Marine Diesel Oil) and low sulphur MGO is similar. So it is assumed the MGO price in table 6.5 will be used as fuel cost for the diesel engines for easy comparison. As the SOFC will use the LNG cargo in the LNG ship as fuel, the cost of the LNG fuel will be the same as the LNG cargo price where the cargo is being loaded. Although the LNG price in table 6.5 already very attractive compare with oil fuel, but the LNG cargo from a LNG export terminal, such as Qatar or Brunei, at whole sale volume will even cheaper than that. Therefore for this particular case of LNG ship, it is very safe to assume the LNG fuel price is the same as the LNG cargo being transported.

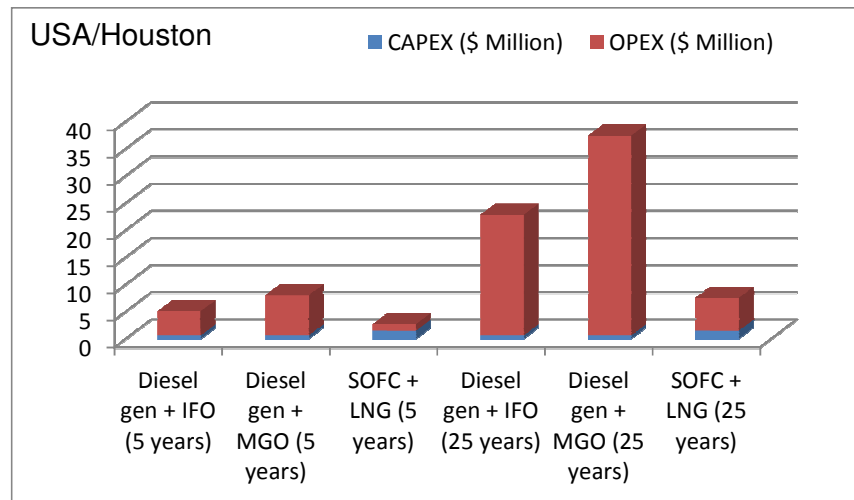
As introduced in section 6.5.1, the SOFC system (Seimens CHP250) have a typical electrical output efficiency of 47% calculating on the lower heating value of 50 (MJ/kg) for methane. While the diesel engine generating used for the original LNG ship has a electrical output efficiency of around 35.3% based on a lower heating value of 43 (MJ/kg) for diesel fuel, specific fuel consumption of 217 (g/kWh) and electrical generator conversion efficiency of 91.5% (Caterpillar 2308 specification, 2013).

Based on the assumptions of the costs as above, the comparison of CAPEX and OPEX between original diesel generating plant and the 750 (kW) SOFC conceptual design is summarized in table 6.6.

**Table 6.6: Economic comparison between diesel generating plant and SOFC system**

		750 (kW) Diesel generating plant fuelled by diesel oil	750 (kW) SOFC fuelled by pure methane
CAPEX (USD)		640,000	1,500,000
OPEX (USD)	Fuel consumption (kg/h)	177.87	114.9
	Fuel consumption (MJ/h)	7648.41	5745
	Fuel consumption (MMBtu/h)	7.24	5.44
	Fuel consumption (MMBtu/year)	63,422	47,654

Based on the information provided in table 6.5 and 6.6, a comparison of diesel generating and SOFC system is performed. The comparison takes into account the types of fuel used, bunkering location, and years of ship operation. The comparison results are indicated in figure 6.10 as below.



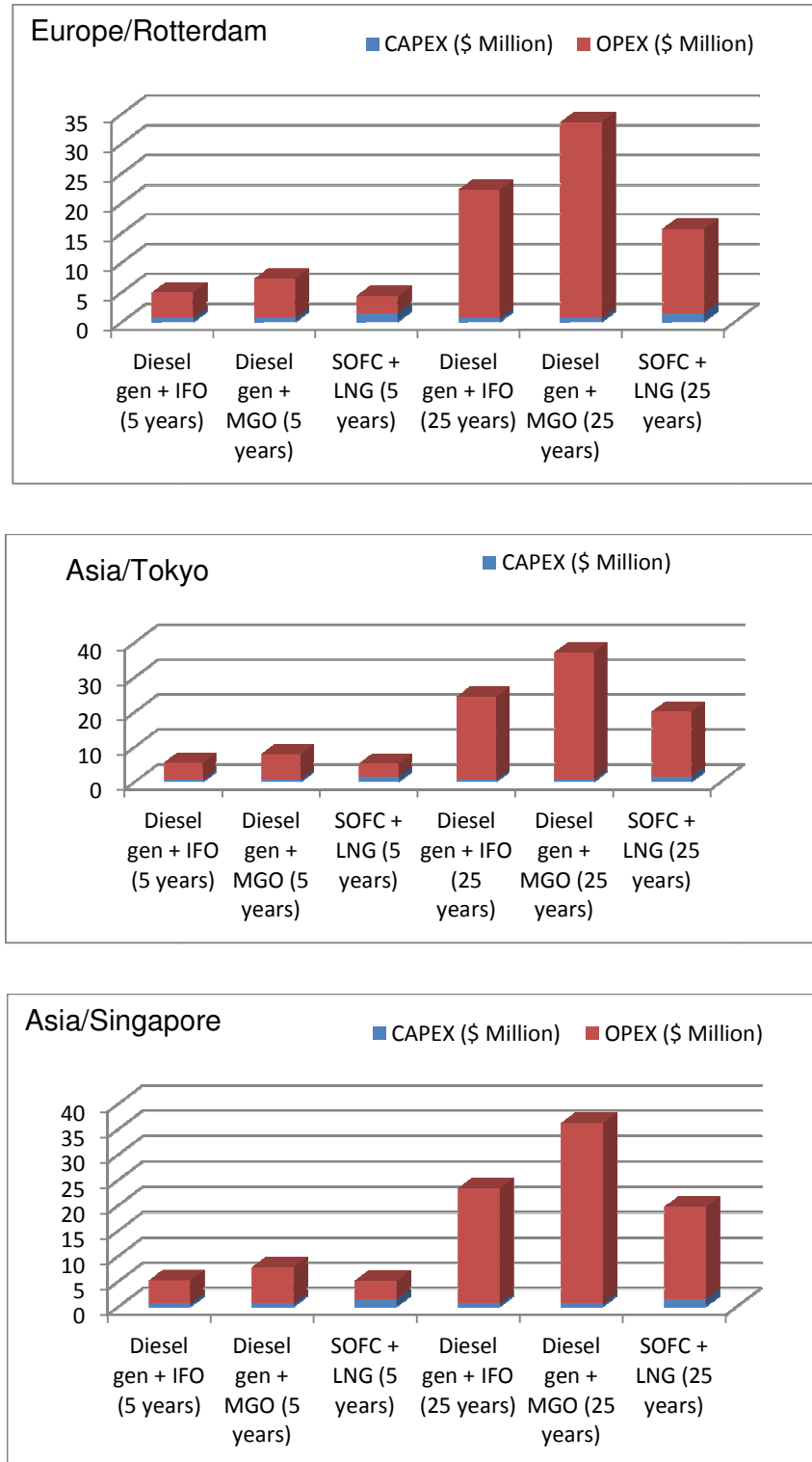


**Figure 6.10: CAPEX and OPEX estimation for 750 (kW) diesel generation and SOFC**

From the comparison in figure 6.10, the CAPEX is only taken a small share of the overall running cost for all scenarios. It is also clearly indicated the favourable cost saving by replacing diesel auxiliary plant with SOFC system for the 12,000 m<sup>3</sup> LNG ship.

In the US, after five years running, the overall cost saving including CAPEX and OPEX will be around 6.14 million US dollars; while after a 25 year running of the ship's life, it could save an astonishing 30.7 million US dollars when comparing diesel generation using MGO and SOFC using LNG, thanks to the high efficiency of SOFC and the low cost of LNG in America.

In Asia (Tokyo and Singapore) where the bunker price difference for fuel oil and LNG is not significant, SOFC system using LNG can also half the overall cost compare with diesel generation using MGO as fuel. Even if compare with diesel generation using IFO as fuel it can also achieve over 20% overall cost saving.

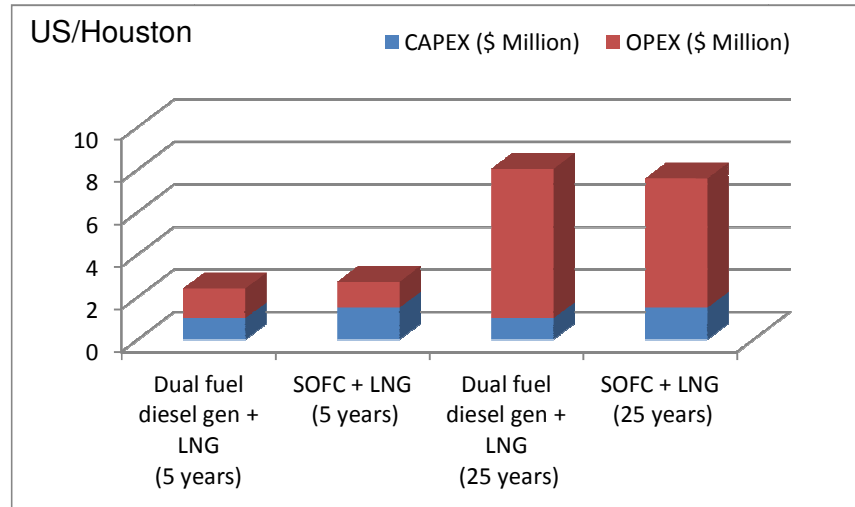
In Europe the LNG price is less expensive than Asia but much higher than US. The overall cost saving including CAPEX and OPEX will be around 3.76 million US dollars; while after a 25 year running of the ship, it could save 18.8 million US dollars when comparing diesel generation using MGO and SOFC using LNG, thanks to the high efficiency of SOFC and the relatively low cost of LNG in Europe.

The above comparison arguably maximized the advantages of high efficacy and low cost of LNG for SOFC system for this particular case study, due to that there is no dual fuel diesel or gas burning engine are commercially available for a few hundred kilowatts range. However if looking at a wider application for SOFC as auxiliary power generation for merchant ships, then competition from the latest dual fuel and gas engine technology has to be taken into account. In this respect, the benefit of low LNG fuel cost will be wiped out if comparing SOFC to dual fuel diesel generating plant. The most recent model of marine dual fuel engine such as Wartsilar 34 DF power generating plant (Wartsila 34DF engine, 2013) will have 40.6 % electrical efficiency when burning methane as fuel (Brake specific fuel consumption 8510 kJ/kWh) based on the electrical

generator conversion efficiency at 96% (Wartsila 34DF engine and generating sets, 2013 specification, 2013). The cost for SOFC installation is unchanged at 1.5 million USD while the installation cost for dual fuel engine is changed to 1 million USD considering the higher engine price and the gas supply system. Therefore under these assumptions the economic picture of SOFC compare with dual fuel generating will be changed to table 6.7 and figure 6.11.

**Table 6.7: Economic comparison between Dual fuel diesel generating plant and SOFC system fuelled by methane**

		750 (kW) Diesel generating plant fuelled by methane	750 (kW) SOFC fuelled by methane
CAPEX (USD)		1,000,000	1,500,000
OPEX (USD)	Fuel consumption (MJ/h)	6650	5745
	Fuel consumption (MMBtu/h)	6.298	5.441
	Fuel consumption (MMBtu/year)	55,170	47,663



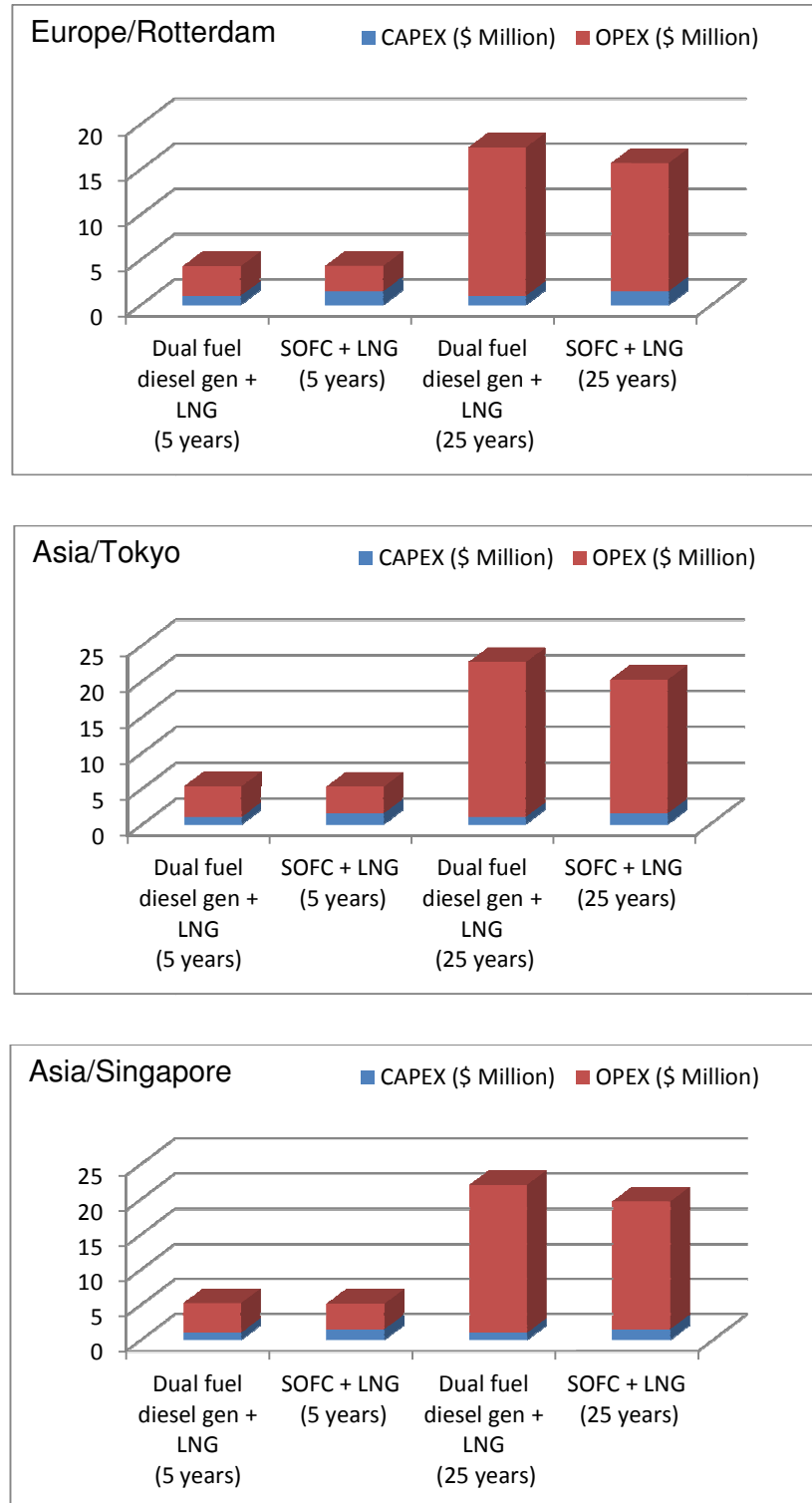


**Figure 6.11: Comparison of 750 (kW) dual fuel engine and SOFC using methane as fuel**

It can be seen from figure 6.11, whilst considering using LNG at all four bunkering locations, SOFC will also prevail to dual fuel engine in terms of overall cost saving thanks to its relatively higher electrical output efficiency. But the competitive advantages are less significant than comparing SOFC with diesel engine. The more expensive capital cost of SOFC also looks negligible compare with the long term fuel cost savings.

On top of advantages of cost saving, SOFC also enjoy the environmental benefit. The sulphur oxidation emission from the SOFC exhaust is near zero thanks to the very low sulphur content in the natural gas fuels. The nitrogen oxide emission from the SOFC exhaust is around 0.5 (ppm) (Forbes, C.A. (2003)) which is also insignificant compare with dual fuel engines or gas engines when using methane as fuel.

## 6.6 Conclusion

Onboard installation of the SOFC is a complicated topic. Safety issues and seagoing environments need to be considered for marine application. The relevant ship rules and regulations are analysed in this chapter. Even though no authorised rules are available at present, traditional shipping rules are applicable for SOFC system applications as indicated by LR and DNV. Industry standards and manufacturing standards are also referable for SOFC marine application.

According to the rules' analysis, various obstacles prevent on board use of large scales of fuel cell power plant. The reasons come from both fuel cell technology and sea going circumstances. Consequently improvement and modification measurements are examined for SOFC systems to be installed onboard ships.

Finally, a conceptual design for 750 (kW) SOFC marine application are proposed in line with the previous technical discussions. The 750 (kW) SOFC system was chosen to installed onboard a 12,000 ( $m^3$ ) LNG carrier to provide electricity power supply for auxiliary services. The system arrangement including fuel gas supply system is

presented. Economical analysis and comparison between the SOFC system and original diesel generating system is also provided. The comparison results show a huge cost saving to replacing diesel generating plant with SOFC system due to the low natural gas price and the high efficiency of SOFC. It also concluded that even compare with gas burning dual fuel diesel engines generating plant, the SOFC will also have advantages in terms of fuel cost saving and environmental benefits.

## Chapter 7 Thesis summary and conclusion

### 7.1 Summary of the thesis

Bearing the characteristics of silent, vibration free, high efficiency and environmental friendliness, SOFC technology has the potential to replace virtually all sources of main and auxiliary power of merchant ships. However the obstacle at the current stage is that of lack of experience of marine SOFC application, which intimidates the potential users to install this novelty onboard. Ship owners want to know how SOFCs will perform in seagoing circumstances. One solution for the problem is to resort to computational simulation which is an effective method to imitate and predict the actual operating status for marine SOFC systems. Therefore, the thesis provided an integrated SOFC marine power system model which can simulate the static and real time performance of SOFC power systems in various working conditions that may occur on ships.

In the thesis, the simulation work of SOFC marine power systems is specified on the characters of high temperature tubular SOFC manufactured by Siemens. The whole SOFC marine power system has been decoupled into subcomponents and subsystems to facilitate the modelling works at the first phase. These subcomponents were computed concerning the mechanism of each part, e.g. SOFC stack was modelled considering electric-chemical reactions, fuel reforming, heat transfer and energy balance; a battery model was established by a hypothetic equivalent circuit; a propulsion train was described according to interaction of propeller, ship hull resistance and electric motor. Then these subcomponent models were integrated into systems which could function together by implementing a viable system control strategy.

Characteristics of dynamic response of the SOFC system are determined by identifying time inertia of the system. For starting the process of a SOFC power system, stack temperature takes hours to warm up to avoid sudden temperature differences and resultant material fatigue malfunction. The temperature profile and thermal stress of the SOFC stack structure was computed using the CFD method. The optimised minimum starting time was then deducted. As for the transient response of the SOFC system at

load change, the time delaying effects from controllers and gases flow manifolds are implied in dynamic modelling.

In the thesis two SOFC power systems were modelled and validated, i.e. a 5 (kW) SOFC power system stand-alone and a 5 (kW) SOFC generating system with battery connection in parallel. Both static and dynamic simulations are performed by using the proposed simulation model. Shipboard installation issues for the SOFC are discussed in the last part of the thesis with a conceptual design of 750 (kW) SOFC auxiliary power system for small LNG ship.

## 7.2 Simulation results validation

The review in chapter 1 concluded that marine application of fuel cells is very rare, especially for SOFC marine applications. Up to today, the only SOFC marine application was the 20 (kW) planar SOFC system installed onboard the Wallenius Car and Truck Carrier “Undine” for testing purposes for the METHAPU project (METHAPU project, 2010). The SOFC was then removed from the ship after testing. Accordingly, finding reliable data to verify the model in this thesis became a difficult job due to the fact that no tubular SOFCs have ever been installed or tested in a marine environment.

In the thesis two sources of testing data were used for verification of the modelling result: The first is from the land-based trial data for FCT’s Beta 5 (kW) tubular SOFC system (Allen, 2004); second is testing data from the METHAPU project as mentioned above.

FCT ran a worldwide trial test at four different places for its 5 (kW) tubular SOFC system. In comparison, the general simulation results of the model used in the thesis are compared with a group of real test data according to the laboratory test from Fort Michigan (Operation and maintenance manual Beta 5 kW SOFC system, 2005). The modelling results are simulated for steady state and are summarised in table 7.1 when

assuming a working temperature of 847 ( $^{\circ}\text{C}$ ). It is obvious that the outcome from steady state simulation has a better system performance than the test data. This is mainly because the active surface area of cells in the simulation model is an ideal value. In practice, not all of the active area of cells is fully used.

In the similar case of the METHAPU project, the onboard testing of the SOFC was not running on nominal power due to the unstable operation of the pre-reformer at high currents and to prevent carbon formation. However, the sister unit of the SOFC used for the METHAPU project, WFC20 Proto2, was tested in the laboratory at nominal level, where water feed could be discontinued and the nominal stacks loading state could be reached. The test resulted in a 41% net AC electrical efficiency. Approximately 41% overall net efficiency also partially verified the model simulation of the 43.8% outcome, although different types of SOFC were used.

**Table 7.1: Comparison of simulation results with test data**

System		Simulation results	Ford Michigan ALFA
Net power	AC (W)	1979	1700
	Overall AC Efficiency	43.8%	37.8%
	DC (W)	2328	2192
	Efficiency	51.5%	48.7%
Stack	Power (W)	2616	2492
	Efficiency	58%	55.4%
Heat recovery	Hot Water (W)	1403	1400
	Overall Efficiency	31.1%	31.1%
Fuel energy	W (LHV)	4513	4498
Overall System Efficiency		74.9%	68.9%

In order to verify the practical requirements for ship application, a questionnaire to shipbuilding engineers, ship designers and classification surveyors was conducted from June to October 2012. The respondents include: 24 machinery engineers and electrical engineers, having at least five years' experience in ship outfitting related work, from various ship yards of the China Shipbuilding Industry Corporation; two ship design engineers from Shanghai Merchant Ship Design & Research Institute; and two ship surveyors from Lloyd's Register London Design Support Office. In the survey questionnaire, the practically accepted error rate for main and auxiliary power was asked. The survey results show that an acceptable overall error range for modelling can be as high as 2% to 5% for main propulsion power. This is because in this error range, the final sea acceptance test figure can be adjusted by using related design factors. It is also concluded that, for most of the shipbuilding contract, a 2% to 5% deviation in main power is tolerable. The survey also shows that a "relative accurate" dynamic simulation model covering all key components of the system and with a reasonable simulation time is desired and appreciated.

Based on the criteria of the industry survey results, as explained above, the simulation result for fuel efficiency of the SOFC stack of 2.4% difference to laboratory testing is acceptable. It is also noted that the simulation model assumes 100% usage of active surface area of cells. In practice, not all of the active area of cells is fully used. If a correction factor is added, then the simulation will have a near perfect result.

Verification of the dynamic simulation results for a lump sum SOFC model is a very difficult job, because the lump sum model comprises of so many factors (such as, stack temperature response, chemical reaction rate, air flow rate response time, fuel gas flow rate response time, battery response time, electric motor response time, and control device response time) which can affect the time domain response. It is also the first time a full system lump sum model for a SOFC marine system has been introduced. There is no readily available ship trial data or similar testing data to date. Therefore, a like to like comparison of existing Ship Classification Rules for oil engine propulsion is used to verify the dynamic simulation result of the lump sum SOFC marine model.

According to the Lloyd's Register Rules and Regulations for the Classification of Ships (2012), Part 5, Chapter 2, Item 5.3.4, “For alternating current installations, . . . Momentary speed variations with load changes are to return to and remain within one per cent of the final steady state speed. This should normally be accomplished within five but in no case more than eight seconds”. That is to say for a marine used alternating current electrical power device, the dynamic output of the device shall return to one percent of the steady state speed within five but not more than eight seconds.

As discussed and concluded in section 5.2.2 of the thesis, overall response time of a required load change for the lump sum model is around 1.1 to 1.5 seconds (see figure 5.11 and 5.12). This result is well within the required five seconds response time required for marine diesel engines.

### 7.3 Conclusions

The thesis proposed an integrated and real time model which can simulate both the steady state and dynamic response of SOFC power system. The model considered the influences of pre-reforming, internal reforming process of fuel gas, temperature change, battery response, mechanical drive chain, electrical drive chain and time delays caused by the control system. Based on the simulation results at both steady state and dynamic state, the following conclusions can be drawn:

- The simulation results are very close to the data of manufacturer’s running test in terms of general operating characters.
- The dynamic character of the SOFC is largely determined by two time constants namely, stack temperature time constant  $\tau_{stack}$  and inlet and outlet manifold time constant  $\tau_{manifola}$ . The constants  $\tau_{stack}$  is determined by SOFC material and mass of SOFC structure and flow rate of air and gas fuel; while  $\tau_{manifola}$  is

determined by volume of manifolds, geometry of flow channel, temperature and characters of air and gas.

- The starting time of the SOFC power system can be reduced dramatically by optimising starting control logic.
- According to dynamic simulation results, when the SOFC system is running at stand-alone mode, it could meet the requirement of transient load changing as regulated by ship rules. However, the electric power output would be greatly smoothed if the SOFC is paralleled with a battery.

Following a detailed review and examination of shipboard installation issues, it is concluded that the marine installation of an SOFC system can be assessed and examined to comply with relevant ship rules and regulations. The practical approach is to break down SOFC systems into subsystems and devices that can be recognised and applied by traditional ship rules, like the piping system, bunkering line system, storage tank and pressure vessel, electric equipment, control equipment, structure and housing, ventilation, fire fighting and alarm etc. The examination result shows there are many improvements and adjustments are needed for land based SOFC systems to be installed onboard ships. The practical challenges for SOFC marinisation are mainly identified as

- marine operating environment
- volume density of SOFC system
- SOFC output power range
- system durability and reliability
- exhaust heat recovery and integration with ship system
- frequent starting and shutdown arrangement

A conceptual design was proposed in the last part of the thesis. The 750 (kW) SOFC power system is designed to provide auxiliary power supply for a 12,000 ( $m^3$ ) LNG carrier. Economical analysis and comparison between the SOFC system and original diesel generating system showed a huge cost saving thanks to the low natural gas price and the high efficiency of SOFC. It also concluded that even compare with gas burning

dual fuel diesel engines generating plant, the SOFC will also have advantages in terms of fuel cost saving.

To sum up, base on the proposed model and simulation results, SOFC system is capable of satisfying the requirements of ship operations as both propulsion power and auxiliary power. Arguably SOFC could produce large power output with high efficiency and is perhaps most suitable for merchant marine operating environments. It is also expected that the manufacturing technique will gradually improve, which may substantially increase its efficiency and durability. However, technical obstacles need to be conquered to practically install the SOFC system onboard ships. The economical comparison between SOFC and diesel engine system of the conceptual design shows a dramatically fuel cost saving. The massive fuel cost saving and the environmental benefits will make the expensive SOFC capital cost negligible in long term running.

## Reference

Alkaner, S. and Zhou P.L. (2006) 'A comparative study on life cycle analysis of molten carbon fuel cells and diesel engines for marine application', *Journal of Power Sources*, 158, pp. 188-199.

Allen, G. (2004) 'Demonstration program for 5kW SOFC system', *2004 Rural Energy Conference*, Apr 27 2004.

Autissier, N., Larain, D., Van herle, J. and Favrat, D. (2004) 'CFD simulation tool for solid oxide fuel cells', *Journal of Power Sources*, 131, pp. 313–319.

*Bahrain Vision* (2013), Available at:

<http://www.marinetraffic.com/ais/shipdetails.aspx?MMSI=565527000> (Accessed at 12 September 2013)

Batchelor, G. K. (1967) *An Introduction to Fluid Dynamics*. Cambridge Univ. Press, Cambridge, England, 1967.

Bessett, N.F. (1994) *Modeling and Simulation for Solid Oxide Fuel Cell Power Systems*, Ph.D. Thesis, Georgia Institute of Technology, USA.

Bossel, U.G. (1992) *Final Report on SOFC Data Facts and Figures*, Swiss Federal Office of Energy, Berne.

*Bunker world* (2013), Available at:

<http://www.bunkerworld.com/prices/region/maj> (Accessed at 06/11/2013)

Campanari, S. and Iora, P. (2004) 'Definition and sensitivity analysis of a finite volume SOFC model for a tubular cell geometry', *Journal of Power Sources*, 132, pp. 113-126.

- Caterpillar 2308 specification* (2013), Available at:  
<http://marine.cat.com/cda/files/1014960/7/Spec%20Sheets%20-%20Cat%203208%20Propulsion.pdf> (Accessed at 26 September 2013)
- Chan, H., Khor, K. and Xia, Z. (2001) ‘A complete polarization model of a solid oxide fuel cell and its sensitivity to the change of cell component thickness’, *J. of Power Sources*, vol. 93, pp. 130–140.
- Chan, S.H. and Xia, Z.T. (2002) ‘Polarization effects in electrolyte electrode-supported solid oxide fuel cells’, *Journal of Applied Electrochemistry*, 32, pp. 39–47.
- Cheddie, D. and Munroe, N. (2005) ‘Review and comparison of approaches to proton exchange membrane fuel cell modelling’, *Journal of Power Source*, 147, pp. 72-84.
- Chudley, J. and Munson, M. (1997) ‘Power limited design for small craft’, *International conference on power performance & operability of small craft*, Southampton, 1997
- Costamagna, P., Costa, P. and Antonucci, V. (1998) ‘Micro-modelling of solid oxide fuel cell electrodes’, *Electrochimica Acta*, vol. 43-3/4, pp. 375–394.
- Costamagna, P. and Honegger, K. (1998) ‘Modeling of solid oxide heat exchanger integrated stacks and simulation at high fuel utilization’, *Journal of the Electrochemical Society*, 145(11), pp. 3995–4007.
- DeepC project*. (2005) Available at: [www.deepc-auv.de](http://www.deepc-auv.de) (Accessed 28 November 2005)
- Deep-sea cruising AUV URASHIMA*. (2009) Available at:  
<http://www.jamstec.go.jp/e/about/equipment/ships/urashima.html> (Accessed: 2 May 2009)
- Development of a Hybrid Fuel Cell Ferry, Summary Report* (2003) Water Transit Authority. (Accessed: 21 August 2003)
- Electric Warship Technology* (2001) NIAG/SG61 Pre-Feasibility Study. (Accessed: 25 November 2001)

*Failure mode and effects analysis* (2006) IEC 60812, International Electrotechnical Commission, 25-Jan-2006

*FCSHIP project.* (2005) Available at: [www.fcship.com](http://www.fcship.com) (Accessed: 9 July 2005)

*FCSHIP working file* (2004) *Synthesis of open problems and Roadmap for future RTD*, DTR-5.2-06.2004 (Accessed: 30 June 2004)

*FCTESTNET project introduction.* (2005) Available at:  
<http://ie.jrc.ec.europa.eu/fctestnet/> (Accessed at 13 August 2005)

Forbes, C.A. (2003), ‘Solid Oxide Fuel Cells for CHP Application’, *Combined heat and power in New York State*, Available at: [www.nyserda.ny.gov/-/media/Files/EIBD/.../5SOFCFuelCell\\_F Forbes.pdf](http://www.nyserda.ny.gov/-/media/Files/EIBD/.../5SOFCFuelCell_F Forbes.pdf) (Accessed at 11 August 2013)

*German Navy orders two more fuel cell subs.* (2006) Fuel Cells Bulletin, 11, 6.

*GOALDS, European Commission funded research project on Goal Based Damage Stability* (2012) Available at: <http://goalds.org/> (Accessed 26 Jan 2012)

Grove, W. (1938) ‘A small voltaic battery of great energy’, *Philosophical Magazine*, vol. 15, pp. 287-293.

Guzzella, L. (1999) ‘Control oriented modeling of fuel cell based vehicles’, *Presentation in NSF Workshop on the Integration of Modeling and Control for Automotive System*, 1999.

Hagiwara, A., Michibata, H., Kimura, A., Jaszcar, M.P., Tomlins, G.W. and Veyo, S.E. (1999) ‘Tubular solid oxide fuel cell life tests’, *Proceedings of the third international fuel cell conference*, D2-4, pp. 365-368.

Harvld, S.A. (1983) *Resistance and Propulsion of Ships*. Wiley, John & Sons, 1983.

*HotModule power for FellowSHIP project* (2008) Fuel Cells Bulletin, (Accessed: 4 January 2008)

*Hydra (ship)* (2002) Available at: [http://en.wikipedia.org/wiki/Hydra\\_\(ship\)](http://en.wikipedia.org/wiki/Hydra_(ship)) (Accessed: 2 August 2002)

*Hydroxy3000 Hydrogen ship.* (2004) Available at: <http://iese.heig-vd.ch/hydroxy> (Accessed 8 October 2004)

*International Standard for HAZOP studies* (2006) IEC 61882, Hazard and Operability studies-Guide word approach, International Electrotechnical Commission

Iora, P., Aguiar, P., Adjiman, C.S. and Brandon, N.P. (2005) ‘Comparison of two IT DIR-SOFC models: Impact of variable thermodynamic, physical, and flow properties. Steady-state and dynamic analysis’, *Chemical Engineering Science*, 60, pp. 2963–2975.

*ISH logarithmic propeller Diagram for three-bladed propellers.* (1982) Wageningen Series B-3 hand book, 1982

James, B.D., Spisak, A.B. and Colella, W.G. (2012), ‘Cost Estimates of Stationary Fuel Cell Systems’, Available at:  
<http://www.fuelcellseminar.com/media/51164/sta32-2.pdf> (Accessed at 2 August 2013)

Janardhanan, V.M. and Deutschmann, O. (2006) ‘CFD analysis of a solid oxide fuel cell with internal reforming: Coupled interactions of transport, heterogeneous catalysis and electrochemical processes’, *Journal of Power Sources*, 162, pp. 1192–1202.

Jiang, W., Fang, R., Khan, J. A. and Dougal, R. A. (2006) ‘Parameter setting and analysis of a dynamic tubular SOFC model’, *Journal of Power Sources*, 162, pp. 316–326.

Kakac, S., Pramuanjaroenkij, A. and Zhou, X. Y. (2007) ‘A review of numerical modeling of solid oxide fuel cells’, *International Journal of Hydrogen Energy*, 32, pp. 761 – 786.

Kandepua, R., Imslandb, L., Fossa, B. A., Stillerc, C., Thorudc, B. and Bollandc, O. (2007) ‘Modelling and control of a SOFC-GT-based autonomous power system’, *Energy*, 32, pp. 406 – 417.

- Kar, L., Tse, C., Wilkins, S., McGlashan N., Urban, B. and Martinez-Botas, R. (2011) ‘Solid oxide fuel cell/gas turbine trigeneration system for marine applications’, *Journal of Power Sources*, 196, pp. 3149–3162.
- Khaleel, M., Recknagle, K., Deibler, J. and Stevenson, J. (2001) ‘Thermo-mechanical and electrochemistry modelling of planar SOFC stacks’, *Proceedings of the International Symposium, SOFC VII*, Electrochemical Society, pp. 1032–1041.
- Larminie, J. and Dicks, A. (2003) *Fuel Cell Systems Explained*, P59-60.
- Li, P.W. and Chyu, M.K. (2003) ‘Simulation of the chemical/electrochemical reactions and heat/mass transfer for a tubular SOFC in a stack’, *Journal of Power Source*, 124, pp. 487–498.
- Liu, H.C., Lee, C.H., Shiu, Y.H., Lee, R.Y. and Yan, W.M. (2007) ‘Performance Simulation for an Anode-supported SOFC Using Star-CD’, *Journal of Power Sources*, 167, pp. 406–412.
- Liu, Y. and Leong, K.C. (2006) ‘Numerical study of an internal reforming solid oxide fuel cell and absorption chiller co-generation system’, *Journal of Power Sources*, 159, pp. 501-508.
- M50 Programme for type testing of non-mass produced I.C. engines, Unified Requirement* (2013) International Association of Classification Societies (Accessed: 14 March 2013)
- METHAPU project.* (2010) Available at: <http://www.methapu.eu/> (Accessed: 25 October 2010)
- Meusinger, J., Riensche, E. and Stimming, U. (1998) ‘Reforming of natural gas in solid oxide fuel cell systems’, *Journal of Power Sources*, 71, 315–320.
- MTU Sailing boat.* (2003) Available at:

<http://www.fuelcelltoday.com/reference/image-bank/Transport/MTU-Sailing-Boat>  
(Accessed 12 March 2003)

Nelson, P., Bloom, I., Amine, K. and Henriksen, G. (2002) ‘Design modeling of lithium-ion battery performance’, *Journal of Power Source*, 110, pp. 437-444.

Nelson, P., Dees, D., Amine, K. and Henriksen, G. (2003) ‘Modeling the performance of Lithium-ion batteries for fuel cell vehicles’, *Hybrid Vehicle and Energy storage technologies*, SAE Technical Paper, 2003-01-2285.

Newman, J. and Thomas-Alyea, K. (2004) *Electrochemical systems*, Hoboken, NJ, Wiley.

‘Operation and maintenance manual Beta 5kW SOFC system’ (2005) Fuel Cell Technologies Ltd, Report Number: 151-00-030-R-1, September 28th, 2005.

Ovrum, E. and Dimopoulos, G. (2012) ‘A validated dynamic model of the first marine molten carbonate fuel cell’, *Applied Thermal Engineering*, 35, pp. 15-28.

Padulles, J., Ault, G. W. and McDonald, J.R. (2000) ‘An integrated SOFC dynamic model for power system simulation’, *Journal of Power Sources*, 86, pp. 495-500.

*Part 6, Chapter 1, section 2.3.8* (2012) The Rules and Regulations for the Classification of Ships, Lloyd’s Register, London.

*Part 6, Chapter 1, Section 2.10.7* (2012) The Rules and Regulations for the Classification of Ships, Lloyd’s Register, London.

*Part 6, Chapter 1, section 2.12.7* (2012) The Rules and Regulations for the Classification of Ships, Lloyd’s Register, London

‘Permanent magnet synchronous machine’ (2008) *SimPowerSystem reference*, The Mathworks, version Oct 2008.

Pischinger, S., Schonfelder, C. and Ogrzewalla, J. (2006) ‘Analysis of dynamic requirements for fuel cell systems for vehicle applications’, *Journal of Power Source*, 154, pp. 420-427

*Platts LNG daily* (2013), available at:

<http://www.platts.com/IM.Platts.Content/ProductsServices/Products/lngdaily.pdf>  
(accessed 6th November 2013)

Privette, R. M. (1999) ‘2.5 MW PEM Fuel Cell System for Navy Ship Service Power’, *Joint Fuel Cell Technology Review Conference*, 1999 August.

*Program for trials of diesel engines to assess operational capability* (2012) Part 5, Chapter 2, Section 18 of the Rules and Regulations for the Classification of Ships 2012, Lloyd’s Register.

Pukrushpan, J. T., Stefanopoulou, A. G. and Peng, H. (2005) *Control of fuel cell power system*, Springer, USA.

Recknagle, K., Williford, R., Chick, L., Rector, D. and Khaleel, M. (2003) ‘Three dimensional thermofluid electrochemical modelling of planar SOFC stacks’, *Journal of Power Sources*, 113, pp. 109–114.

Recommended air velocities in ducts (2013), *The engineering Tool Box*, available at: [http://www.engineeringtoolbox.com/duct-velocity-d\\_928.html](http://www.engineeringtoolbox.com/duct-velocity-d_928.html) (accessed 3rd December 2013)

Reid, R.C., Prausnitz, J.M. and Poling, B.E. (1987) *The Properties of Gases and Liquids*, McGraw-Hill, New York.

*Requirements for Machinery and Engineering Systems of Unconventional Design*. (2012) Chapter 16, Part 7 of the Rules and Regulations for the Classification of Ships, Lloyd’s Register, Jan 2012.

Rules and guidelines for the use of fuel cell system on board of ships and boats, version 2003 (2003) Germanister Lloyds.

San, B. and Bradshaw, J. (2012) 'Fuel cells for ships: systems, risks and regulations', *11th International Marine Design Conference*, Glasgow, UK, Vol 2, pp. 407-415, 10-14th June 2012.

Sanchez, D., Chacartegui, R., Munoz, A. and Sanchez, T. (2006) 'Thermal and electrochemical model of internal reforming solid oxide fuel cells with tubular geometry', *Journal of power sources*, 160, pp. 1074-1087.

*Siemens Stationary fuel cell performance* (2010) Available at:

<http://www.powergeneration.siemens.com/products-solutions-services/products-packages/fuel-cells/sofc-commercialization/sfc-200-performance/> (Accessed: 12 September 2010)

*Siemens tubular SOFC*. (2013) Available at:

<http://www.powergeneration.siemens.com/products-solutions-services/products-packages/fuel-cells/principle-behind-technology/> (Accessed : 23 Jan 2013)

Singhal, S.C. (1998) 'Advance in solid oxide fuel cell technology', *Proceedings of the 1998 fuel cell seminar*, pp. 266-269.

*SK Summit* (2007) Available at:

[http://www.skshipping.co.kr/jsp/eng/company/fleet/fleet\\_detail.jsp?idx=00001&cateidx=00004](http://www.skshipping.co.kr/jsp/eng/company/fleet/fleet_detail.jsp?idx=00001&cateidx=00004) (Accessed: 23 Feb 2007)

Strazza, C., Del Borghi, A., Costamagna, P., Traverso, A. and Santin, M. (2010) 'Comparative LCA of methanol-fuelled SOFCs as auxiliary power systems on-board ships', *Applied Energy*, 87, pp. 1670–1678.

*Test specification Number 4 for internal combustion engines* (2012) Lloyds Register Type Approval System, Lloyds Register.

*The Rules and Regulations for the Classification of Ships* (2012) Chinese Classification Society.

*The Rules and Regulations for the Classification of Ships, July 2012 version* (2012)  
Lloyd's Register, London

*TRI-ZEN LNG Market Perspective* (February 2013) Available at:  
<http://www.imo.org/OurWork/Environment/PollutionPrevention/AirPollution/Documents/Air%20pollution/LNG%20Bunkers%20Perspective%20February%202013.pdf>  
(Accessed at 9 August 2013)

Tu, H. and Stimming, U. (2004) ‘Advances, aging mechanisms and lifetime in solid-oxide fuel cells’, *Journal of Power Sources*, 127, pp. 284–293.

Van Selow, E.R. and Kraaij, G.J. (2005) ‘Fuel Cell System Development for Frigates’, *Second European Hydrogen Energy Conference*, 22-25 November, 2005, Zaragoza, Spain.

Versteeg, H.K. and Malalasekera, W. (1995) *An Introduction to Computational Fluid Dynamics: The Finite Volume Method*, Wiley, New York.

Veyo, S.E. (2003), ‘Tubular SOFC hybrid power systems’, *Third DOE/UN international conference and workshop on hybrid power system*, Newport beach, USA, 13 May 2003

Wang, F.J. (2004) *Analysis of Computational Fluid Dynamics*, Tsinghua University Press, 2004 September.

*Wartsila 34DF engine*, (2013), Available at:  
<http://www.wartsila.com/en/engines/DF-engines/wartsila34DF> (Accessed at 5 August 2013)

Wendt, H. and Kreysa, G. (1999) *Electrochemical Engineering*, Springer, Berlin.

Yakabe, H., Ogiwara, T., Hishinuma, M. and Yasuda, I. (2001) ‘3-D model calculation for planar SOFC’, *Journal of Power Sources*, 102, pp. 144–154.

Yakabe, H., Ogiwara, T., Yasuda, I. and Hishinuma, M. (1999) 'Model calculation for planar SOFC focusing on internal stresses', *Proceeding of the International Symposium, SOFC VI*, Electrochemical Society, pp. 1087–1098.

Yang, Z., Weil, K. S., Paxton, D. M., and Stevenson, J. W. (2003) 'Selection and evaluation of heat resistant alloys for SOFC interconnect applications', *Journal of the Electrochemical Society*, 150(9), pp. 1188–1201.

Yerramalla, S., Davari, A. and Feliachi, A. (2003) 'Modelling and simulation of the dynamic behaviour of a polymer electrolyte membrane fuel cell', *Journal of Power Source*, 124, pp. 104-113.

*Z4 type DC motor specification* (2008) Available at:

[http://www.tradebub.com/by\\_1882999\\_Z4-DC-motor.htm](http://www.tradebub.com/by_1882999_Z4-DC-motor.htm) (Accessed 19 January 2008)

## Appendix A1: Classification regulations for marine SOFC application

Marine installation of an SOFC system is a relatively comprehensive topic influencing various ship systems such as fuel cell stack onboard installation, bunkering line installation, fuel storage, piping system, fuel cell enclosure (housing) and electrical system installation.

SOFC is a type of high temperature fuel cell which is constructed by using refractory materials seldom seen in the marine industry. Hence, the manufacturing certificates or standards applied for SOFC stack production need to be examined at the first stage. This information should include: design and manufacturing procedures, industry standards applied, materials for key components, quality control system used during design and manufacturing, plans of type testing.

Other than the SOFC stack itself, most components and subsystems used in the fuel cell system, from electrical parts to mechanical parts, are applicable to certain parts of ship rules and regulations. The relevant parts of LR rules has been checked and listed in table A.1.

**Table A.1: LR rule applied for SOFC approval**

Hull structure rules	<i>The Rules and Regulations for the Classification of Ships</i> Part 3: Ship structures general Part 4: Ship structures ship type
Main & auxiliary machinery rules	<i>The Rules and Regulations for the Classification of Ships</i> Part 5, Chapter 1: General requirements for the design and construction of machinery Part 5, Chapter 2: Oil engines Part 5, Chapter 11: Other pressure vessels Part 5, Chapter 12: Piping design requirements Part 5, Chapter 13: Ship piping systems Part 5, Chapter 14: Machinery piping systems
	<i>The Rules and Regulations for the Classification of Natural Gas Fuelled Ships</i>
	<i>The Rules and Regulations for the Construction and</i>

	<p><i>Classification of ships for the Carriage of Liquefied Gas in Bulk</i> Chapter 16: Use of cargo as fuel Chapter 17: Special requirements</p> <p><i>The Rules and Regulations for the Construction and Classification of Ships for the Carriage of Liquid Chemicals in Bulk</i> Chapter 5: Cargo transfer Chapter 12: Instrumentation</p> <p><i>The Ships and Regulations for the Classification of Ships</i> Part 6, Chapter 1: Control engineering systems Part 6, Chapter 2: Electrical engineering</p>
Control, electrical and fire rules	

To specify the topic of plan approval for SOFC marinisation, the 5 (kW) SOFC system used in chapter 4 is examined as a sample according to the rules and regulations mentioned above.

In the following paragraph rules and codes in relation to the 5 (kW) SOFC system installation will be listed in detail with special attention given to LNG carrier installation.

### A1.1 SOFC stack

The SOFC stack is to be constructed in line with manufacturing standards, IMO, IEC and EU standards for fuel cells, e.g. American National Standard for Fuel Cell Power Plants, Uniform Mechanical Code, National Fire Code and National Electric Code.

The burner and heat exchanger inside the SOFC system are to be of a certificated type.

The fuel cell stack is to be leak tested at 1.1 times the maximum allowable working pressure.

### A1.2 Fuel cell room (housing) and operating environment

A means of drainage and a bilge alarm in the fuel cell room are to be provided.

One additional gas detector in the fuel cell room is to be installed close to the fuel inlet of the fuel cell stack or wherever leakage is most likely to occur.

Fuel cell room entrance doors are to be gas-tight and self-closing.

The material used for fuel cell housing construction is to be grade A and AH36 according to LR material rules.

The mass of the fuel cell system should be taken into effect when calculating the strength of the fuel cell housing structure.

A lifting test should be carried out before final lifting and fitting of the fuel cell room

If the fuel cell room is intended to be installed above the open deck, then the roof structure is to be self-draining and kept free of snow and ice.

### A1.3 General arrangement

If SOFC stacks are used for supplying essential consumers, then redundancy shall be ensured.

All parts of the SOFC and the directly associated components containing fuel during normal operation shall be arranged in an enclosed space that shall be properly ventilated and monitored by gas detection systems.

The installation spaces of the SOFCs and their directly associated components shall be separated from the spaces used for fuel storage.

Spaces in which fuel storage tanks are located shall be separated from conventional machinery spaces and the other parts of the SOFC system. If the installation space is

adjacent to a space with potential fire load, separation by means of an A-60 bulkhead is required. Tanks, which are part of the ship structure, shall be separated from other spaces by means of cofferdams (Rules and guidelines for the use of fuel cell system on board of ships and boats, 2003).

SOFC Systems shall be located in separate spaces. The installation spaces of SOFC stacks and directly associated components shall be arranged outside of accommodation, service and machinery spaces and control rooms, and shall be separated from such spaces by means of a cofferdam or an A-60 bulkhead. Installation in a conventional machinery space is admissible, on condition that a suitable enclosure is provided (Rules and guidelines for the use of fuel cell system on board of ships and boats, 2003).

Anti-collision chocks are to be provided to ensure that the manufacturer's maximum shock load limits are not exceeded.

#### A1.4 Ventilation

Ventilation systems must be permanently installed and are not allowed to be connected to those of other ship spaces.

The extracted air must be monitored for fuel constituents.

The ventilation system shall be designed for at least 30 air changes per hour with regard to the total geometric volume of the empty space. If the ventilation system fails, an alarm must be generated.

Suitable design of the spaces shall ensure that no gas can accumulate in recesses or pockets. (Rules and guidelines for the use of fuel cell system on board of ships and boats, 2003)

All ventilation fans and fire dampers are to be capable of being stopped from a safe remote location in the event of fire.

Protection screens of not more than 13 (mm) square mesh shall be fitted in outside openings to ventilation ducts.

The outlet of the ventilation duct is to be fitted with suitable flame wire gauze.

Bunkering hoses are to be of an approved type and to be stored in a safe and well ventilated location on open deck.

#### A1.5 Fuel storage container

Material for container and pressure vessel is to be provided with LR test certificate. Storage tank should be designed and tested according to the LR Rule for Natural Gas Fuelled Ships and IMO's International Code for the Construction and Equipment of Ships Carrying Liquefied Gases in Bulk (IGC Code).

Level gauge and swash-plate need to be provided.

Sloshing assessment of tank must be carried out to determine the sloshing pressure and thickness of swash-plates and effect of sloshing load on tank walls.

A quick closing valve is to be fitted to the fuel storage tank. The quick closing valve is to be capable of being closed both remotely and locally. The quick closing valve and its control is to be of steel construction or of an acceptable fire tested design.

Leakage test is to be provided after onboard installation.

#### A1.6 Bunkering and fuel transfer

The fuel supply systems are to comply with the requirements of the relevant section of the Rules for Ships for Liquefied Gases, where applicable like Part 7 Chapter 2 Section 5, 9 and 17 of LR rules.

All welds in the bunkering system are to be full penetration butt weld. Those welds located after the gas detection point are to be tested by 100% volumetric non-destructive test.

Provision to shut off the gas is to be made in the gas firing supply lines immediately before the lines enter the compartment in which the equipment is installed. The shut off arrangements are to be of the double block and vent type, and are to be operable at the equipment or the equipment control position and at a position in a safe area remote from the equipment.

Fuel transfer systems shall be permanently installed and completely separated from other pipeline systems.

The bunkering procedure and measurement of dealing with safety and effectively with gas leaks are to be approved.

The bunkering line is to be supported and protected against mechanical damage.

An emergency stop for the bunkering pump is to be fitted in a safe location.

A leakage test for the bunkering line is to be carried out.

#### A1.7 Control and electric

The SOFC power system is required to have the following functions applicable:

- Over-load protection
- Over-pressure protection
- Maximum working stresses
- Explosion protection and fire protection

- Automatic shutdown on system failure

The SOFC alarm system is to be such that should an alarm be acknowledged and a second fault occur prior to the first fault being rectified, audible and visual alarms will operate again (Part 6, Chapter 1, section 2.3.8 of The Rules and Regulations for the Classification of Ships, Lloyd's Register, 2012).

The SOFC control and alarm system is to be provided with self-monitoring facilities such that hardware and functional failure will initiate an audible and visual alarm (Part 6, Chapter 1, Section 2.10.7 of The Rules and Regulations for the Classification of Ships, Lloyd's Register, 2012).

According to the IMO's Safety of Life at Sea (SOLAS) code, the control systems for the fuel cell are required essentially to be independent or designed so that failure of one system does not degrade the performance of another system. The automatic starting, operational and control systems are required to have provisions for manually overriding the automatic controls; and the failure of the systems is not to prevent the use of the manual override.

There are to be means of ensuring that fuel cell system machinery and equipment are functioning in a reliable manner with arrangements for regular inspections and tests to ensure continuous reliable operation. The fuel cell alarm system is required to be designed on the fail-to-safety principle to ensure that any serious malfunction in machinery operation which presents an immediate danger initiates the automatic shutdown of that part of the plant and gives an alarm.

If the SOFC system is used as a power source, software would be required to comply with the regulations of 'LR's Software Conformity Assessment System – Assessment module GEN1' (Part 6, Chapter 1, section 2.12.7 of The Rules and Regulations for the Classification of Ships, Lloyd's Register, 2012).

If the SOFC system is used as a test unit, it is recommended to connect to an emergency switchboard.

### A1.8 Piping system

Flexible hoses and pipes used are to be of an approved type.

Mechanical pipe couplings are to be type approved and the number of connections is to be kept to a minimum.

The fuel supply and return line are to be hydraulically tested to 1.5 times the design pressure.

A leakage test is to be carried out after the hydraulic test.

The exhaust system is to be leak tested at 1.1 times the maximum working pressure.

The purge system is to be hydraulic pressure tested at 1.5 times the maximum allowable working pressure.

All welded pipe connections are to be full penetration welds.

Fuel and exhaust pipes should be welded with two fillet welds.

### A1.9 Fire fighting

Gas detection devices are to be fitted under valves in line of pipelines which carry flammable gas and liquid. The gas alarm is to be wired to the engine room alarm and control system. A dedicated fire extinguishing system is to be provided for the fuel cell room.

Extra fire detectors and extinguishing devices should be installed in both the fuel cell room and natural gas storage tanks where fuel leakage may occur. Fire extinguishing system should be located outside the space of the fuel cell room. A CO<sub>2</sub> extinguishing device is also applicable since the fuel cell room is a relatively self-enclosed space. The

alarm and emergency shutdown functions must be provided and can be triggered independently. The fuel cell malfunction alarm system and switch off function is activated when the explosion limit is reached. The control panel of the monitoring and alarm system is displayed in the engine control room for regular safety checks.

#### A1.10 Materials

Materials used in the SOFC system, e.g. pipes, valves and fittings, are to be in accordance with Class I materials to comply with LR rules Part 2 “manufacture, testing and certification of materials”. However, massive amounts of unconventional materials are used in fuel cells, e.g. zirconia ceramic and strontium doped lanthanum manganite. Currently, there is no reference or experience of using these materials on board ships. The approval of fuel cell material should comply with industry used regulations in respect of fuel cell manufacturing.

#### A1.11 Seagoing circumstances

Fuel cell systems to be applied to ships shall be able to cope with ambient reference conditions at sea, such as acceleration, ship motion, inclination and temperature. The following, table A.2, shows the operating conditions required by classification rules and satisfactory conditions of solid oxide fuel cell systems.

**Table A.2: SOFC under seagoing circumstances**

	<i>Rules requirement</i>	<i>SOFC satisfactory</i>
Static athwartship inclination	15 degrees	Ok
Dynamic athwartship inclination	22.5 degrees	Ok
Static fore and aft inclination	5 degrees	Ok
Dynamic fore and aft inclination	7.5 degrees	Ok
Barometric pressure ambient	1000 (mbar)	Ok
Engine room temperature	45 (°C)	Ok

Suction air temperature	45 (°C)	Ok
Relative humidity	60%	Ok
Salt in air	0 to 50 (ppm)	Depends on SOFC
Vibration	Depends on engine system	Depends on SOFC

It can be seen that ship inclination, humidity and ambient temperature have not much effect on SOFC performance. Solid oxide fuel cell systems will be placed in an environment of salty air. Apparently salt particles have no chemical reactions with cathode materials like  $L_aC_oO_3$  and  $L_aS_r M_n O_3$ . The Ballard PEMFC has been tested with salty air of 50 ppm. The testing report from the METHAPU project also indicates the tolerance of marine environments for SOFCs after modification. The results show that the salty air has no or limited effect on fuel cell performance (Privette, 1999).

Anti-shock measures need to be adopted for the installation, because some materials used in SOFCs are fragile. In order to minimise the vibration effect from the propulsion engines location of the fuel cell room should be avoided at the same deck level as the main engines and propulsion shaft. In addition, elastic supports are also required to reduce the vibration and shock effect on the SOFC. Mechanical accelerometers are equipped with connection to the alarm system within the SOFC module, to monitor shock situations and report to the alarm system accordingly.

#### A1.12 Trial

If SOFCs are used for supplying essential consumers, then every fuel cell stack shall be subjected to a performance test at the manufacturer's works. The electrical and thermal output of the fuel cells shall be verified by means of a suitable performance test.

The SOFC system shall be subjected to the following trials after installation onboard:

- Function trials of components
- Trials of protective devices and protective system

- Trials of the fire extinguishing system
- Function trials of the SOFC system
- Function trials of interaction of the SOFC system with the ship system

#### A1.13 Dependability and maintenance

SOFC system dependability analysis is to be carried out by methods of FMECA and HAZOP. The SOFC stack and its immediate supporting system, e.g. supply of fuels and electrical equipment, need to be checked to ensure that risk mitigation measures have been achieved. A single failure in SOFC system will not cause degradation or loss of system performance and will not result in unsafe operating conditions.

Even though researchers and manufacturers claim that fuel cells need less maintenance work than conventional combustion engines, this view point is still questionable when fuel cells work in harsh sea conditions. The maintenance work of the SOFC system comes from BOP components, such as battery charging, water methanol tank charging, filter and desulphuriser replacement. Other maintenance work is partly attributed to the monitor and alarm systems.

#### A1.14 Quality control system and manufacturing control procedure

General description detailing the extent of the machinery or engineering system, the shipboard services it is to provide, its operating principles, and its functionality and capability when operating in the environment to which it is likely to be exposed under both normal and foreseeable abnormal conditions. The general description is to be supported by the following information as applicable:

- (a) System block diagram.
- (b) Piping and instrumentation diagrams.

- (c) Description of operating modes, including: Start-up, shut-down, automatic, reversionary, manual and emergency.
- (d) Description of safety related arrangements, including:
  - Safeguards, automatic safety systems and interfaces with ship's safety systems.
- (e) Description of connections to other shipboard machinery, equipment and systems, including: Electrical, mechanical, fluids and automation.
- (f) Plans of physical arrangements, including: Location, operational access and maintenance access.
- (g) Operating manuals, including: Instructions for start-up, operation, shut-down, instructions for maintenance, instructions, for adjustments to the performance and functionality and details of risk mitigation arrangements.
- (h) Maintenance manuals, including: Instruction for routine maintenance, repair following failure, disposal of components and recommended spares inventory.

Project process documentation including the following procedures and the results of applying the procedures including:

- (a) Project management
- (b) Requirements definition
- (c) Quality assurance
- (d) Design definition
- (e) Risk management
- (f) Configuration management
- (g) Verification

(h) Integration

(j) Validation (certification and survey)